DISSECTING PLANT INNATE IMMUNITY USING SNC1 – A SENSITIVE IMMUNE RECEPTOR

by

Yu Ti Cheng

B. Sc., The University of British Columbia, 2004

A THESIS SUBMITTED IN PARTIAL FULFILLMENT OF
THE REQUIREMENTS FOR THE DEGREE OF

DOCTOR OF PHILOSOPHY

in

The Faculty of Graduate Studies
(Genetics)

THE UNIVERSITY OF BRITISH COLUMBIA
(Vancouver)

May 2013

Abstract

Plants rely on innate immunity to fight pathogens. Among plant defence mechanisms, Resistance (R) proteins play essential roles in recognizing pathogens and mounting robust defence responses. *snc1*, a mis-regulated plant *Resistance* (*R*) gene mutant, exhibits distinctive morphological and autoimmune phenotypes. To identify the signalling components downstream of R protein-mediated defence, forward genetic screens were conducted in the *snc1* background.

From the screens, fifteen novel *mos* (*modifier of snc1*) mutants were identified, of which, I studied *mos7* and *mos9* for my PhD thesis. Both *mos7* and *mos9* partially suppress all *snc1*-related autoimmune phenotypes. MOS7 is an Arabidopsis homolog of human and Drosophila Nucleoporin 88 (Nup88) required for protein nuclear retention. Partial loss-of-function alleles of *Nup88* in Drosophila and mammalian cells fail to accumulate NF-κB in the nucleus and result in immune deficiency. We found that several defence related proteins have altered distribution/abundance in *mos7*, including snc1. This study highlights the importance of nucleocytoplasmic trafficking in plant immunity.

mos9 contains a mutation in a gene encoding a protein of unknown function. Immunoprecipitation followed by mass spectrometry identified a SET domain-containing protein, ATXR7, as an interactor of MOS9. Previous studies showed that ATXR7 methylates lysine 4 of histone H3 (H3K4) and this methylation is required for proper transcriptional activation of *Flowering Locus C* (*FLC*). We found reduced expression of two *R* genes, *SNC1* and *RPP4*, in *mos9* and *atxr7*. Also, H3K4 marks close to *SNC1* are reduced in *mos9*. My research on MOS9 illustrated the importance of histone modification in regulating plant immune receptor transcription.

Serendipitously, I worked on an F-box protein, CPR1. From the genetic and biochemical data, we found that at least two R proteins, SNC1 and RPS2, are being regulated by CPR1. Our study is the first report with evidence suggesting how plant R proteins are negatively regulated by the ubiquitin-26S proteasome.

Overall, my PhD thesis research provides evidence that plant immunity is under tight control at multiple levels. My work furthers our knowledge on how plant immune responses are regulated.

Preface

The work described in this thesis is the culmination of research from September 2006 through April 2013. Below is a list of manuscripts (published or in preparation) that comprise this thesis, and the contribution made by the candidate.

Chapter 1, Section 3 – Ubiquitination in NB-LRR R protein-mediated immunity was modified from the manuscript:
Cheng Y.T. and Li X. (2012). Ubiquitination in NB-LRR-mediated immunity. Current Opinion in Plant Biology. 15(4):392–399. Edited by Pamela Ronald and Ken Shirasu.

- X. Li conceived of, wrote and prepared the manuscript. The candidate prepared Figure 1.1 and Table 1.1 based on the text written by X. Li.

Chapter 2 – Nuclear pore complex component MOS7/Nup88 is required for innate immunity and nuclear accumulation of defence regulators in Arabidopsis was modified from the manuscript:
Cheng Y.T., Germain H., Wiermer M., Bi D., Xu F., Garcia A.V., Wirthmueller L., Despres C., Parker J.E., Zhang Y., and Li X. (2009). Nuclear pore complex component MOS7/Nup88 is required for innate immunity and nuclear accumulation of defense regulators in Arabidopsis. Plant Cell 21(8): 2503-2516.

- The *mos7* mutant was generated and isolated by Y. Zhang and X. Li. The candidate performed the following experiments under the instruction and supervision of X. Li and Y. Zhang: map-based cloning of *mos7* and single mutant characterization including morphology, abiotic responses and disease assays. Confocal microscopy of MOS7-GFP (transgenic line generated by Y. Zhang) and nuclear export/import assay system (Haasen et al., 1999) was conducted by D. Bi; confocal microscopy images of mos7-GFP (transgenic line generated by the candidate) were taken by the candidate with great help and advice from Dr. EunKyoung Lee. Protein fraction of snc1-GFP (transgenic line generated by Y. Zhang) was performed by H. Germain; protein fractionation of NPR1-GFP and EDS1 was performed by M. Wiermer. F. Xu and A. Garcia performed protein fractionation experiments shown in Figure 2.11A and Figure 2.11B, respectively, and wrote the corresponding materials and methods sections. The candidate, H. Germain, M. Wiermer and X. Li wrote the manuscript. X. Li supervised the work done by the candidate and prepared the manuscript.

Chapter 3 – Regulation of transcription of NB-LRR-encoding genes SNC1 and RPP4 via H3K4 tri-methylation was modified from the prepared manuscript:
Xia S., Cheng Y.T., Huang S., Win J., Soards A., Jinn T-L, Jones J.D., Kamoun S., Chen S., Zhang Y., and Li X. Regulation of transcription of NB-LRR-encoding genes *SNC1* and *RPP4* via H3K4 tri-methylation. Manuscript in preparation.

- The *mos9* mutant was generated and isolated by Y. Zhang and X. Li. S. Xia performed map-based cloning and the candidate conducted TAC clone and single gene transgene complementation. T-L Jinn provided a construct for single gene complementation of *mos9*. The candidate performed mutant characterization including morphology, salicylic acid analysis, disease assays and gene expression analysis and isolated the *mos9* single mutant. The candidate performed disease assays using *At1g56420* RNAi knock-down lines (generated by the candidate). The candidate, J. Win, A. Soards, S. Kamoun and X. Li analyzed the evolutionary trends of MOS9 and the MOS9 homolog, At1g56420. The candidate generated the MOS9-GFP transgenic line and conducted confocal microscopy and protein fractionation using the line. The candidate used the same MOS9-GFP transgenic line for immuno-purification of MOS9-GFP associated proteins and prepared samples for mass spectrometry. S. Chen performed the mass spectrometry and data analysis. The candidate generated *atxr7 snc1* and *atx1 snc1* double mutant plants and performed mutant characterization on these plants. The candidate, S. Xia and S. Huang performed chromatin immunoprecipitation (ChIP) experiments; the candidate and X. Li analyzed the ChIP data. The candidate and X. Li wrote the manuscript. X. Li supervised the work done by the candidate, S. Xia and S. Huang, and prepared the manuscript.

Chapter 4 – Stability of plant immune receptor Resistance proteins is controlled by SCF-mediated protein degradation was modified from the manuscript:
Cheng Y.T., Li Y., Huang S., Huang Y., Dong X., Zhang Y., and Li X. (2011). Stability of plant immune-receptor resistance proteins is controlled by SKP1-CULLIN1-F-box (SCF)-mediated protein degradation. Proceedings of the National Academy of Sciences of the United States of America. 108 (35): 14694-14699. Edited by Paul Schulze-Lefert.

- The candidate and Y. Li performed most of the experiments under the supervision of X. Li and Y. Zhang. S. Huang identified the mutation in the *cpr1-1* allele isolated by X. Dong's group. Y. Huang isolated the *35S:CPR1* in *snc1* transgenic line used in this study and performed disease assays using *Hyaloperonospora arabidopsidis*. The candidate, X. Dong, Y. Zhang and X. Li wrote the manuscript. X. Li supervised the work done by the candidate and prepared the manuscript.

Table of Contents

List of Tables

List of Figures

List of Abbreviations

35S	a very strong constitutive promoter found in Cauliflower mosaic virus (CaMV); the coefficient of sedimentation of viral transcript whose expression is naturally driven by this promoter is 35S
ABA	abscisic acid
ABRC	Arabidopsis Biological Resource Center
ACIF1/*ACRE189*	Avr9/Cf-9–Induced F-Box 1 (or Avr9/Cf-9 Rapidly Elicited gene 189) in Nicotiana benthamiana
ACRE276/*PUB17*/*ARC1*	Avr9/Cf-9 Rapidly Elicited gene 276 (in N. benthamiana); Plant U-Box 17 (in A. thaliana); Arm Repeat Containing 1 (in B. napus)
ACT1	Actin 1
AGO1	Argonaute 1
amiRNA	artificial microRNA
Apaf1	Apoptotic protease activating factor 1
APC/C	Anaphase-Promoting Complex or Cyclosome
AtCDC5	Arabidopsis thaliana Cell Division Cycle 5
ATL9	Arabidopsis tóxicos en levadura 9
ATX1	Arabidopsis homolog of trithorax 1
ATXR7	Arabidopsis Trithorax-Related 7
AUS/IAA1	Auxin-responsive protein or Indoleacetic Acid-Induced protein 1
Aux/IAA	Auxin/Indole-3-Acetic Acid protein
IAA	Indole-3-Acetic Acid
Avr	avirulent or avirulence
Avr3a	an avirulence effector from *Phytophthora infestans*
Avr4	an avirulence effector from *Cladosporium fulvum*
Avr9	an avirulence effector from *Cladosporium fulvum*
avrB	Avirulence protein B; an avirulence effector from *Pseudomonas syringae* pv. *Glycinea*
avrPphB	An avirulence effector from *Pseudomonas syringae* pv. *phaseolicola*
avrPto	an avirulence protein from *Pseudomonas syringae*
avrPtoB	an avirulence protein from *Pseudomonas syringae*
avrRpm1	An avirulence protein isolated from *Pseudomonas syringae* pv. *maculicola* strain M2
avrRps4	An avirulence protein isolated from *Pseudomonas syringae* pv. *pisi*
avrRpt2	An avirulence protein isolated from *Pseudomonas syringae* pv. *tomato*
Ax21	activator of *Xa21*-mediated immunity
BAH1/NLA	benzoic acid hypersensitive1 or NITROGEN LIMITATION ADAPTATION

BAT2	HLA-B Associated Transcript 2
BBI1	BLAST AND BTH-INDUCED-1
BCAS2	Breast Cancer-Amplified Sequence 2
BLAST	Basic Local Alignment Search Tool
BTB	BR-C, ttk and bab (also known as the POZ domain); a protein-protein interaction motif
CC	coiled-coil
CEBiP	Chitin Elicitor Binding Protein
CED4	Cell death protein 4
CERK1	CHITIN ELICITOR RECEPTOR KINASE 1
Cf-9	a tomato resistance gene that confers resistance to *Cladosporium fulvum* that expressing the *Avr9* avirulence gene
cfu	colony forming unit
ChIP	chromatin immunoprecipitation
CHS	chalcone synthase; a cytosolic protein
CIP29	cytokine-induced protein 29
Col	an Arabidopsis ecotype; it is also referred as wild type in this thesis work
COP1	Constitutively photomorphogenic 1
CPR1/CPR30	Constitutive Expresser of *PR* Genes 1; also known as Constitutive Expresser of *PR* Genes 30
CRM1	Chromosomal Region Maintenance 1; also named Exportin 1 (XPO1)
CTLH domain	C-terminal to LisH domain
Cul1	Cullin 1
DDB1	UV-damaged DNA-binding protein 1
DDM1	Decrease in DNA methylation 1
DIC	Differential interference contrast; a microscopy illumination technique to enhance the contrast in unstained, transparent samples
Dif	Dorsal-related immunity factor
DND1	Defense no Death 1
DND2	Defense no Death 2
Dorsal	a conserved eukaryotic transcription factor in Drosophila that binds to DNA sequence motif kappa-B
DRF1	defense-related F-box protein 1
DUB	deubiquitinating enzyme
DWD	DDB1 binding WD40 protein
E1	ubiquitin-activating enzyme
E2	ubiquitin-conjugating enzyme
E3	ubiquitin ligase
EDM2	ENHANCED DOWNY MILDEW 2

EDS1	Enhanced Disease Susceptibility 1
EFR	EF-Tu receptor
EF-Tu	bacterial Elongation Factor Tu
EMS	Ethyl methanesulfonate; a chemical mutagen
ETI	effector-triggered immunity
Fen	fenthion-sensitivity gene
fH	free hyphae
FLAG	an epitope protein tag compose of a single or repeated DYKDDDDK sequence
FLC	Flowering Locus C
FLS2	FLAGELLIN-SENSITIVE 2
GFP	green fluorescent protein
G-patch	glycine-rich nucleic acid binding domain
GUS	beta-glucuronidase; a reporter gene system used in this thesis
H3K4	lysine 4 of histone H3
H3K4me3	tri-methylation of H3K4
H3K9	lysine 9 of histone H3
H.a.	*Hyaloperonospora arabidopsidis*
HA	hemagglutinin; an epitope protein tag compose of a single or repeated YPYDVPDYA sequence
HCF173	High Chlorophyll Fluorescence Phenotype 173
HDA19	HISTONE DEACETYLASE 19
HECT	Homologous to the E6-AP Carboxyl Terminus; an 40 kDa catalytic domain found at the C-terminus of HECT-class E3 ubiquitin protein ligases
HKMT	histone lysine methyl transferase
HP1/DDB1	high pigment-1; also known as UV-damaged DNA-binding protein-1
HR	hypersensitive response
HRT	HYPERSENSITIVE RESPONSE TO TCV
HSP90	HEAT SHOCK PROTEIN 90
HUB1	HISTONE MONOUBIQUITINATION 1
ICS1	Isochorismate Synthase 1
INA	2,6-dichloro-isonicotinic acid; an SA analog
InDel	insertion/deletion
Inf	infestin; A 10 kDa elicitor protein produced by *Phytopthora infestans*
IP	Immunoprecipitation
I-κB	inhibitor of kappa B
JAtY	a TAC library consisting of 36,864 clones, constructed using pYLTAC17 as vector and providing 14x coverage of the Arabidopsis genome

KEG	KEEP ON GOING
KOW	Kyprides, Ouzounis, Woese
LAZ2	LAZARUS 2; an H3K4 methyltransferase
LAZ5	LAZARUS 5; a TIR-type NB-LRR protein
L*er*	Landsberg *erecta*; an Arabidopsis ecotype
LisH domain	Lissencephaly type-1-like homology domain
LPS	lipopolysaccharide
LRES	Long Range Epigenetic Silencing
LRR	leucine-rich repeat
MAC3	MOS4-ASSOCIATED COMPLEX SUBUNIT 3
MAC5	MOS4-ASSOCIATED COMPLEX SUBUNIT 5
MAMP	microbe-associated molecular pattern
MAP	Mitogen-activated protein
Mbo	Members only
MG132	a proteasome inhibitor
Mla10	a barley *Mla* allele that encodes CC-type NB-LRR protein that confers isolate-specific disease resistance against the barley powdery mildew fungus *Blumeria graminis* f sp *hordei* (*Bgh*)
MOS	Modifier of *snc1*
MOS1	Modifier of *snc1*, 1; a BAT2 domain containing protein
MOS2	Modifier of *snc1*, 2; a G-patch and KOW domains containing protein
MOS3	Modifier of *snc1*, 3; also known as AtNup96 or SAR3
MOS4	Modifier of *snc1*, 4; a nuclear protein homologous to human Breast Cancer-Amplified Sequence (BCAS2)
MOS5	Modifier of *snc1*, 5; also known as UBIQUITIN-ACTIVATING ENZYME 1 (UBA1), one of the two Arabidopsis Ubiquitin-activating enzymes
MOS6	Modifier of *snc1*, 6; also known as IMPORTIN ALPHA 3 (IMPA-3)
MOS7	Modifier of *snc1*, 7; homologous to human and Drosophila Nup88
MOS8	Modifier of *snc1*, 8; also known as ENHANCED RESPONSE TO ABA 1 (ERA1)
MOS9	Modifier of *snc1*, 9
MOS10	Modifier of *snc1*, 10; also known as Topless-Related 1 (TPR1)
MOS11	Modifier of *snc1*, 11; homologous to the human RNA binding protein CIP29
MOS12	Modifier of *snc1*, 12; an Arabidopsis cyclin L homolog
MOS14	Modifier of *snc1*, 14; a nuclear importer of serine-arginine rich (SR) proteins
mRNP	messenger ribonucleoprotein
MS medium	Murashige and Skoog medium; a plant growth medium

NB-LRR	nucleotide binding-leucine rich repeat
NDR1	Non-Race Specific Disease Resistance 1
NES	nuclear export signal
NF-kB	nuclear factor kappa-light-chain-enhancer of activated B cells
NLR	Nod-like Receptor or nucleotide binding and leucine-rich repeat-containing R protein
NLS	nuclear localization signal or sequence
NOD	Nucleotide oligomerization domain
NPR1	NONEXPRESSER OF *PR* GENES 1
NTC	PRP Nineteen Complex
Nup107-160	nuclear pore subcomplex contributes to proper kinetochore functions
Nup214	nucleoporin 214kDa that functions in CRM1-Dependent Nuclear Protein Export
Nup88	nucleoporin 88kDa that functions in CRM1-Dependent Nuclear Protein Export
Nup96	nucleoporin 96kDa (often known by the name of its yeast homolog Nup145C); its Arabidopsis homolog is MOS3 (also known as SAR3)
O	oospores
OD	optical density
P0	a viral-coded F-box protein that function in suppressing Post-Transcriptional Gene Silencing (PTGS; an important antiviral defence system in plants)
p50	a 50 kDa TMV helicase fragment that induces the N-mediated HR in tobacco
PAD4	Phytoalexin Deficient 4
SDS-PAGE	sodium dodecyl sulfate polyacrylamide gel electrophoresis
PAMP	pathogen-associated molecular pattern
PEPC	Phosphoenolpyruvate carboxylase
PM	Plasma membrane
PR	pathogenesis-related
PRL1	Pleiotropic Regulatory Locus 1
PRR	pattern recognition receptor
Psm ES4326	*Pseudomonas syringae* pv. *maculicola* strain ES4326
Pst DC3000	*Pseudomonas syringae* pv. *tomato* strain DC3000
PTI	PAMP-triggered immunity
PUB	PLANT U-BOX
pv	Pathovar
qRT-PCR	Quantitative reverse transcriptase PCR
QS	quorum sensing
R	Resistance

RAR1	REQUIRED FOR *MLA12* RESISTANCE 1
RBS	Rubisco Small Subunit terminator
RBX	RING box protein 1; also known as Regulator of Cullin 1 (ROC1)
RGA1	REPRESSOR OF GA 1; a member of the DELLA protein family
RHC1	RING-H2 finger C1
RIN2	RPM1-interacting protein 2
RIN3	RPM1-interacting protein 3
RING	Really Interesting New Gene
RING1	a RING finger domain protein with E3 ligase activity
RLK	receptor-like kinase
RNAi	RNA interference
RPM1	RESISTANCE TO *P. SYRINGAE* PV *MACULICOLA* 1
RPP2	RECOGNITION OF *PERONOSPORA PARASITICA* 2
RPP4	RECOGNITION OF *PERONOSPORA PARASITICA* 4
RPP7	RECOGNITION OF *PERONOSPORA PARASITICA* 7
RPS2	RESISTANT TO *P. SYRINGAE* 2
RPS4	RESISTANT TO *P. SYRINGAE* 4
RPS5	RESISTANT TO *P. SYRINGAE* 5
RRS1	RESISTANT TO *RALSTONIA SOLANACEARUM* 1; also known as AtWRKY52 or SENSITIVE TO LOW HUMIDITY 1 (SLH1)
RT-PCR	reverse transcriptase PCR
Rx	Resistance against potato virus X
RxLR	a motif containing Arg, any amino acid, Leu, Arg, and is located on the N-terminal of secreted oomycete effectors
SA	Salicylic acid
SAG101	senescence-associated gene 101
SAR	systemic acquired resistance
SAR3	SUPPRESSOR OF AUXIN RESISTANCE 3; also known as MOS3 or AtNup96
SCF	Skp1-Cullin-F-box
SET	Drosophila Su(var)3-9, Enhancer of zeste [E(z)], and Trithorax
SGT1	Suppressor of G2 Allele of SKP1
SKP1	Suppressor of Kinetochore Protein 1
SNC1	suppressor of *npr1*, constitutive, 1
snc1-r1	the revertant mutant of *snc1* that has 10 nucleotides deleted in the first exon of *SNC1*
snc1-r3	the revertant mutant of *snc1* that has the entire *RPP4* cluster on chromosome 4 deleted
SON1	suppressor of *nim1-1*
SPL11	spotted leaf 11

SPX	SYG1/Pho81/XPR1; a protein domain usually exists at the N-terminal of a protein that has function in G-protein associated signal transduction
SR protein	serine-arginine rich proteins
SRFR1	SUPPRESSOR OF RPS4-RLD 1
STAND	signal transduction ATPases with numerous domains
TAC clone	transformation competent artificial chromosome; a modified version of bacterial artificial chromosome (BAC)
TCV	Turnip crinkle virus
T-DNA	transfer DNA
TGA2	TGACG Sequence-Specific Binding Protein 2
TGN	trans-Golgi network
TIR	Toll/interleukin-1 receptor
TIR1	transport inhibitor response protein 1
TMV	Tobacco mosaic virus
TN	trailing necrosis
TPL	TOPLESS
TPR1	TOPLESS-RELATED 1
TREX	TRanscription-EXport
TRN-SR	Transportin-SR
Ub	ubiquitin
UBA1	E1 ubiquitin-activating enzyme 1
UBC	E2 ubiquitin-conjugating enzyme
UBP	ubiquitin-specific protease
UPS	ubiquitin-26S proteasome system
VIGS	virus-induced gene silencing
VIP1	VirE2-interacting protein
VirE2	a type IV secreted protein from Agrobacterium that binds to single-stranded DNA and facilitate delivery of T-DNA to plant cells
VirF	an Agrobacterium type IV secreted F-box protein
WD40 repeat	also known as the WD or beta-transducin repeat; a short structural motif of approximately 40 amino acids, often terminating in a tryptophan-aspartic acid (W-D) dipeptide
WRKY domain	a 60-amino acid-protein domain defined by the conserved sequence WRKYGQK together with a zinc-finger-like motif
WT	wild type
Xa21	A rice resistance locus that confers disease resistance to *Xanthomonas oryzae* pv. *Oryzae*
XB3	XA21-binding protein 3
Xoo	*Xanthomonas oryzae* pv. *oryzae*
XPO1	Exportin 1

1 Literature Review – Introduction

1.1 Plant Immunity

1.1.1 Non-Host Resistance

Plants are constantly confronting pathogen challenges in nature. However, most of the plants are healthy most of the time; fatal diseases that kill an entire plant species are rare. This is due to the fact that over the long evolutionary period, plants have evolved sophisticated mechanisms to fight against a broad spectrum of pathogens.

The two types of plant-pathogen interactions are non-host and host. Non-host resistance is the resistance shown by an entire plant species against a specific pathogen. In the non-host interaction, plants have physical or chemical barriers, for example, the cuticle, plant cell walls, or antimicrobial secondary metabolites, present on the plant surface that prevent or stop pathogens from initiating an infection (Fan and Doerner, 2012). A number of studies also indicate that certain types of non-host defence might be active and involve vesicle trafficking (Collins et al., 2003; Lipka et al., 2005; Stein et al., 2006; Bednarek et al., 2009). The non-host defence, the molecular mechanisms of which remain largely unknown, provides robust protection to the entire plant species to all isolates of a pathogenic microbial species (Nurnberger and Lipka, 2005; Hardham et al., 2007).

1.1.2 Host Immunity

1.1.2.1 Recognition of Pathogens

In the host-pathogen interactions, pathogens are able to overcome and breach the physical or chemical barriers of the host plants. However, the attempted invasion can trigger a defence mechanism called the basal defence. The plants use trans-membrane pattern recognition receptors (PRRs), which are often receptor-like kinases (RLKs) to detect broadly conserved and indispensable components of microbe/pathogen-associated molecular patterns (MAMPs/PAMPs). Well-known examples of MAMPs are prokaryotic elongation factor-Tu (EF-Tu), flagellin, and lipopolysaccharide (LPS) of Gram-negative bacteria, glucans and glycoproteins from oomycetes, and chitin of fungal pathogens (Boller and Felix, 2009).

Over the past ten years, knowledge has been accumulated on a few PAMPs from pathogens and cognate plant receptors that can recognize them (Segonzac and Zipfel, 2011). Well-known PRRs in plants include: the flagellin receptor FLS2 and EF-Tu receptor EFR from Arabidopsis, chitin receptor CERK1 and CEBiP from Arabidopsis and rice, respectively, and rice Xa21 that recognizes Ax21 (activator of Xa21-mediated immunity) from *Xanthomonas* species and related genera (Monaghan and Zipfel, 2012).

Rice *Xa21* disease resistance locus that confers resistance to most strains of the Gram-negative bacterium *Xanthomonas* oryzae pv *oryzae (Xoo*) that causes bacterial blight has been identified almost 20 years ago (Song et al., 1995). *Xa21* encodes a receptor-like kinase consisting of leucine-rich repeats (LRRs) in the extracellular domain and a serine/threonine kinase in the intracellular domain. Later it was found that Xa21 recognizes a type I secreted sulfated peptide derived from the Ax21 (activator of Xa21-mediated immunity) (Lee et al., 2009). Secreted mature Ax21 acts as a quorum sensing (QS) factor in *Xoo* that is important for motility, biofilm formation and virulence (Han et al., 2011).

Another well-studied PRR-PAMP pair is FLS2 that has been identified in nearly all plant species tested so far, and flagellin, which is the building block of flagellum, an important structure for bacterial motility. FLS2 from the model plant Arabidopsis and rice Xa21 are both RLKs, and share sequence and structural similarities. FLS2 has extracellular LRR domain, a single membrane-spanning domain and an intracellular serine/threonine kinase domain. The extracellular LRR domain of FLS2 recognizes the presence of bacterial flagellin and activates defence responses through a series of mitogen-activated protein (MAP) kinase cascades via its kinase domain (Gomez-Gomez et al., 2001; Dunning et al., 2007).

1.1.2.2 Signalling Downstream of PRR

Perception of signature PAMPs by plant cell surface PRRs and activation of downstream defence responses is a quick process including ion fluxes across the plasma membrane (e.g. increase in Ca^{2+} influx) in 30 seconds to 2 minutes, oxidative burst within a few minutes, signal transduction via MAP kinase cascade and defence gene activation, callose deposition, stomatal closure and increased accumulation of plant defence hormone salicylic acid (Tsuda et al., 2008; Nicaise et al., 2009). Using flagellin, one of the best characterized PAMPs, more and more mechanistic details are unveiled about the signalling components and events downstream of PAMP-triggered immunity (PTI; [Block and Alfano, 2011; Segonzac and Zipfel, 2011]).

The described receptor-PAMP recognition triggers the defence responses to stop pathogens from colonization. Although the responses are relatively quick, the resistance activated by plants is relatively weak. This type of defence response is exerted regardless of species or races of pathogens. Because of its weak defence response, plants may develop disease symptoms under some conditions (Ingle et al., 2006; Bittel and Robatzek, 2007; Ma and Berkowitz, 2007; Underwood et al., 2007).

1.1.2.3 Suppression of PAMP-Triggered Immunity by Pathogen Effectors

Over evolutionary time, successful pathogens have acquired the ability to overcome PAMP-Triggered Immunity (PTI), a basal level of plant defence, by secreting virulent effectors and mounting successful invasion. For example, one of the studies on suppression of host PTI by a pathogen effector comes from the bacterial type III secreted effector, AvrPtoB (Munkvold and Martin, 2009). AvrPtoB is one of the effectors from *Pseudomonas syringae*. It contains a C-terminal E3 ligase domain that ubiquitinates plant PRRs FLS2 and CERK1, a fungal chitin

receptor that also plays a role in immunity against bacterial pathogens , and promotes their degradation (Gohre et al., 2008; Gimenez-Ibanez et al., 2009), leading to successful colonization.

1.1.2.4 Recognizing Effectors by Host Resistance Proteins

In the "arms race" between plants and pathogens, the selective pressure on host plants leads to the co-evolution of plant Resistance (R) proteins, which specifically recognize pathogen effectors, and trigger race-specific disease resistance, known as R protein-mediated resistance (the recognized effectors are also called Avirulent (Avr) factors as their presence can now trigger host immunity; [Chisholm et al., 2006; DeYoung and Innes, 2006; Jones and Dangl, 2006]). R protein-mediated resistance is believed to be an amplified version of the basal resistance (Tao et al., 2003; Thilmony et al., 2006; Truman et al., 2006). It exerts robust responses to fight against invading pathogens. In most cases, specific recognition of a pathogen attack triggers a series of local defence responses including generation of an oxidative burst, induction of ion exchange reaction, activation of defence gene expression, and ultimately culminates in a hypersensitive response (HR), a robust defence response that is caused by rapid programmed cell death at the site of infection (Nurnberger and Scheel, 2001; Greenberg and Yao, 2004). While the local plant tissue is battling against pathogens by R protein-mediated resistance, a danger signal is sent out to distal tissues to develop systemic resistance, known as systemic acquired resistance (SAR). As a result, the entire plant becomes more resistant to secondary infections (Durrant and Dong, 2004).

1.1.3 Plant R Proteins

R protein-mediated resistance is one of the most effective defence mechanisms in plants. The genetics of this kind of defence mechanism was first described by H. H. Flor in the 1940's. Flor's gene-for-gene model stated that the resistance phenotype can only be observed when the host plant carries a dominant *Resistance* (*R*) gene and the infecting pathogen carries a cognate dominant *Avirulent* (*Avr*) gene. The products of *R* genes probably recognize, either directly or indirectly, the presence of specific *Avr* gene products produced by the pathogen; this specific *R*-*Avr* recognition event, in turn, through complex signal transduction, elicits defensive responses observed as the resistant response.

Over time, plants evolved a large collection of structurally similar R proteins, which can recognize a wide array of Avr effectors (Bergelson et al., 2001). With a few exceptions, most plant R proteins belong to the intracellular nucleotide-binding leucine-rich repeat (NB-LRR) protein family. They are structurally very similar to animal Nucleotide Oligomerization Domain (NOD) immune receptors, and are referred to as Nod-like receptors (NLRs; or nucleotide-binding domain leucine-rich repeat containing proteins (Ting and Davis, 2005)).

Genome sequence analyses revealed that there are 149 NB-LRR encoding genes in the Arabidopsis genome (Meyers et al., 2003). The presence of the NB domain suggests that R protein activity may require ATP/GTP binding and/or hydrolysis which could result in conformational changes that regulate downstream signalling (Jiang and Wang, 2000; Harton et

al., 2002). The variable 20-30 amino acids-long leucine-rich motifs, which are present in proteins ranging from viruses to eukaryotes, have been known for providing structural framework for protein-protein interactions (Kobe and Kajava, 2001). The amino-termini of plant NB-LRR proteins are thought to be involved in activating downstream signalling pathways. Plant NB-LRR proteins can be divided into two subgroups based on their amino-termini. One group is the coiled-coil (CC) NB-LRR proteins that have an α-helix-rich N-terminus predicted to form coiled-coil structures. The other group is the TIR-NB-LRR class whose N-terminal domain has significant similarity to the Drosophila Toll and human interleukin-1 receptors (TIR) (Jebanathirajah et al., 2002; DeYoung and Innes, 2006). The wide range of the amino-terminal domains allows NB-LRR proteins to interact with different partners and to activate various signalling pathways (Aarts et al., 1998; Inohara et al., 2005).

1.1.3.1 R Protein Structure and Regulation

R protein-mediated plant immunity is a robust defence mechanism; however, an un-controlled defence response is detrimental to plant development and has a high fitness cost (Purrington, 2000; Heil and Baldwin, 2002; Heidel et al., 2004). Experimental evidence suggests that NB-LRR proteins are held in an auto-inhibited state through intra-molecular interactions (Rairdan and Moffett, 2006; Takken and Tameling, 2009; Du et al., 2012). Furthermore, proper R protein folding and stability are critical for its function (Kadota et al., 2010; Zhang et al., 2010).

The NB domain containing proteins are a subclass of the STAND superfamily proteins (Signal Transduction ATPases with Numerous Domains). Proteins of the STAND family are known to be involved in many biological processes including immunity, apoptosis (e.g. Apaf1 and CED4) and transcriptional regulation (Danot et al., 2009). At present, no crystal structure of a plant NB domain is available. With the help of structurally homologous proteins, Apaf1, CED4 and several STAND ATPases, it was predicted that plant NB domain forms a compact globular structure when the protein is in its resting state (Takken et al., 2006; Takken and Tameling, 2009).

The C-terminal LRR domain of plant NB-LRR proteins is the most variable region of the protein (McHale et al., 2006). Because of its highly rich polymorphisms (e.g. repeat lengths and non-canonical LRR motifs) among homologous NB-LRR proteins, it is hard to construct an accurate structural model based on a single template. Fortunately, with the abundant plant LRR structures in the protein database, the composite model of LRR structure is deduced to form a horseshoe-like shape (Sela et al., 2012).

Recently, the crystal structures of the CC domain for the NB-LRR R protein Mla10 from barley (Maekawa et al., 2011) and the TIR domain of the NB-LRR protein L6 from flax (Bernoux et al., 2011) have been solved. Each CC domain forms a helix-loop-helix structure and then two CC domains intertwine to form a tightly rod-shaped homodimer. The crystal structure of TIR domain of L6 shows a globular shape similar to the structure of the Arabidopsis protein consisting only of a TIR domain, AtTIR (At1g72930; Chan et al., 2010). Based on the crystal structures and the NB-LRR R protein mutant studies, it is believed that in the absence of pathogens, the NB-LRR proteins are kept in an auto-inhibited state by intra-molecular interactions between the different domains, but are, at the same time, exquisitely competent for detecting pathogen effectors. Release from inhibition by an effector or endogenous stress

stimulus triggers a series of conformational changes to initiate downstream defence signalling cascades (Takken et al., 2006; Takken and Tameling, 2009).

Besides the auto-inhibition by the structural constraints of the R proteins, these immune receptors are also regulated at two levels: 1) chaperone-assisted protein folding/maturation, and 2) control of NB-LRR levels by targeted protein degradation. Genetic screens that looked for components that are essential for R protein-mediated resistance uncovered a protein complex with three core members, RAR1 (Required for Mla12 Resistance 1), SGT1 (Suppressor of the G2 allele of SKP1) and HSP90 (Heat Shock Protein 90) as key players in regulating NB-LRR protein stability and activity (Shirasu et al., 1999; Warren et al., 1999; Austin et al., 2002; Azevedo et al., 2002; Muskett et al., 2002; Tör et al., 2002; Hubert et al., 2003; Takahashi et al., 2003). However, the mechanistic functions of the RAR1-SGT1-HSP90 complex in maintaining NB-LRR protein stability and activity remain elusive.

The involvement of SGT1 in R protein stability and the involvement of yeast SGT1 in Skp1-Cullin-F-box protein (SCF) ubiquitin ligases that target regulatory proteins for degradation (Kitagawa et al., 1999) suggest a route of R protein regulation through protein degradation.

1.1.3.2 R Protein Signalling

Several components have been shown to be involved in signalling downstream of an activated R protein. They are EDS1 (Enhanced Disease Susceptibility 1) and PAD4 (Phytoalexin Deficient 4) downstream of TIR-type R proteins (Wiermer et al., 2005) and NDR1 (Non-Race Specific Disease Resistance 1) in the CC-type R protein mediated resistance (Knepper et al., 2011) (Figure 1.1).

EDS1 and its interacting partner PAD4 are essential components of both basal and TIR-NB-LRR R proteins-mediated resistance in Arabidopsis (Feys et al., 2001). *EDS1* encodes a protein whose amino-terminus has similarities to eukaryotic lipases and it functions upstream of plant defence hormone salicylic acid (SA; Falk et al., 1999). *PAD4*, identified in a screen for phytoalexin deficiency in response to pathogen attack, encodes another lipase-like protein. PAD4 was also shown to have an important function in SA signalling (Jirage et al., 1999). In addition to their roles in signal transduction, EDS1 and PAD4 interaction is important in the positive feedback regulation of SA accumulation (Feys et al., 2001; Wiermer et al., 2005).

NDR1 was originally identified as a component in resistance against the virulent bacterial pathogen *Pseudomonas syringae* pv *tomato* DC3000 (*Pst* DC3000) in Arabidopsis (Century et al., 1997). Although the biochemical and cellular function of NDR1 remains elusive, several CC-type of NB-LRR proteins' function require NDR1, including RPS2, RPMl, RPS5 (Century et al., 1997; Knepper et al., 2011).

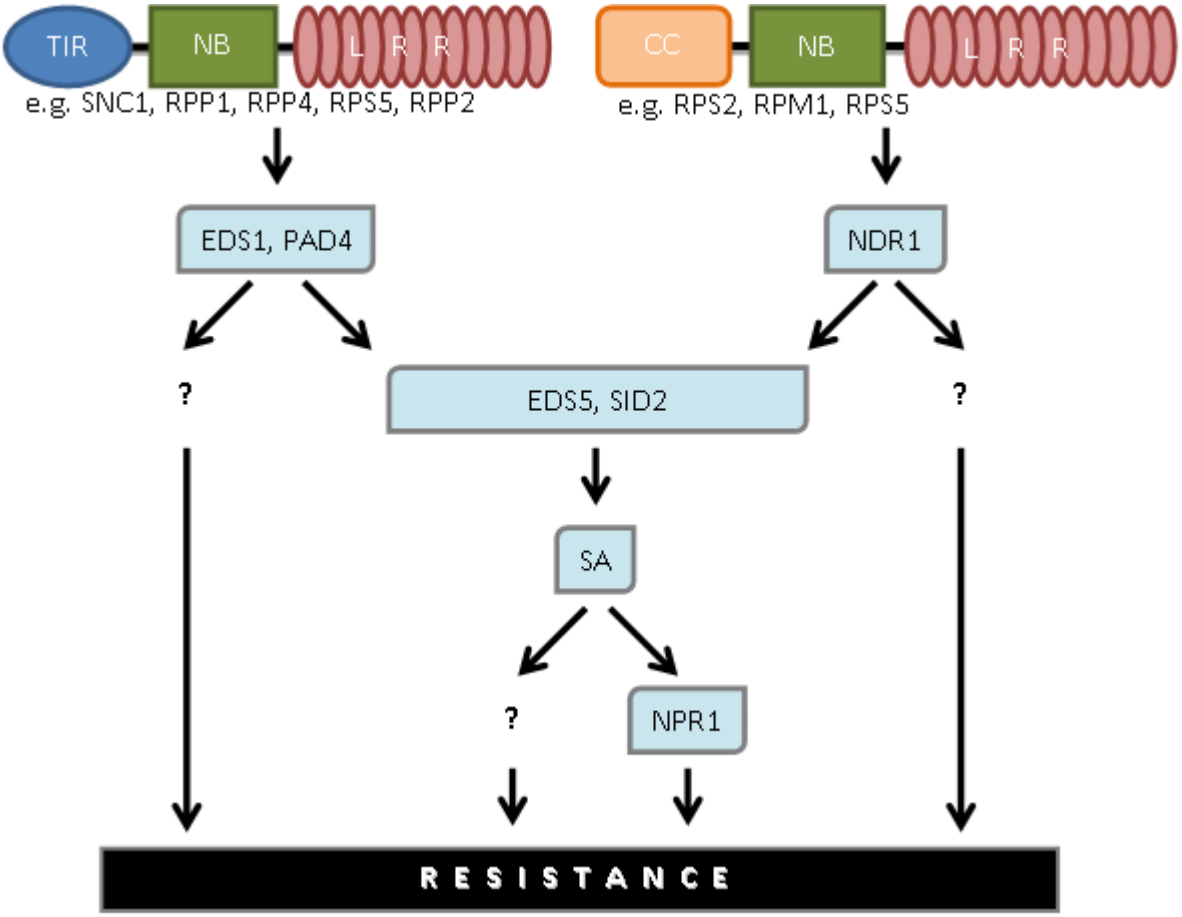

Figure 1.1: Signaling components downstream of TIR-type and CC-type NB-LRR R proteins.

1.2 Dissecting Plant Immunity Using *snc1* and Modifiers of *snc1* in Arabidopsis

1.2.1 *snc1*: A Unique Gain-of-Function Mutant of a TIR-Type NB-LRR R Protein

Genetic analysis of Arabidopsis mutants with impaired SAR response has led to the identification of a positive regulator of SAR, *NPR1* (*Non-Expresser of PR-1*) (Cao et al., 1994; Cao et al., 1997). Mutations in the *NPR1* gene abolish SA-induced *Pathogenesis-Related* (*PR*)-gene expression and resistance to pathogens, whereas overexpression of *NPR1* to enhance resistance to pathogens showed no obvious negative effects (Cao et al., 1998; Yuan et al., 2007).

A unique gain-of-function mutant, *suppressor of npr1-1, constitutive 1* (*snc1*) constitutively expresses *PR* genes and exhibits resistance against two virulent pathogens: the bacterial pathogen, *Pseudomonas syringae* pv *maculicola* ES4326 (*Psm* ES4326), and the oomycete pathogen, *Ha* Noco2 (Li et al., 2001) in the *npr1* mutant background. SNC1, an R protein of the TIR-NB-LRR class, is a member of the *Resistance to Peronospora parasitica 4* (*RPP4*) *R* gene cluster on chromosome IV in Arabidopsis ecotype Columbia. In *snc1*, a single amino acid substitution in the linker region between the NB and LRR domains renders the SNC1-mediated signal transduction constitutively active in the absence of pathogens (Zhang et al., 2003). Because *snc1* plants direct most of their energy toward defending against a non-existing pathogen, they have limited resources for other biological processes (Purrington, 2000; Heil and Baldwin, 2002; Heidel et al., 2004). As a result, the *snc1* plants have very unique morphological phenotypes, including small stature and curly leaves. In addition, a high level of SA was also detected in *snc1*, and it is partially responsible for the *snc1* phenotypes (Zhang et al., 2003a). Epistasis analysis of this dominant mutation showed that there are several important components of SNC1-mediated immunity, including EDS1 and PAD4 (Zhang et al., 2003).

The first plant *R* gene was cloned about twenty years ago (Johal and Briggs, 1992; Martin et al., 1993), yet little is known about the signalling components downstream of activated R proteins. To gain more insights on how danger signals are transduced from an activated R protein to downstream defence activation, a *snc1* suppressor screen was conducted.

1.2.2 The *MOS* Screen

Because of the distinct morphology of *snc1* and constitutive activation of defence response in this mutant that mimics an activated R protein-mediated resistance in the absence of a pathogen, *snc1* has become an extraordinary tool for dissecting the signalling required for defence activation. Genetic screens were performed to search for suppressors of *snc1*. Several mutagenesis methods including radiation mutagenesis by fast neutron bombardment, chemical mutagenesis by ethyl methanesulfonate (EMS) and Agrobacteria-mediated T-DNA mutagenesis were carried out in the *snc1* mutant background to screen for mutants that suppress or block *snc1* autoimmune phenotypes.

In the primary screen, putative mutants that lost the *snc1* small stature and stunted growth morphology, and restore close to wild type morphology, were selected. To validate that the

putative mutants that passed the primary screen are indeed defence-related mutants, the secondary screen was conducted to look for mutants that lost the enhanced *PR* gene expression and constitutive resistance against the virulent pathogen *Ha* Noco2. From these screens, several mutant alleles of *PAD4* were obtained, suggesting that the screens were successful. A total of fifteen *mos* (*modifier of snc1*) mutants were identified from the screens. These *mos* lines resulted in the identification of genes/proteins with functions in: 1) epigenetic regulation of *SNC1* transcription, 2) RNA processing and splicing, 3) nucleo-cytoplasmic trafficking of RNA molecules and proteins, 4) transcriptional regulation of defence related genes, and 5) protein modifications. The diverse array of MOS proteins identified from the *snc1* suppressor screens demonstrates the spatial and temporal complexity of plant defence signalling pathways required to activate robust and finely controlled resistance responses.

1.2.3 Modifiers of *snc1* (MOSes)

1.2.3.1 Epigenetic Regulation of SNC1 Transcription: MOS1

MOS1, the first MOS identified, is a HLA-B Associated Transcript 2 (BAT2) domain-containing protein that is conserved in plants and animals (Li et al., 2010b); none of the BAT2-containing proteins have been previously functionally characterized. Analysis of *snc1* transcription level in *mos1* revealed that *snc1* transcript is greatly reduced when *MOS1* is mutated, and this suppression of *snc1* expression by *mos1* can be released in the *Decrease in DNA methylation 1* (*DDM1*) mutant background. The *ddm1* mutant has drastically reduced levels of DNA methylation, and a change of H3K9 methylation (the ninth lysine residue of histone H3; a transcription repression mark) with H3K4 methylation (transcription activation mark; [Gendrel et al., 2002]). Further analysis revealed that DNA methylation is altered in the upstream region of endogenous *SNC1* in *mos1* mutant background; however, the expression level of *snc1* transgene is not affected, suggesting that MOS1 may function in regulating gene expression through chromatin remodelling. The identification and functional studies of MOS1 show that the expression level of *R* genes is under tight regulation (Li et al., 2010b; Li et al., 2011). Like MOS1, BAT2-containing proteins in other systems could also function in regulating gene expression through chromatin modification.

1.2.3.2 RNA Processing/Metabolism and Splicing Machinery: MOS2, MOS3, MOS4, MOS11, and MOS12

a) RNA processing: MOS2

mos2 is a partial suppressor of *snc1*. Unlike *mos1*, which has no defects in basal and R protein mediated resistance, *mos2* mutant plants are more susceptible to virulent pathogens and are compromised in R protein resistance mediated by RPM1, RPS4, and RPP4 (Zhang et al., 2005). Map-based cloning revealed that *MOS2* encodes a nuclear protein that contains a G-patch (glycine-rich nucleic acid binding domain) and two KOW (Kyprides, Ouzounis, Woese) domains.

G-patch is a conserved domain that has been shown to mediate RNA-protein interactions (Aravind and Koonin, 1999). KOW, another conserved domain, could function in protein-protein interactions (Steiner et al., 2002). The exact role that MOS2 plays in plant immunity remains elusive; however, the presence of G-patch and KOW domains suggests that MOS2 may function through binding to certain RNA molecules.

b) RNA splicing machinery: MOS4 and MOS12

RNA splicing is a process in eukaryotes that modifies nascent pre-messenger RNA (pre-mRNA) molecules by removing introns and adjoining exons to generate mature mRNA molecules for translation. Proper RNA splicing is not only essential for biological functions of a gene, but also generates alternative splice variants for proper spatial and temporal expression of a gene (Kelemen et al., 2013).

MOS4 is a conserved nuclear protein in both plant and animal kingdoms (Palma et al., 2007). Its homolog in humans is Breast Cancer-Amplified Sequence 2 (BCAS2). BCAS2 is a member of spliceosome-associated PRP Nineteen Complex (NTC) (Neubauer et al., 1998). Like BCAS2, MOS4 associates with NTC through direct interaction with AtCDC5 (Arabidopsis Cell Division Cycle 5), a key component of the NTC. Like mutation in *MOS4*, mutation in *AtCDS5* can also suppress the auto-immune phenotypes of *snc1*. Analyses of transcript variants in several alternatively spliced genes in *mos4* and *atcdc5* mutant backgrounds revealed that splicing patterns of *SNC1* and *RPS4*, two TIR-type NLR encoding genes, were altered, whereas the splicing patterns of several house-keeping genes were unaffected (Palma et al., 2007; Xu et al., 2012). This result suggests that MOS4 and AtCDC5 have specific roles in regulating splicing patterns of defence related genes.

Another MOS found to be involved in RNA splicing is MOS12 (Xu et al., 2012). MOS12 is a protein with two conserved cyclin domains at the N terminus. Its closest homolog in humans is cyclin L, which is required for pre-mRNA splicing (Loyer et al., 2008). Analysis of transcript variants in *mos12* mutant background found that the splicing patterns of *SNC1* and *RPS4* are changed. These changes in splicing pattern are associated with suppression of *snc1* autoimmune phenotypes and compromised RPS4-mediated immunity. Immunoprecipitation of MOS12 followed by western blot analysis showed that MOS12 associates with MOS4, consistent with the role of MOS12 in RNA splicing.

c) mRNA export: MOS3 and MOS11

Once the transcript of a gene is fully processed, it needs to be translocated from the nucleus to the cytoplasm for translation. This translocation process through the nuclear pore complex, which is highly conserved across eukaryotes, plays an important role in regulation of gene expression (Chinnusamy et al., 2008). Two MOS proteins identified in the suppressor screen, MOS3 and MOS11, are involved in mRNA export from the nucleus.

MOS3 (also known as NUP96 or SAR3) is a member of the Nup107-160 nuclear pore sub-complex (Zhang and Li, 2005; Parry et al., 2006). Mutations in *MOS3* lead to partial suppression of *snc1*'s autoimmunity and compromised basal immunity, as well as RPP4-, RPM1-, and RPS4-mediated immunity. In vertebrate and yeast cells, defects in the Nup107-160 complex result in the accumulation of mRNA within the nucleus (Fabre et al., 1994; Dockendorff et al., 1997; Vasu et al., 2001). A similar defect was also observed in *mos3*/*sar3* mutant plants (Parry et al., 2006; Germain et al., 2010).

MOS11 is a conserved eukaryotic protein; its homologous human protein is the RNA binding protein CIP29 (Germain et al., 2010). CIP29 is a member of the TREX (TRanscription-EXport) mRNA export complex (Dufu et al., 2010), which was first identified as a complex that functions in messenger ribonucleoprotein (mRNP) export (Reed, 2003). Like *MOS3*, mutations in *MOS11* lead to accumulation of mRNA within the nucleus (Germain et al., 2010). Epistasis analysis between *mos3* and *mos11* revealed that MOS3 and MOS11 might function in the same pathway (Germain et al., 2010). It is possible that MOS11 binds to mRNA molecules and facilitates their translocation from the nucleus, where they are generated, to the cytoplasm, where they are translated, through the Nup107-160 nuclear pore complex. Interestingly, although accumulation of poly(A) mRNAs was observed in the nucleus, null mutations of *MOS3* and *MOS11* are not lethal (Zhang and Li, 2005; Parry et al., 2006; Germain et al., 2010). This suggests that MOS3 and MOS11 may play roles in specifically exporting certain, likely defence related, mRNA molecules.

The identification of a large number of MOS proteins with roles in RNA processing and splicing in the *snc1* suppressor screen demonstrates the importance of RNA metabolism and translocation of mature mRNA molecules, from the nucleus to the cytoplasm, in plant defence signalling.

1.2.3.3 Nucleo-Cytoplasmic Trafficking: MOS6 and MOS14

Another class of MOS proteins identified are those involved in nucleo-cytoplasmic trafficking. MOS6 (Palma et al., 2005) is an essential component of the nuclear import machinery. *MOS6* encodes one of eight importin α homologs in Arabidopsis. The function of importin α is to recognize and facilitate the transport of proteins bearing nuclear localization signal (NLS) from the cytoplasm to the nucleus (Lange et al., 2007). One potential function of MOS6 is to recognize and import proteins involved in disease response signalling into the nucleus.

An additional MOS that plays a role in nucleo-cytoplasmic trafficking and defence is MOS14 (Xu et al., 2011). MOS14 is a nuclear protein that has high homology to animal Transportin-SR (TRN-SR) proteins. TRN-SR shows amino acid sequence homology to members of the importin β superfamily, and it functions specifically as the nuclear import receptor for serine-arginine rich (SR) proteins, which are important components of the pre-mRNA splicing machinery (Reed and Cheng, 2005). In *mos14* background, several SR proteins fail to properly localize inside the nucleus. Also, splicing patterns of two *R* genes, *SNC1* and *RPS4*, whose splicing patterns are important for their functions, are altered in *mos14*. Altered *snc1* and *RPS4* splicing patterns in *snc1 mos14* and *mos14*, respectively, all correspond with compromised SNC1- and RPS4-mediated defence responses.

Identification of essential components of the nuclear import machinery through the *snc1* suppressor screen reveals the importance of nuclear-cytoplasmic trafficking in plant innate immunity.

1.2.3.4 Transcriptional Repressor: MOS10

One unique *MOS* gene identified in the *snc1* suppressor screen was *MOS10* (also known as *TPR1; Topless-Related 1*). *MOS10* encodes a protein with an N-terminal Lissencephaly type-1-like homology (LisH) domain, a C-terminal to LisH (CTLH) domain and twelve WD (tryptophan-aspartic acid)-40 repeat at the C terminus (Zhu et al., 2010). MOS10 is closely related to Topless (TPL). TPL together with TRPs (TOPLESS-related proteins) are thought to be involved in transcription repression of auxin-dependent genes during embryogenesis (Long et al., 2006; Szemenyei et al., 2008). SNC1 is found to associate with MOS10/TPR1, and MOS10/TPR1 represses the expression of negative regulators of immunity, including *Defense no Death 1* (*DND1*) and *Defense no Death 2* (*DND2*) (Zhu et al., 2010). The identification of MOS10/TRP1 suggests that the expression of negative immune regulators needs to be repressed in R protein-mediated immune responses.

1.2.3.4 Protein Modifications: MOS5 and MOS8

mos8, another suppressor of *snc1* that completely abolishes resistance against virulent pathogens, identified a gene found to be allelic to *Enhanced Resistance to Abscisic acid 1* (*ERA1*). *ERA1* encodes the β subunit of plant farnesyl-transferase (Cutler et al., 1996). Protein farnesylation is a post-translational modification process that prenylates the carboxy-terminus of specific cellular signalling proteins (Sorek et al., 2009). The *era1* mutant phenotypes, first described by Pei et al. (1998), have prolonged seed dormancy and stomatal closure due to an enhanced response to abscisic acid (ABA). *mos8* plants have enhanced susceptibility to virulent bacterial pathogen *Psm* ES4326 and oomycete pathogen *Ha* Noco2, indicating the importance of prenylation in basal resistance. Responses to avirulent pathogens mediated by R proteins of RPM1, RPS4 and RPP4, are partially compromised in *mos8*, demonstrating the involvement of prenylation in the highly divergent pathogen-specific signalling pathways (Goritschnig et al., 2008).

MOS5 encodes UBA1, one of two ubiquitin-activating (E1) enzymes in Arabidopsis (Goritschnig et al., 2007). *mos5* mutant plants exhibit somewhat enhanced disease susceptibility, indicating a minor involvement of *MOS5* in basal resistance against virulent bacterial pathogens. Also, mutations in *MOS5* compromise the RPS2-mediated resistance but not resistance mediated by other R proteins tested (RPM1 and RPS4). This differential susceptibility to avirulent pathogens suggests that ubiquitination pathway mediated by MOS5 is required in activation and downstream signalling of certain R proteins (Goritschnig et al., 2007). The identification of MOS5 in the *snc1* suppressor screen, as well as other defence related components of the ubiquitination pathway by other research groups, suggest that protein ubiquitination plays an important role in plant immunity.

1.3 Ubiquitination in NB-LRR R Protein-Mediated Immunity[1]

1.3.1 Introduction

Ubiquitination is a common protein modification where the 76-amino-acid ubiquitin (Ub) moiety is covalently attached to the lysine (Lys) residues of a substrate protein. More than 5% of the Arabidopsis proteome is predicted to be involved in the ubiquitination-26S proteasome pathway (Smalle and Vierstra, 2004), suggesting that this pathway plays essential roles in diverse biological processes and cellular signalling. The consequences of ubiquitination vary and often depend on the ubiquitination site of the substrate, the position of the Lys in the Ub moiety being utilized, and the length of the Ub attachments. Monoubiquitination is usually associated with endocytosis or histone modification (Schnell and Hicke, 2003; Umebayashi, 2003; Weissman et al., 2011). By contrast, polyubiquitination with four or more Ubs typically results in the targeting of the substrate for degradation by the 26S proteasome, although it can occasionally activate the protein (Thrower et al., 2000; Pickart and Fushman, 2004; Sun and Chen, 2004). After degradation of the protein substrate by the proteasome, Ubs are recycled through deubiquitinating enzymes (DUBs). DUBs counteract ubiquitination and play a key role in determining the fate and activities of the target substrates. Thus, besides their housekeeping roles, DUBs may potentially regulate signal transduction through monitoring the balance of their ubiquitinated and non-ubiquitinated protein substrates (Komander et al., 2009).

The covalent attachment of Ub is a multi-step biochemical reaction performed by an ATP-dependent conjugation cascade involving an E1 (Ub-activating enzyme, UBA), an E2 (Ub-conjugating enzyme, UBC), and an E3 (Ub ligase) (Weissman, 2001; Smalle and Vierstra, 2004). Substrate specificity is mainly determined by the E3s, therefore it is not surprising that the Arabidopsis genome encodes only two E1s and 37 E2s, but 1415 E3s (Kraft et al., 2005). The E3s can be further subdivided into six classes depending on their different conserved domains and mode of action (Figure 1.2A and 1.2B). HECT, RING-type, and U-box proteins are simple E3s that can work alone with an E1 and an E2. The transfer of Ub by the RING or U-box E3s is direct and does not involve ubiquitination of the E3, while HECT E3s are ubiquitinated first before transferring the Ub to the substrate. There are also more elaborate E3s that are composed of protein complexes with multiple components that are often Cullin-based (Figure 1.2B) (Vierstra, 2009; Hua and Vierstra, 2011). The best known complex E3s in plant biology contain F-box proteins. In Arabidopsis, there are over 700 F-box protein-encoding genes, which function in almost all biological processes (Somers and Fujiwara, 2009).

[1] A version of this section has been published. Yu Ti Cheng and Xin Li. (2012) Current Opinion in Plant Biology 15: 392–399

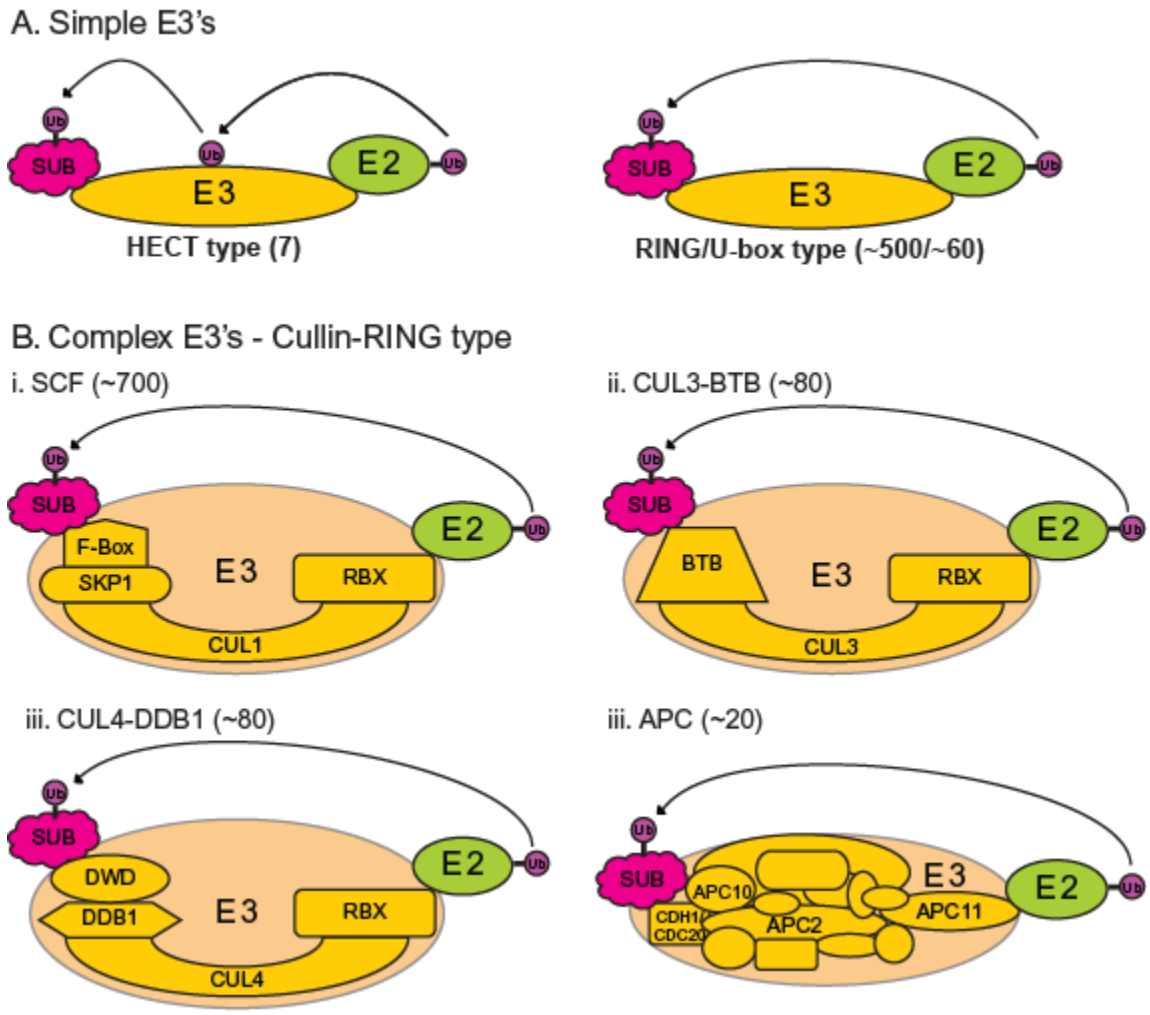

Figure 1.2: Ubiquitination pathway and different classes of E3s.

(A) Diagrams of the simple E3s and their different modes of actions. HECT (Downes et al., 2003), RING-type (Kraft et al., 2005; Stone et al., 2005), and U-box (Yee and Goring, 2009) proteins can work alone with the E1 and E2. The transfer of Ub by the RING or U-box E3s is direct, while that by HECT E3s is indirect. The RING finger (also called zinc finger) domain is stabilized by Zn^{2+} in coordination with its Cys and His residues, while the U-box is mostly stabilized through salt-bridges and hydrogen bonds.

(B) Complex E3s, which are often Cullin-based.
The number of different E3-encoding genes predicted in the Arabidopsis genome is in parentheses along with the E3 types (Capron et al., 2003; Gingerich et al., 2005; Lee et al., 2008; Hua et al., 2011).

1.3.2 E3s in R Protein-Mediated Immunity

E3s are the major specificity determinants in ubiquitination reactions. A number of E3s are implicated in the regulation of plant immunity (Table 1.1A). These E3s were typically identified from analysis of knockout or over-expression phenotypes of the encoding genes. In most cases, the target proteins of the E3s are unknown which makes it difficult to define the exact roles of these E3s in the regulation of plant defence.

1.3.2.1 Light Regulation of R Protein Stability

Light is required for resistance against turnip crinkle virus (TCV) mediated by the Arabidopsis NB-LRR R protein HRT (Jeong et al., 2010). Analysis of HRT protein levels under different light conditions showed that its stability is regulated by light. HRT proteins are degraded under dark or blue-light induction, resulting in susceptibility to TCV. Blue-light-dependent HRT degradation can be blocked by the proteasome inhibitor MG132, indicating that the degradation of HRT is 26S proteasome-specific. Although HRT interacts with the E3 ligase COP1, the exact role of COP1 in HRT1 degradation remains to be determined. Regulation of the HRT levels by protein degradation raises interesting questions on whether other plant growth parameters, such as humidity and temperature, could also affect the stability of NB-LRR R proteins.

1.3.2.2 F-Box Protein ACIF1 in R Protein-Mediated Immunity

ACRE189/ACIF1 is an F-box protein with LRR repeats identified from the Avr9/Cf-9 Rapidly Elicited (ACRE) screen in tomato. It was shown to be recruited to Skp1-Cullin-F-box (SCF) E3 ubiquitin ligase complexes. Silencing of tobacco ACIF1 suppresses the HR responses by various elicitors such as Avr9, Avr4, AvrPto, Inf and the p50 helicase of *Tobacco mosaic virus*. Silencing of ACIF1 in tomato attenuates Cf-9-dependent HR, but not Cf-9-mediated resistance, suggesting that ACIF1 targets a negative regulator of HR for degradation (van den Burg et al., 2008). Future identification of the target protein of ACIF1 may help us better understand how HR is activated during R protein-mediated defence responses.

1.3.2.3 MAC3A/MAC3B in the Splicing of R Genes

Arabidopsis MAC3A and MAC3B are two redundant U-box E3 ligases homologous to yeast and human PRP19, implicated in mRNA splicing. MAC3 is a core member of the MOS4-associated complex (MAC) containing MOS4, AtCDC5, PRL1, MAC5 and other proteins (Monaghan et al., 2009). Knocking out both *MAC3A* and *MAC3B* phenocopies *mos4,* and not only suppresses autoimmunity mediated by *snc1*, but also attenuates resistance mediated by other R proteins. The MAC was recently found to associate with MOS12, a cyclin L homolog that is critical for

splicing (Xu et al., 2012). Splicing patterns of TIR-NB-LRR-type *R* genes *SNC1* and *RPS4* are altered in *mos12-1*, *mos4*, *Atcdc5* mutants, as well as *mac3a mac3b*, indicating that MOS12 and the MAC regulate proper splicing of target *R* genes. How the MAC3 E3 controls *R* gene splicing remains unclear. Future identification of the MAC3 targets will help us illuminate its role in splicing regulation.

1.3.2.4 Other E3s

Arabidopsis BAH1 and Pepper RING1 (CaRING1) are two RING-type E3s recently shown to be involved in regulating plant immunity (Lin et al., 2008; Lee et al., 2011). However, their mode of action and therefore their contribution to R protein-mediated resistance remains to be determined.

CaRING1 exhibits E3 ligase activity and localizes to the plasma membrane. It is induced by *Xanthomonas* infection. VIGS silencing of *CaRING1* causes enhanced susceptibility, reduced *Pathogenesis-Related* (*PR*) gene expression and decreased salicylic acid accumulation, while over-expression of *CaRING1* enhances resistance to both *Pseudomonas* and oomycete pathogens. These data suggest that the CaRING E3 probably targets a negative regulator of defence for degradation. When *CaRING1* is silenced, the negative regulator accumulates and causes enhanced susceptibility (Lin et al., 2008; Lee et al., 2011).

BAH1 encodes an E3 ligase with RING and SYG1/Pho81/XPR1 (SPX) domains of unknown function. It was identified from a forward genetics screen searching for mutants hypersensitive to benzoic acid, which was suggested to contribute to Isochorismate Synthase 1 (ICS1)-independent SA synthesis. The *bah1* mutant plants accumulate higher SA after bacterial infection and are more resistant to pathogen infections. SA accumulation in *bah1* is only partly dependent on *ICS1* (Yaeno and Iba, 2008). So far, there is no biochemical data supporting its E3 ligase role. Whether it targets a positive regulator of SA synthesis for degradation remains to be determined.

1.3.2.5 Components Associated with E3: SRFR1 and SGT1 in Stability Control of NB-LRR R Proteins

SRFR1 is a protein involved in the regulation of NB-LRR R protein-mediated defence responses (Kim et al., 2010; Li et al., 2010a; Bhattacharjee et al., 2011). The *srfr1* mutant plants display constitutive defence responses. The constitutive defence responses in *srfr1* can be largely suppressed by loss-of-function mutations in *SNC1*. SRFR1 associates with SNC1, RPS4 and RPS6 *in planta* (Kim et al., 2010; Li et al., 2010a; Bhattacharjee et al., 2011). In *srfr1* mutants, levels of multiple NB-LRR R proteins, including SNC1, RPS2 and RPS4, are increased (Li et al., 2010a), suggesting that SRFR1 functions in the negative regulation of NB-LRR R protein accumulation.

SGT1 was originally identified as a co-chaperone of HSP90. The HSP90-RAR1-SGT1 chaperone complex is required for proper folding and accumulation of NB-LRR R proteins (Shirasu, 2009). Surprisingly, a deletion mutant of SGT1b can suppress the reduced accumulation and loss of function of the NB-LRR R protein RPS5 in *rar1* (Holt et al., 2005).

SGT1 also interacts with SRFR1 (Li et al., 2010a). Like in *srfr1* mutants, the SNC1 protein level is similarly increased in *sgt1b*, suggesting that SRFR1 and SGT1 function together to negatively regulate the SNC1 protein levels (Li et al., 2010a). In yeast, SGT1 is a member of the SCF complex (Kitagawa et al., 1999). SGT1 was also found to associate with components of the SKP1-Cullin1-F-box (SCF) complex in plants (Liu et al., 2002). Thus, it is likely that SGT1 and SRFR1 serve as chaperones or scaffolds in the SCF complex to target a group of R proteins. They may also be critical in determining the substrate specificity of SCF complex through their protein-protein interaction interface.

1.3.3 E1s and E2s in R Protein-Mediated Immunity

Arabidopsis has two E1s, UBA1/MOS5 and UBA2. The *mos5* mutant was identified in a suppressor screen of *snc1* (Goritschnig et al., 2007). It is required for *snc1*-mediated defence responses. The *mos5* mutant plants also have defects in resistance specified by the NB-LRR R protein RPS2, and display enhanced disease susceptibility. While *uba2* single mutant plants have no obvious phenotypes, the *mos5 uba2* double mutant is lethal, indicating that UBA1 and UBA2 have partially redundant functions. In the Arabidopsis genome, there are 37 E2s. No individual E2s have been identified to be required for the regulation of plant immunity, suggesting high levels of redundancy among these E2 enzymes.

A requirement for MOS5 in resistance mediated by SNC1 suggests the existence of at least one E3 functioning as a positive regulator of defence responses in *snc1*. It either targets a key negative regulator(s) for degradation or activates a positive regulator by mechanisms like monoubiquitination. Since E1 participates in a large number of ubiquitination reactions, *mos5/uba1* probably affects the stability of many proteins targeted by different E3s.

1.3.4 DUBs in R Protein-Mediated Immunity

In Arabidopsis, the 27 ubiquitin-specific proteases (UBPs) form one of the largest classes of de-ubiquitinating enzymes (DUBs) (Yan et al., 2000). Like the E2s, they fall into distinctive subfamilies of two to five members, suggesting a high level of redundancy. Only one pair of UBPs, UBP12 and UBP13, have been implicated in plant immunity (Ewan et al., 2011). Loss of both UBP12 and UBP13 leads to seedling lethality, indicating a crucial role for these proteins in plant growth and development. In Arabidopsis, the RNAi-co-silenced *UBP12/UBP13* plants exhibit enhanced *PR* gene expression and disease resistance against virulent *Pseudomonas* bacteria. In tobacco, silencing the *UBP12* homolog *NtUBP12* leads to increased Cf-9-mediated HR, while overexpression of *AtUBP12* or *NtUBP12* suppresses the HR response. These data suggest that UBP12/13 has a conserved function in regulating plant defence responses.

The targets of UBP12/13 that are involved in regulating plant defence remain to be determined. Since UBPs de-ubiquitinate their targets, reduction of the activity of UBP12/13 should lead to increased ubiquitination and degradation of target proteins. Thus, the target proteins of UBP12/13 are most likely negative regulators of plant immunity. Because the

ubiquitinated form of a target sometimes is the active form of the protein, it is also possible that UBP12/13 is involved in de-ubiquitination of a positive regulator of plant immunity.

1.3.5 Conclusions and Perspectives

In recent years, ubiquitination has emerged as one of the key mechanisms involved in regulating NB-LRR R protein-mediated plant defence responses. At the level of the immune receptor, control of the stability of NB-LRR proteins by SCF-mediated protein degradation appears to be critical for preventing over-accumulation of the receptors and constitutive activation of immune responses without the presence of pathogens. Downstream of plant R proteins, increasing evidence suggests that ubiquitin-26S proteasome system (UPS) is also critical for both positive and negative regulation of defence responses. As ubiquitination-mediated protein degradation leads to rapid changes in protein levels in response to stimuli, it could be used to regulate the stability of many downstream components of NB-LRR proteins.

Among the 1415 E3s in Arabidopsis, most are still without an assigned biological function, perhaps due to redundancy and/or subtle E3 mutant phenotypes that are difficult to observe. Many of these E3s may potentially be involved in plant immunity. Future research using targeted reverse genetics approaches and carefully-designed novel forward genetic screens may enable us to find these elusive E3 regulatory components of plant immunity and decipher how they control the defence output in response to pathogen attack. As always, one of the biggest challenges is to find the protein substrates of the E3s involved in plant immunity. New methods, such as global protein stability profiling (Yen and Elledge, 2008), can potentially be adapted for use in plants to address this predicament.

1.3.6 Manuscript Acknowledgements

We cordially thank members of Dr. Jane Parker's laboratory (Servane Baufumé, Katharina Heidrich and Dr. Jane Parker), Dr. Yuelin Zhang and Ms. Kaeli Johnson for careful reading of the manuscript. Research in the authors' laboratory is supported by Natural Sciences and Engineering Research Council (NSERC) Discovery grant program from Canada and the William Dewar Cooper Endowment Fund of UBC Botany Department.

Table 1.1: List of E3 ubiquitin ligases from plants and pathogens that have been shown to play roles in plant immunity.

a) Plant E3s that have been shown to be involved in ETI. PM: Plasma membrane, TGN: trans-Golgi network.

Name	Type of E3	Substrates	Positive (+) or negative (-) regulation	Localization	References
CMPG1/ACRE74	U-box		+		(Gonzalez-Lamothe et al., 2006; Bos et al., 2010)
RHC1	RING-type		+	PM	(Cheung et al., 2007)
DRF1	F-box		+		(Cao et al., 2008)
ACIF1/ACRE189	F-box		+		(van den Burg et al., 2008)
RIN2/RIN3	RING-type		+	PM	(Kawasaki et al., 2005)
RING1	RING-type		+	PM	(Lin et al., 2008; Lee et al., 2011)
PRP19/MAC3	U-box		+		(Monaghan et al., 2009)
HUB1	RING-type	H2B	+		(Dhawan et al., 2009)
ACRE276/PUB17/ ARC1	U-box		+		(Yang et al., 2006)
SON1	F-box		–		(Kim and Delaney, 2002)
BAH1/NLA	RING-type		–		(Yaeno and Iba, 2008)
COP1	CUL4-RING	HRT	–	Nucleus	(Jeong et al., 2010)
SPL11	U-box		–	Entire cell	(Zeng et al., 2004)
KEG	RING-type		– in ABA signaling	TGN	(Stone et al., 2006; Gu and Innes, 2011)

b) Plant E3s that are involved in PTI.

Name	Type of E3	Substrates	+/–	Localization	References
HP1/DDB1	CUL4-DDB1		+		(Liu et al., 2012)
BBI1	RING-type		+		(Li et al., 2011)
XB3	RING-type		+		(Wang et al., 2006)
ATL9	RING-type		+	ER	(Berrocal-Lobo et al., 2010)
PUB22/PUB23/PUB24	U-box		–	cytosol	(Trujillo et al., 2008)
PUB12/PUB13	U-box	FLS2	–		(Lu et al., 2011)

c) Pathogen E3s or proteins from pathogen that target host E3s to promote disease in the host plant.

Name	Organism	Type of E3/Protein	Substrates	References
Avr3a	*P. infestans*	RxLR containing secreted effector protein	CMPG1	(Bos et al., 2010; Yaeno et al., 2011)
AvrPtoB	*P. syringae pv tomato*		CERK1, Fen, FLS2	(Gohre et al., 2008; Gimenez-Ibanez et al., 2009)
VirF	*Agrobacterium*	F-box	VIP1 VirE2	(Tzfira et al., 2004)
P0	*Polerovirus*	F-box	AGO1	(Baumberger et al., 2007)

1.4 Thesis Objectives

The *snc1* suppressor screen has uncovered a number of novel players in plant immunity. **The primary aim of this thesis research was to positionally clone and perform functional studies on two *MOS* mutants, *mos7* and *mos9*, identified in the *snc1* suppressor screen.** *mos7* and *mos9* were identified from the same mutagenized *snc1* population generated using fast neutron bombardment. By studying the functions that MOS7 and MOS9 play in plant immunity, we hope to gain better insights in how plants, which are sessile organisms, strive for survival by responding rapidly to pathogenic microbial invasions.

While studying MOS7 and MOS9, a paper published in the Plant Journal by Dr. Guoying Wang's group (Gou et al., 2009) attracted our attention. This study described an F-box protein encoding gene, *CPR30*, which plays a negative role in plant defence. Prior to this study little was known about how stability of plant R proteins is controlled, and there were very few reports on the relationship between ubiquitin-proteasome pathway and plant immunity. The data of Guo et al. (2009) suggested that SNC1 may be a target of CPR30. This interesting finding prompted me to further pursue the role CPR30 plays in plant immunity, and led to the third objective of my thesis research: **to understand how SNC1 stability is controlled and the function of CPR30 in plant immunity**.

2 Nuclear Pore Complex Component MOS7/Nup88 is Required for Innate Immunity and Nuclear Accumulation of Defence Regulators in Arabidopsis[2]

2.1 Introduction

Innate immunity in plants against microbial pathogen infection is a dynamic process that requires stimulus-dependent spatial and temporal action of its defence regulatory components. One of the most effective disease resistance mechanisms is mediated by resistance (R) proteins. Upon infection, an R protein recognizes a specific pathogen effector (termed Avirulence [Avr] protein) and mounts a fast and robust response leading to a local hypersensitive response, a form of programmed cell death, to restrict pathogen growth and spread (Jones and Dangl, 2006). Many *R* genes have been cloned and the majority encodes proteins containing NB-LRR domains in which the NB is a central nucleotide binding site and LRRs are C-terminal leucine-rich repeats. There are two subclasses of NB-LRR proteins, varying according to their N termini (Martin et al., 2003; Belkhadir et al., 2004; McHale et al., 2006). TIR-NB-LRR type R proteins carry an N-terminal Toll interleukin receptor (TIR) domain, while the CC-type has a predicted coiled-coil domain (also called leucine zipper domain) at its N terminus. These two NB-LRR classes differ in their initial mode of signalling since TIR-NB-LRR proteins activate resistance and cell death through EDS1/PAD4/SAG101 (for Enhanced Disease Susceptibility1/Phytoalexin-Deficient4/Senescence Associated Gene 101) complexes, whereas CC-NB-LRR proteins commonly use NDR1 (for Non Race-Specific Disease Resistance1) (Century et al., 1997; Aarts et al., 1998; Feys et al., 2005; Wiermer et al., 2005). NDR1 associates with the plasma membrane, while EDS1 interacts with PAD4 and SAG101 in distinct complexes in the cytosol and nucleus (Coppinger et al., 2004; Feys et al., 2005). Downstream of EDS1 and NDR1, pathways converge at the synthesis of the defense hormone salicylic acid (SA), a sufficient and necessary signal for systemic acquired resistance (SAR) (Vernooij et al., 1994). SAR represents systemic responses induced throughout the plant to enhance resistance. NPR1 (for Nonexpresser of *PR* genes 1) is a key positive regulator of SAR whose monomerization and nuclear accumulation is essential for its activity in stimulating defence gene expression (Cao et al., 1997; Mou et al., 2003; Tada et al., 2008).

The detailed biochemical functions of NB-LRR proteins have started to emerge in recent years. They are normally under tight negative control, but upon infection, the release of repression seems to be the driving force for the resistance responses. For example, the *Arabidopsis thaliana* defence modulator RPM1-interacting protein 4 (RIN4) negatively regulates two different CC-NB-LRR type R proteins, RPM1 and RPS2 (Mackey et al., 2002; Axtell and Staskawicz, 2003; Mackey et al., 2003; Kim et al., 2005). Although most NB-LRR proteins are predicted to be cytosolic (Jones and Dangl, 2006), the CC-NB-LRR class proteins MLA1 and MLA6 localize partially to and function inside the nucleus (Shen et al., 2007). Upon infection, recognition of its cognate fungal effector induces MLA interaction with repressive WRKY

[2] A version of this chapter has been published. Yu Ti Cheng, Marcel Wiermer, Hugo Germain, Dongling Bi, Fang Xu, Ana V. Garcia, Lennart Wirthmueller, Charles Despres, Jane E. Parker, Yuelin Zhang, and Xin Li. (2009) *The Plant Cell* 21:2503-2516.

transcription factors, leading to deregulation of downstream defense gene expression. Also, the TIR-type NB-LRR proteins, N in tobacco (*Nicotiana tabacum*) and RPS4 in Arabidopsis, need to accumulate in nuclei to function (Burch-Smith et al., 2007; Wirthmueller et al., 2007). These recent discoveries suggest there may be a general requirement for nuclear localization of R proteins or their downstream signalling components in R-mediated resistance.

Previous studies of MOS3 (for Modifier of *snc1*,*3*; Zhang and Li, 2005), MOS6 (Palma et al., 2005), and RanGAP2 (Sacco et al., 2007; Tameling and Baulcombe, 2007) reveal the importance of two nucleocytoplasmic trafficking pathways in plant innate immunity: mRNA export and nuclear localization signal (NLS)-dependent nuclear protein import. It is not known whether other nucleocytoplasmic trafficking machineries, such as the one governing nuclear export signal (NES)-mediated nuclear protein export, contribute to plant disease resistance. MOS3/NUP96/SAR3 is required for mRNA export (Dong et al., 2006; Parry et al., 2006), and mutations in *MOS3* confer enhanced susceptibility to both virulent and avirulent pathogens. Also, mutations in *MOS6*, an Importin α homolog responsible for importing proteins with an NLS to the nucleus, compromise plant defense against pathogen infection. RanGAP2, another component of the protein nuclear import machinery, interacts with the NB-LRR protein Rx, and silencing of *RanGap2* impairs Rx-mediated resistance (Sacco et al., 2007; Tameling and Baulcombe, 2007).

Both MOS3 (Zhang and Li, 2005) and MOS6 (Palma et al., 2005) were identified in a forward genetic screen aimed at finding components that function downstream of R protein activation. In *snc1* (for *suppressor of npr1-1, constitutive 1*), a point mutation resulting in an E-to-K change in the linker region between the NB and LRR of an *RPP4* homolog, renders this TIR-type R protein constitutively active without pathogen recognition (Zhang et al., 2003a). As a consequence, *snc1* mutant plants are dwarf, accumulate high levels of SA, and exhibit enhanced disease resistance against virulent pathogens (Li et al., 2001; Zhang et al., 2003a). As a TIR-NB-LRR protein, *snc1* was accordingly found to be fully dependent on EDS1/PAD4, whose nucleocytoplasmic partitioning and complex formation is probably under tight control (Feys et al., 2005; Wiermer et al., 2005).

In this study, we report the isolation, positional cloning, and detailed functional analysis of *MOS7.* A partial loss-of-function mutation, *mos7-1*, suppresses *snc1* autoimmune phenotypes, while complete loss of *MOS7* in *mos7-2* and *mos7-3* mutants causes lethality. In the *mos7-1* single mutant, basal defence against virulent pathogens, local resistance conditioned by several TIR- and CC-type NB-LRR R proteins, and SAR responses are impaired. *MOS7* encodes a protein homologous to the human Nup88 nucleoporin. In *Drosophila melanogaster* and human, mutations in Nup88 enhance CRM1 (for Chromosomal Region Maintenance 1; also named Exportin 1; XPO1)-dependent nuclear export of activated NF-κB transcription factors (Roth et al., 2003; Xylourgidis et al., 2006). In this study, we establish that MOS7 is required for appropriate nuclear accumulation of the autoactivated R protein snc1, as well as the downstream defence signalling components EDS1 and NPR1.

2.2 Results

2.2.1 Identification of the *mos7-1* Mutant

The *mos7-1* mutant was identified from a MOS (modifier of *snc1*) forward genetic screen with fast neutrons, as described earlier (Zhang and Li, 2005). *snc1* plants have a stunted stature and curly leaves due to constitutive defense activation (Zhang et al., 2003a). The suppressor screen was designed to search for mutants that resemble wild-type morphology and abolish constitutive pathogen resistance in *snc1*. *mos7-1 snc1* double mutant plants are larger than *snc1* plants (Figure 2.1A). In *snc1* plants, several *Pathogenesis Related* (*PR*) defense marker genes are constitutively expressed. Analysis using RT-PCR showed that *PR-1* and *PR-2* expression was suppressed in *mos7-1 snc1* compared with *snc1* (Figure 2.1B).

snc1 plants exhibit enhanced resistance against virulent pathogens, including the bacterium *Pseudomonas syringae* pv. *maculicola* (*Psm*) ES4326 and the oomycete pathogen *Hyaloperonospora arabidopsidis* (*H.a.*; previously named *Peronospora parasitica* or *Hyaloperonospora parasitica*) Noco2 (Zhang et al., 2003a). To determine whether the *mos7-1* mutation alters the *snc1* autoimmune response, we inoculated *mos7-1 snc1* double mutant plants with these pathogens. As shown in Figures 2.1C and D, *mos7-1 snc1* double mutants had lost enhanced resistance to both pathogens. Bacterial growth in *mos7-1 snc1* was even higher than in wild-type plants (Figure 2.1D).

SA levels are elevated in the *snc1* mutant (Li et al., 2001). To determine whether *mos7-1* affects SA accumulation in *snc1*, SA was extracted and measured from *mos7-1 snc1* plants. As shown in Figures 2.1E and F, levels of free and total SA in *mos7-1 snc1* were similar to those of wild-type plants and approximately fourfold lower than in *snc1*. Therefore, *mos7-1* fully suppresses all known autoimmune phenotypes of *snc1*.

When *mos7-1 snc1* was backcrossed with *snc1*, the F1 progeny had *snc1* morphology. Of 40 F2 plants, 28 were *snc1*-like, whereas 12 were wild type–like. The 1:3 wild type to *snc1*-like ratio ($\chi^2 = 0.53$; $P > 0.1$) together with the F1 phenotype are consistent with *mos7-1* being a single, recessive nuclear mutation.

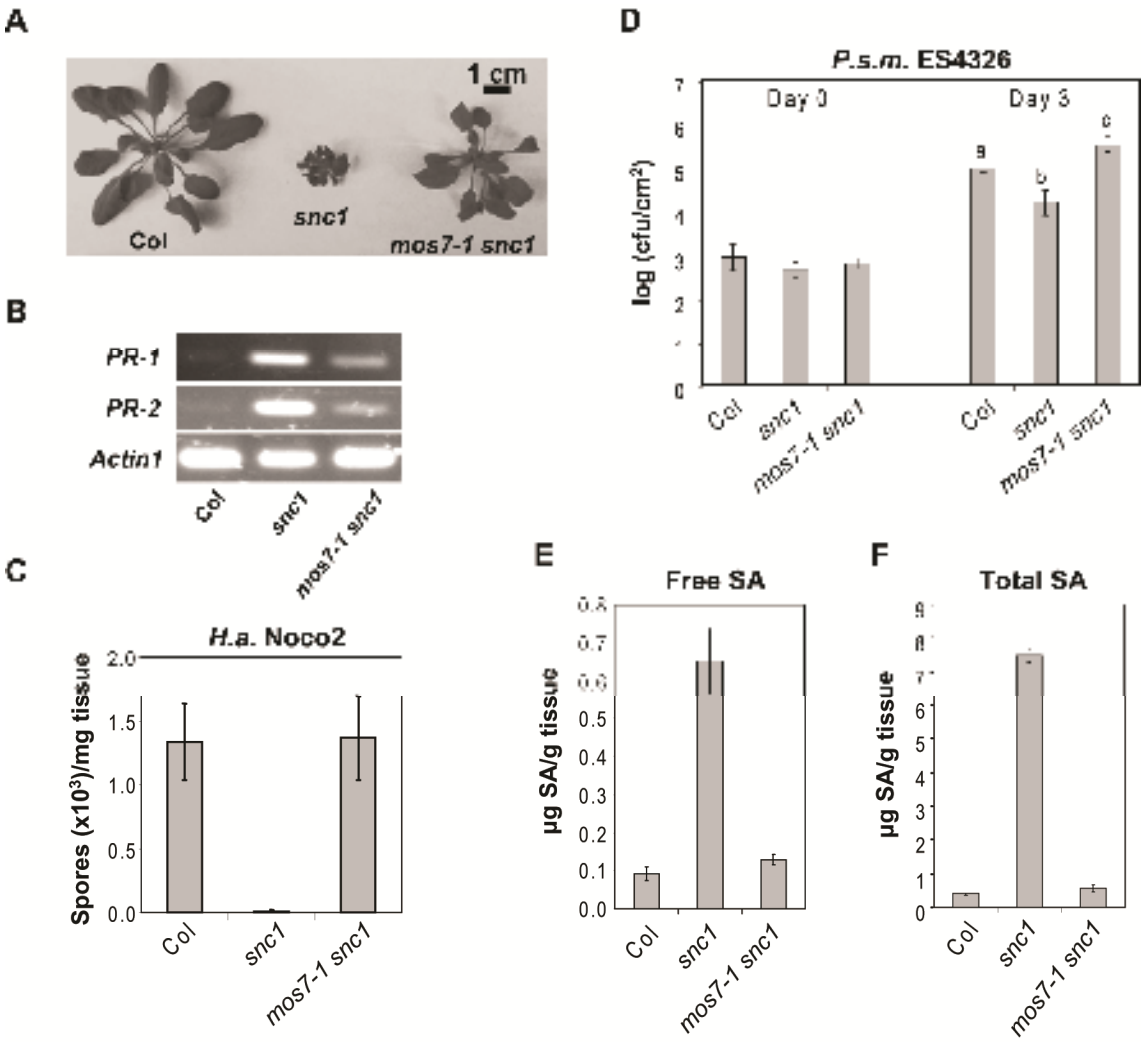

Figure 2.1: *mos7-1* suppresses the autoimmune responses in *snc1*.

(A) Morphology of five-week-old soil-grown plants of Col, *snc1*, and *mos7-1 snc1*.
(B) *PR* gene expression in *mos7-1 snc1*. RNAs were prepared from three-week-old plants grown on MS media and reverse transcribed to obtain total cDNA. The cDNA samples were normalized by real-time PCR using *Actin1*. *PR-1*, *PR-2*, and *Actin1* were amplified by 31 cycles of PCR using equal amounts of total cDNA, and the products were analyzed by agarose gel electrophoresis with ethidium bromide staining.
(C) Two-week-old soil-grown seedlings were inoculated with *Ha* Noco2 at a concentration of 50,000 conidia per ml of water and the number of conidia was quantified 7 days post inoculation (dpi). Bars represent means of four replicates ± standard deviation (SD).
(D) Five-week-old soil-grown plants were infiltrated with *Psm* ES4326 (OD600=0.0001) and colony forming units (cfu) were quantified at 0 and 3 dpi, respectively. Bars represent means of six replicates ± SD. All data were analyzed by one-way analysis of variance (one-way ANOVA). Different letters indicate statistically significant differences between genotypes ($P<0.05$).
(E) Free and (F) total SA were extracted from five-week-old plants and analyzed by HPLC. Bars represent the average of four replicates ± SD.

2.2.2 Map-Based Cloning of *mos7-1*

A positional cloning approach was used to identify the mutation in *mos7-1* leading to the suppression of *snc1*. To map *mos7-1*, *mos7-1 snc1* in Columbia (Col) ecotype was crossed with Landsberg *erecta* (L*er*) containing the introgressed *snc1* mutation, L*er-snc1* (Zhang and Li, 2005). Linkage analysis was performed on 24 F2 plants that had lost the *snc1* morphology. The *mos7-1* locus was found to have linkage with markers on the top arm of chromosome 5 that unfortunately was not introgressed from L*er* to L*er-snc1*. Therefore, a population of 1056 F3 plants was generated for fine mapping from F2 progeny that were homozygous for *snc1* and heterozygous for *mos7-1* from another cross between *mos7-1 snc1* and L*er*. The *mos7-1* mutation was narrowed to the region between markers MOP10 and MJJ3 on chromosome 5 (Figure 2.2A). To identify the molecular lesion in *mos7-1*, a set of overlapping PCR fragments covering coding sequences in this region were amplified from *mos7-1 snc1* and sequenced. Comparing sequences from the mutant with the Arabidopsis genome sequence revealed a 12-bp deletion in the fourth exon of *At5g05680* (Figure 2.2 B and C) that leads to an in-frame deletion of four amino acids at the N terminus of MOS7 (Figure 2.3). BLAST analysis showed that MOS7 is related to human Nup88 and Drosophila Mbo (Members only) proteins (Figure 2.3). MOS7 is the only Nup88 homolog in Arabidopsis. The homology between MOS7 and Nup88 and Mbo extends throughout the entire length of the protein.

To confirm that *MOS7* is *At5g05680*, a wild-type copy of *At5g05680* under the control of its own promoter was transformed into *mos7-1 snc1*. Among 12 T1 transgenic plants obtained, all displayed *snc1*-like morphology (Figure 2.2D). Progeny of T1 plants carrying the *MOS7* transgene were tested for resistance against *Ha* Noco2. Constitutive resistance to *Ha* Noco2 was restored in the transgenic plants (Figure 2.2E), indicating that *At5g05680* is able to complement *mos7-1* and that *MOS7* is *At5g05680*. Two additional mutant alleles of *MOS7* were obtained from the ABRC. *mos7-2* (SALK_129301) contains a T-DNA insertion in the third intron and *mos7-3* (SALK_085349) has a T-DNA inserted in the sixth exon of *MOS7* (Figure 2.2B). We were unable to identify plants that are homozygous for either *mos7-2* or *mos7-3* from >200 progeny of plants heterozygous for the mutations, indicating that null mutations of *MOS7* are lethal. This is consistent with the lethality phenotype of null *mbo* alleles in Drosophila (Uv et al., 2000). The viability and recessive nature of *mos7-1* suggest that it is a partial loss-of-function allele of *MOS7*.

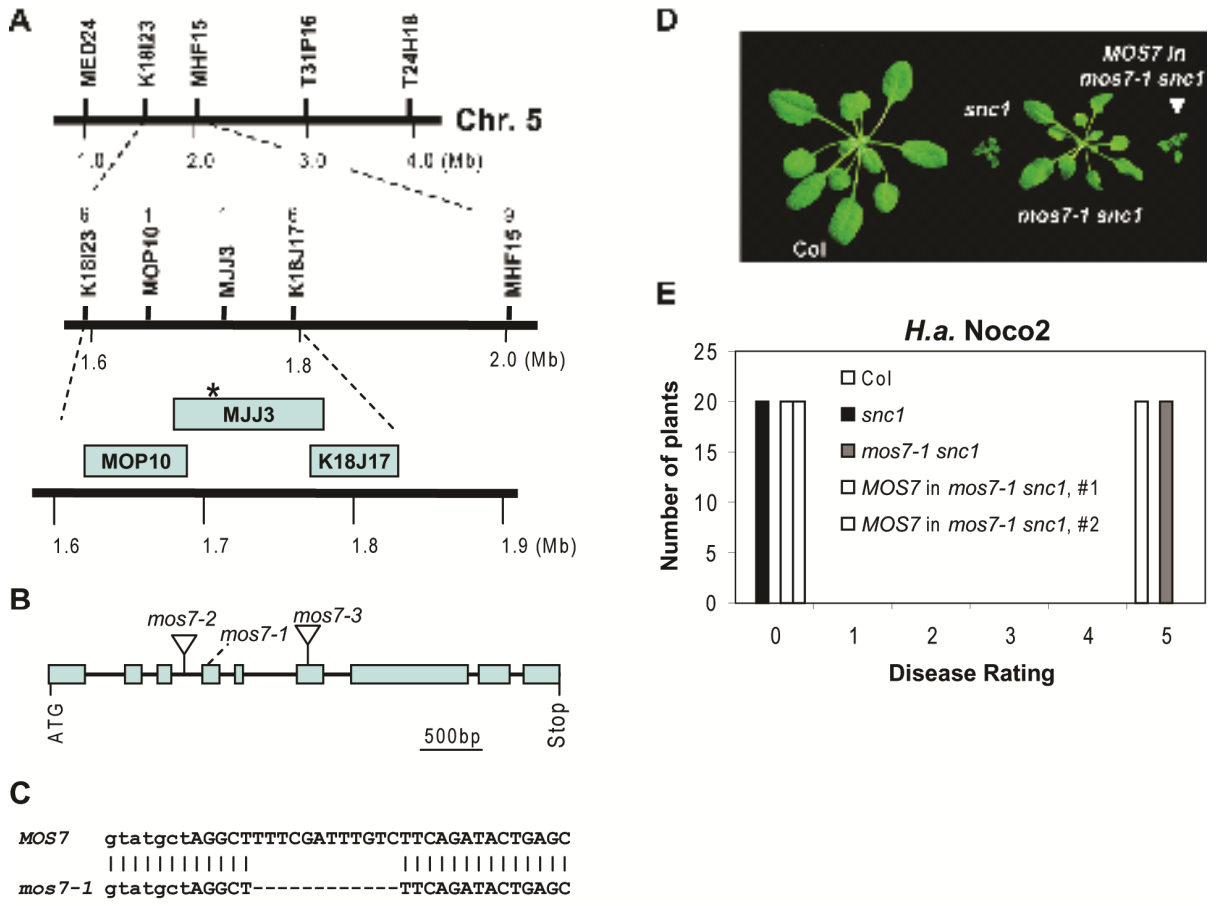

Figure 2.2: Map-based cloning of *mos7-1*.

(A) Map position of the *mos7-1* locus on chromosome 5. BAC clones and number of recombinants are indicated. Asterisk indicates the physical location of the *mos7-1* locus.
(B) Gene structure of *At5g05680*. The exons are indicated by boxes, and the introns are represented by solid lines. Locations of *mos7-1* deletion and T-DNA insertions of *mos7-2* (SALK_129301) and *mos7-3* (SALK_085349) are indicated.
(C) *mos7-1* deletion site in the MOS7 gene. Lower and upper case letters indicate intron and exon, respectively.
(D) Morphology of wild type Col, *snc1*, *mos7-1 snc1*, and a representative transgenic line containing *MOS7* transgene driven by its native promoter in *snc1 mos7-1*.
(E) Resistance of Col, *snc1*, *mos7-1 snc1*, and a *MOS7* complementing line in *snc1mos7-1* against *Ha* Noco2. The infection was rated as follows on 20 plants 7 days after infection by counting the number of conidiophores per infected leaf: 0, no conidiophores on the plants; 1, no more than 5 conidiophores per infected leaf; 2, 6 to 20 conidiophores on a few of the infected leaves; 3, 6 to 20 conidiophores on most of the infected leaves; 4, 5 or more conidiophores on all infected leaves; 5, 20 or more conidiophores on all infected leaves.

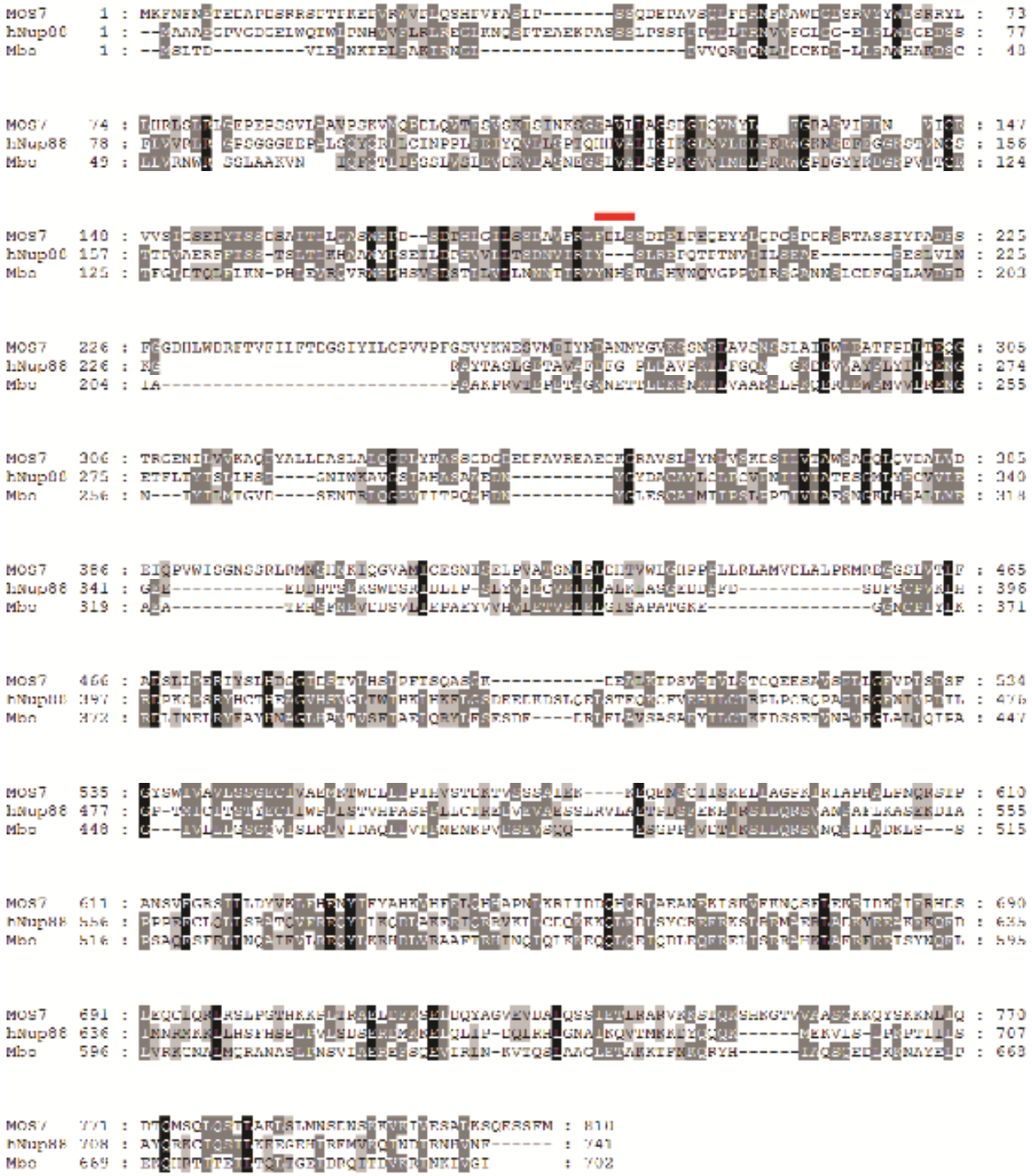

Figure 2.3: Amino acid alignment of MOS7, human Nup88, and Drosophila Nup88.

Amino acid sequences from Arabidopsis MOS7 (accession number NP_196187), Drosophila DNup88 (Mbo; accession number NP_524330), and human hNup88 (accession number NP_002523) were aligned using ClustalW2 (Larkin et al. 2007). Sequence identities and similarities were shaded using Genedoc. Red bar indicates the 4 amino acids deleted in mos7-1. Identical amino acids are shaded in black, and amino acids with similar properties are shaded in grey.

2.2.3 *mos7-1* Single Mutant Plants Exhibit Enhanced Disease Susceptibility

To test whether *MOS7* contributes to basal defence against virulent pathogens, *mos7-1* plants were challenged with *Psm* ES4326 at a concentration of OD_{600} = 0.0001. Wild-type plants usually develop no disease symptoms at this low dose; however, subtle disease symptoms were observed on *mos7-1* plants 3 days after inoculation. When bacterial growth was determined, ~10-fold more bacteria accumulated in *mos7-1* than in wild-type leaves (Figure 2.4A). Therefore, *MOS7* contributes to basal resistance.

2.2.4 *MOS7* is Required for Resistance Mediated by Multiple R Proteins

To determine whether MOS7 is involved in resistance mediated by other TIR-NB-LRR R proteins, we challenged the *mos7-1* single mutant with *Ha* Emwa1 and *P.s. tomato* DC3000 carrying *avrRps4* that are recognized by RPP4 (van der Biezen et al., 2002) and RPS4 (Hinsch and Staskawicz, 1996), respectively. As shown in Figures 2.4B and C, the *mos7-1* mutation markedly reduced resistance mediated by RPP4. By contrast, RPS4 resistance was only slightly compromised.

We then tested whether resistance mediated by CC-NB-LRR–type R proteins is also impaired in *mos7-1* by inoculating plants with *Psm* ES4326 carrying *avrB* or *Pst* DC3000 carrying *avrPphB* that encode effector proteins recognized by RPM1 (Grant et al., 1995) and RPS5 (Simonich and Innes, 1995), respectively. The *mos7-1* mutant supported ~30-fold more bacterial growth compared with wild-type plants when challenged with *Psm* ES4326 carrying *avrB* (Figure 2.4D). Also, *mos7-1* was highly susceptible to *Pst* DC3000 carrying *avrPphB*, the extent of bacterial growth being the same as in susceptible *ndr1* plants (Figure 2.4E). These data show that *mos7-1* compromises resistance mediated by both TIR- and CC-NB-LRR proteins, although the degree of its effect varies depending on the R protein tested.

2.2.5 *mos7-1* is Compromised in SAR

Initiation of local R protein-mediated resistance primes uninfected tissues against subsequent infections by a broad range of pathogens, a process termed systemic acquired resistance (SAR). As a result, the entire plant becomes more resistant to secondary infections (Durrant and Dong, 2004). To test whether SAR is affected in *mos7-1* plants, we first treated leaves locally with *Psm* ES4326 expressing *avrB* at a density of OD_{600} = 0.2 to trigger a hypersensitive response. A high dose of virulent *Psm* ES4326 (OD_{600} = 0.001) was then infiltrated into the distal leaves 24 hours after SAR induction. Wild-type plants showed a significant decrease in bacterial growth in *avrB* pretreated plants compared with mock-inoculated ones. By contrast, leaves of *mos7-1* supported bacterial growth in systemic leaves of both *avrB* pretreated and untreated plants; this bacterial growth was similar to that seen in the SAR-defective *npr1-1* mutant (Figure 2.5A). Therefore, the SAR response is abolished in *mos7-1*. A defect in SAR was also reflected by the inability of *mos7-1* to boost *PR-1* expression in systemic tissue after local *avrB* induction (Figure 2.5B).

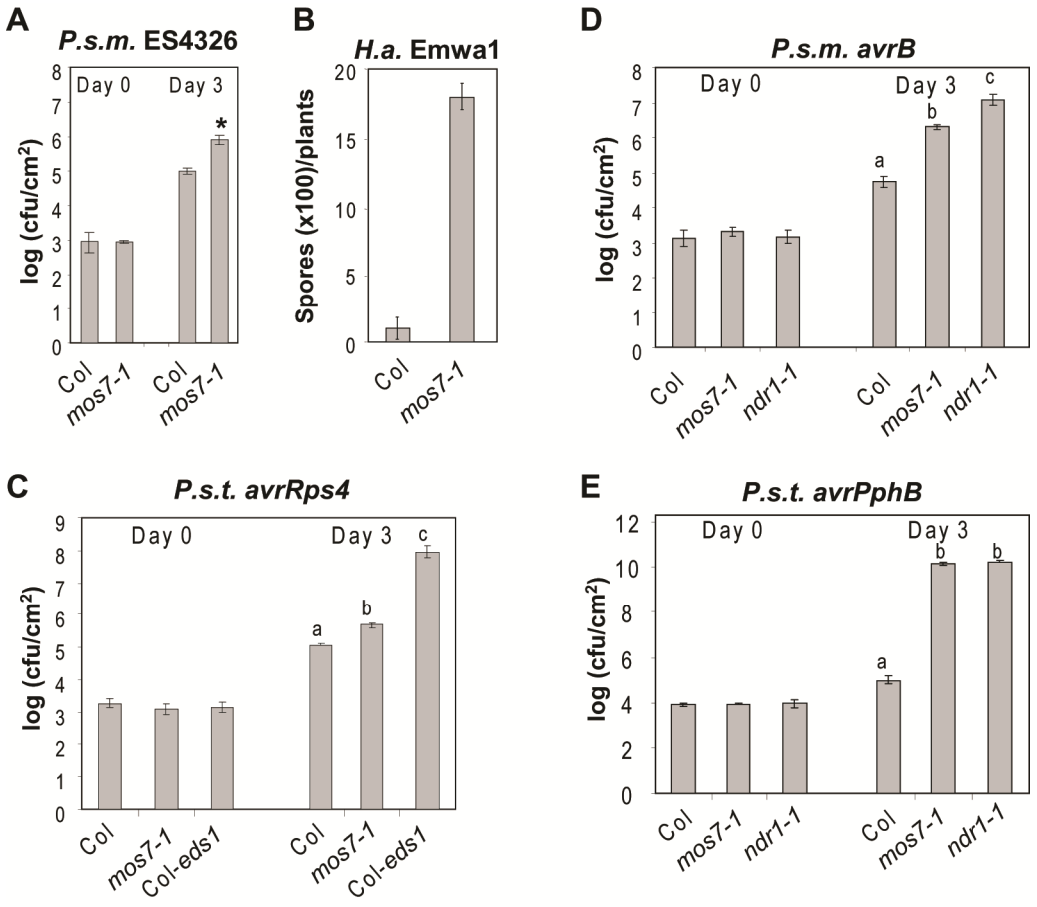

Figure 2.4: Altered basal and R-protein mediated resistance in *mos7-1* single mutant plants.

(A) Enhanced disease susceptibility to *Psm* ES4326 in *mos7-1*. The plants were infiltrated with the bacteria at OD_{600} = 0.0001. Leaf discs within the infiltrated area were taken at Day 0 and Day 3 to measure the bacterial growth. Bars represent means of six replicates ± SD. Susceptibility toward *Psm* ES4326 in *mos7-1* is significantly enhanced compared to Col as indicated by the asterisk ($p<0.0001$, t test).

(B to E) *mos7-1* mutant plants were challenged with the indicated avirulent pathogens carrying effectors that can trigger the cognate R protein-mediated resistance. (B) 50,000 conidia/ml was used for *Ha* Emwa1 inoculation. (C-E) For bacterial pathogens, an inoculation dose of OD_{600} = 0.002 was used. Bars represent means of six replicates ± SD. Statistical analyses of the bacterial growth assays in C, D, and E were done by using one-way ANOVA provided by StatsDirect statistical software (StatsDirect Ltd. http://www.statsdirect.com. England: StatsDirect Ltd. 2008). Statistical differences among the samples are labelled with different letters ($P<0.05$).

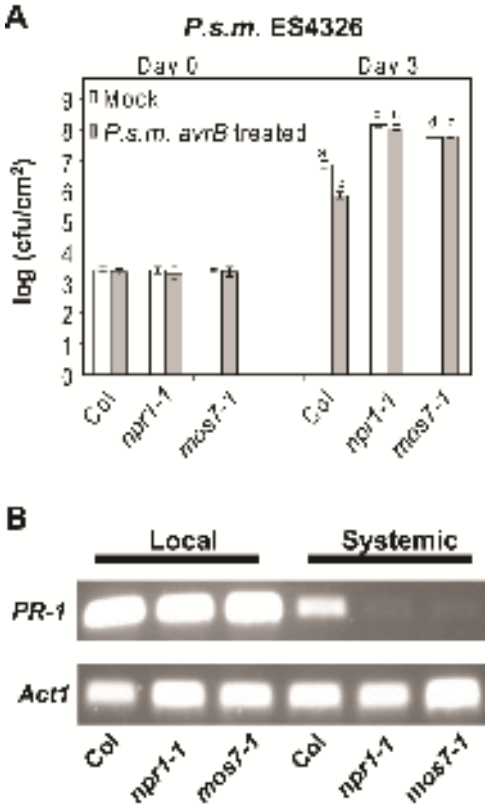

Figure 2.5: Systemic acquired resistance is compromised in *mos7-1*.

(A) Growth of *Psm* ES4326 in five-week-old Col, *npr1-1* and *mos7-1* plants pre-inoculated with *Psm* ES4326 *avrB* in 10 mM MgCl2 (grey bars) or 10mM MgCl2 alone (mock; white bars). Bars represent means of four replicates ± SD. Different letters indicate statistically significant differences between genotypes ($P<0.05$).
(B)RT-PCR for *PR-1* on RNA extracted from local and systemic leaves of the indicated genotypes pre-treated with *Psm* ES4326 *avrB*. *Actin1* was used as control.

2.2.6 MOS7 Localizes to the Nuclear Rim

To explore the roles of MOS7 in plant innate immunity further, we investigated its subcellular localization. Initially we used the native promoter of *MOS7* to drive expression of MOS7 with green fluorescent protein (GFP) fused to its C terminus. Although *MOS7-GFP* expressed under the native promoter complemented the *mos7-1* mutation in regards to all *snc1*-suppressing phenotypes, we did not observe any green fluorescence using confocal fluorescence microscopy, probably due to low abundance of the fusion protein. A construct containing *MOS7* fused to a C-terminal GFP tag under the control of the constitutive *35S* promoter was then made and transformed into the *mos7-1 snc1* mutant. A green fluorescence signal was observed at the nuclear rim (Figures 2.6A and B). The nuclear rim localization was observed in all cell types examined, including root cells (Figures 2.6A and B) and leaf pavement cells (Figure 2.6A). Concentration of GFP signal at the nuclear envelope is consistent with MOS7 being a member of the nuclear pore complex, as predicted by its similarity to nuclear pore components human Nup88 and Drosophila Mbo. The *35S∴MOS7-GFP* transgene not only complemented the morphological phenotypes of *mos7-1 snc1* (Figure 2.6C) but also restored a constitutive defense response against virulent *Ha* Noco2 (Figure 2.6D), suggesting that the MOS7-GFP fusion protein localizes correctly inside the cell.

2.2.7 Nuclear Accumulation of snc1 Resistance Protein is Reduced in *mos7-1*

Recent studies on tobacco N and Arabidopsis RPS4, two TIR-type NB-LRR proteins, revealed that both are present in the cytoplasm and nucleus and that their nuclear pools are important for triggering immune responses (Burch-Smith et al., 2007; Wirthmueller et al., 2007). However, the mechanism that regulates their partitioning between the cellular compartments remains elusive. The TIR-type R protein SNC1 contains a predicted NLS and two NES motifs. Since *mos7-1* was identified as a genetic suppressor of *snc1*, one obvious candidate protein whose cellular distribution could be affected by *mos7-1* is snc1. We therefore made a *snc1-GFP* fusion gene construct driven by its own promoter and transformed this into *snc1-r3* that contains a deletion of the entire *RPP4* cluster. *snc1-r3* was identified as an *snc1* revertant allele from the MOS screen (Zhang et al., 2003a) and was used in this study to avoid potential interference by endogenous SNC1-related proteins. Of many transgenic plants obtained, we were unable to find lines that consistently exhibited green fluorescence, probably due to low levels of the fusion protein. We selected one line with a single insertion site that exhibits a *snc1*-like morphology and crossed it with *mos7-1* to generate a *mos7-1 snc1-r3* line expressing the identical *snc1-GFP* transgene. Homozygous *snc1-GFP* transgenic plants were much smaller than *snc1* plants, probably due to overexpression of the transgene in this particular line. *mos7-1* partially suppressed the morphological phenotypes of *snc1-GFP* in *snc1-r3* (Figure 2.7A) and constitutive defence against virulent *Ha* Noco2 (Figure 2.7B). Immunoblot analysis showed that total snc1-GFP levels were similar in *snc1-r3* and *mos7-1 snc1-r3* (Figure 2.7C). Further fractionation revealed that snc1-GFP was present in both the nuclear-depleted and nuclear fraction (Figure 2.7D). When band intensities were measured by Quantity One 4.6.1 software (Bio-Rad), we estimated from repeated experiments that the majority of snc1 protein accumulates in the cytoplasmic

compartment with 5.6 to 11.5% in the nucleus (Figure 2.7D). In *mos7-1*, there was a significant increase of snc1-GFP protein in the cytoplasm, whereas the nuclear pool of snc1-GFP was reduced (Figure 2.7D), ranging between 2.5 and 2.9% of total snc1 protein. We reasoned that the altered cellular distribution of snc1-GFP likely contributes to the *snc1*-suppressing phenotype of *mos7-1*.

In Drosophila and human, mutations in Nup88 enhance NES-mediated nuclear export (Roth et al., 2003; Xylourgidis et al., 2006). We further tested whether adding an NES to snc1-GFP would affect snc1-mediated resistance. When a construct expressing snc1-GFP-NES driven by its native promoter was transformed into wild-type Col, none of the T1 transgenic plants showed *snc1*-like morphology, while 61% of the transgenic plants carrying the control *snc1-GFP* transgene in Col showed *snc1*-like morphology. The numbers here support that snc1 nuclear localization might be critical for its autoimmunity. Enhancing nuclear export of snc1-GFP results in reduced autoimmunity, a similar effect as observed in *mos7-1*.

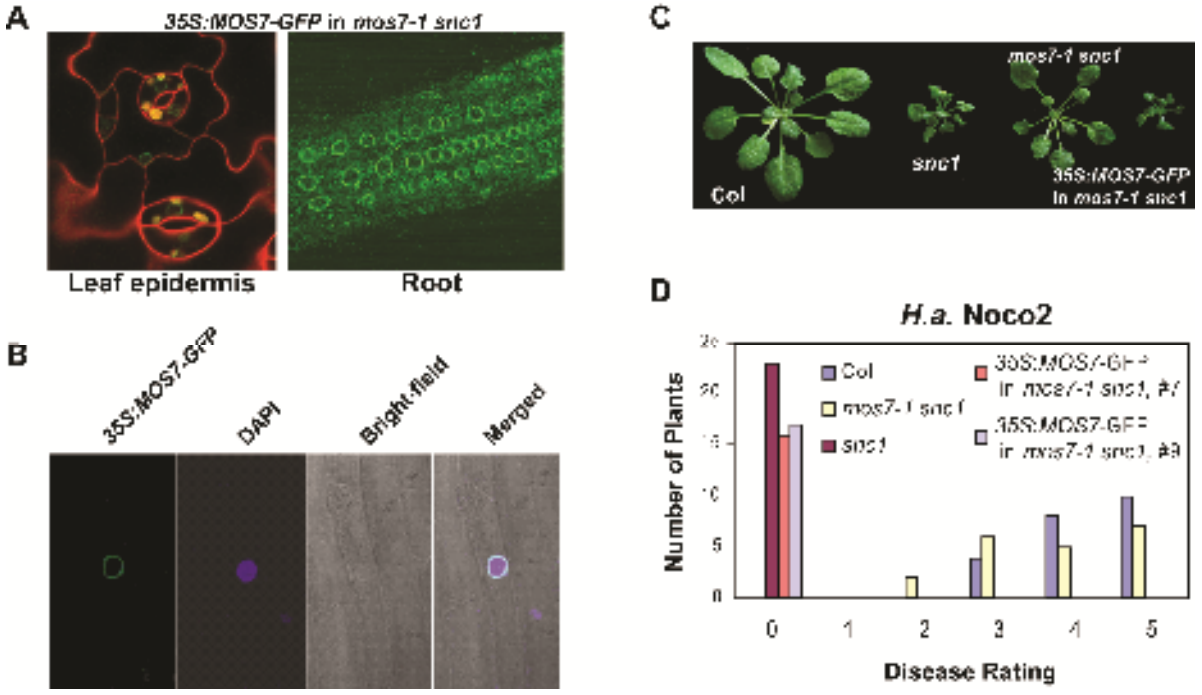

Figure 2.6: Subcellular localization of MOS7-GFP.

(A) MOS7-GFP fluorescence in leaf pavement and root cells of *mos7-1 snc1* transgenic plants expressing *MOS7-GFP* under the control of *35S* promoter. Plant cell walls were stained with 5mg/ml propidium iodine (red) in the left panel.
(B) MOS7-GFP fluorescence, DAPI staining of the nucleus, bright-field, and merged fluorescence channels in root cells. Pictures in (A) and (B) were taken on 2-week-old plate-grown plants.
(C) Complementation of *mos7-1* by *MOS7-GFP* expressed by the *35S* promoter.
(D) Restoration of enhanced disease resistance in *mos7-1 snc1* transformed with *MOS7-GFP* driven by *35S* promoter. The disease ratings are as described in Figure 2.2E.

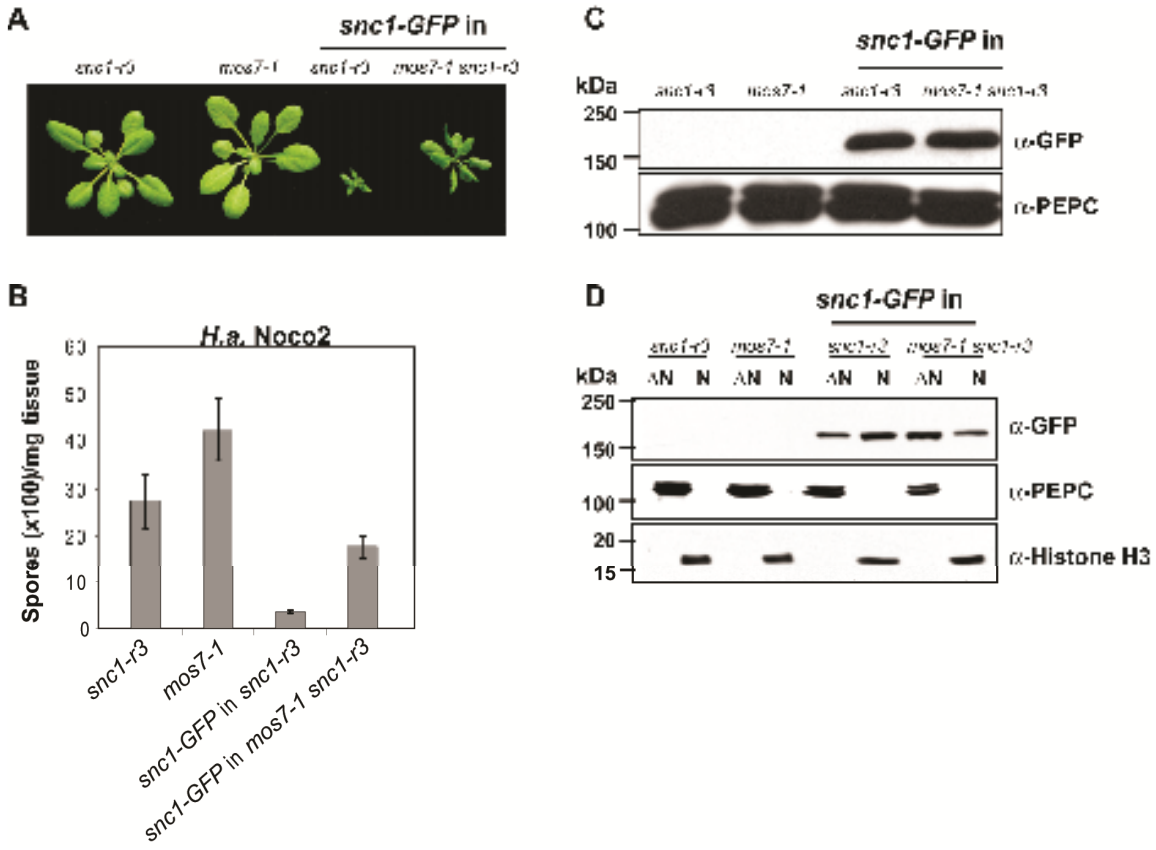

Figure 2.7: Abundance and cellular distribution of snc1-GFP in *mos7-1 snc1-r3*.

(A) Morphology of three-week-old plants of *snc1-r3*, *mos7-1*, *snc1-GFP* in *snc1-r3*, and *snc1-GFP* in *mos7-1 snc1-r3*.
(B) *Ha* Noco2 growth on the same genotypes as (A).
(C) Immunoblot analysis of snc1-GFP expressed under its native promoter in total protein extracts of unchallenged leaf tissues in *snc1-r3* and *mos7-1 snc1-r3*. Equal loading was monitored by probing the membrane with anti-PEPC.
(D) Immunoblot analysis of snc1-GFP in nuclei-depleted (ΔN) and nuclear (N) protein extracts of the indicated genotypes. Anti-PEPC was used as a cytosolic marker and anti-Histone H3 was used as a nuclear marker. Nuclear protein extracts (N) were 25x concentrated as compared to nuclei-depleted fractions (ΔN)

2.2.8 Nuclear Accumulation of NPR1 is Reduced in *mos7-1*

In Drosophila, the MOS7 homolog DNup88/Mbo affects an immune response against bacterial infection through nuclear retention of master immune regulators of the NF-κB family (Uv et al., 2000; Xylourgidis et al., 2006). Upon infection, the I-κB homolog Cactus becomes degraded, allowing the Rel/NF-κB proteins Dorsal and Dif to translocate to the nucleus and activate gene expression. During this process, DNup88 attenuates CRM1-mediated nuclear export of Dorsal and Dif, leading to their nuclear accumulation, whereas *nup88* mutant larvae exhibit enhanced nuclear export of the Rel/NF-κB proteins and fail to activate an immune response (Uv et al., 2000; Roth et al., 2003; Xylourgidis et al., 2006).

The plant defence regulator NPR1 controls basal resistance and SAR downstream of the defence hormone SA and displays a somewhat analogous pattern of activation as NF-κB. Using *35S* promoter-driven *NPR1-GFP*, it was shown that under non-inducing conditions, NPR1 is sequestered in the cytoplasm as an oligomeric complex (Mou et al., 2003; Tada et al., 2008). Upon SA application, increased SA levels result in a change of the cellular redox state that in turn leads to monomerization of NPR1, allowing it to translocate from the cytosol to the nucleus to regulate downstream *PR* gene expression. The SAR defect observed in *mos7-1* mutant plants (Figures 2.5) prompted us to investigate the contribution of MOS7 to NPR1 nuclear accumulation.

To avoid artifacts that can result from overexpression from the *35S* promoter, we constructed an *NPR1-GFP* fusion gene driven by its native promoter. When the *NPR1-GFP* transgene was transformed into the null *npr1-3* mutant, none of the transgenic lines consistently exhibited green fluorescence even upon SAR induction, suggesting that levels of the fusion protein in the transgenic plants are very low. We selected one line that carried a single transgene insertion and complemented fully all *npr1* phenotypes, suggesting that NPR1-GFP expressed by its own promoter functions similarly to wild-type NPR1 protein. The *NPR1-GFP* transgenic line was then crossed with *mos7-1* to create a *mos7-1 npr1-3* double mutant expressing the same NPR1-GFP protein. As shown in Figure 2.8A, NPR1 total protein levels increased markedly in both the wild type and the *mos7-1* mutant upon SAR induction by spraying plants with the SA analog 2,6-dichloroisonicotinic acid (INA). Lower amounts of NPR1 protein accumulated in *mos7-1* before and after SAR induction compared with the wild type. No differences in *NPR1* transcript abundance were observed between uninduced *npr1-3* and *mos7-1 npr1-3* tissues determined by RT-PCR (Figure 2.8B), suggesting that reduced NPR1 accumulation in *mos7-1* likely results from decreased protein synthesis or stability rather than reduced transcription.

We further investigated the cellular distribution of NPR1-GFP in *mos7-1* before and after INA induction by comparing NPR1-GFP levels in nuclear and nuclei-depleted protein extracts of untreated and INA-induced tissues. As shown in Figure 2.8C, lower levels of NPR1-GFP accumulated in nuclei of both healthy and INA-induced *mos7-1* plants than in the wild type. In contrast with the preferential depletion of nuclear snc1 in *mos7-1* tissues, lower amounts of NPR1-GFP were also observed in nuclei-depleted (cytosolic) extracts of INA-treated *mos7-1* compared with the wild type (Figure 2.8C). Since *mos7-1* plants exhibit a SAR defect and nuclear accumulation of NPR1 is required for SAR induction, these data suggest that NPR1 may not be able to attain sufficient abundance in the nucleus for activation of SAR in *mos7-1*.

It is notable that NPR1-GFP expressed under its native promoter was detected in the nucleus of uninduced tissues (Figure 2.8C); this pattern was observed in multiple independent

NPR1-GFP transgenic lines. This partitioning contrasts with data derived from *NPR1-GFP* expressed under control of the *35S* constitutive promoter that showed a cytoplasmic localization of NPR1 without SAR induction (Mou et al., 2003). To rule out the possibility that unchallenged plants were already stressed, causing increased nuclear translocation of NPR1-GFP, we analyzed the expression of the SAR marker gene *PR-1* in the same uninduced tissues from which nuclear extracts were generated. No *PR-1* transcripts were detected in uninduced tissues, whereas strong expression was detected after INA induction (Figure 2.8B), suggesting that the observed nuclear pool of NPR1 represents its uninduced state. These data suggest that NPR1 is present in the nucleus of both uninduced and INA-induced tissues.

2.2.9 EDS1 Nuclear Accumulation is Reduced in *mos7-1*

Another key plant immune regulator known to localize to both cytosol and nucleus is EDS1 (Feys et al., 2005). We investigated whether accumulation and cellular distribution of native EDS1 is affected by *mos7-1*. As with NPR1, EDS1 total protein was reduced in *mos7-1* mutant plants compared with Col wild type (Figure 2.9A), although the wild type and *mos7-1* have comparable *EDS1* transcript levels (Figure 2.9B). In *mos7-1*, the ratio of EDS1 distributing in the cytosol and nucleus was not strongly affected. However, overall lower accumulation of EDS1 resulted in only very low levels being detected in *mos7-1* nuclei (Figure 2.9C). We conclude that MOS7 is also necessary for EDS1 protein accumulation in the nucleus. The effect of *mos7-1* on EDS1 nuclear accumulation may also contribute to the ability of *mos7-1* to suppress *snc1*.

2.2.10 Nuclear Accumulation of HDA19, CDC5, and TGA2 is Not Affected in *mos7-1*

One enigma to *mos7-1* is its specificity. Lethality of *MOS7* null alleles indicates that wild-type MOS7 is probably required for general nuclear export. While *mos7-1* appeared not to exhibit pleiotropic phenotypes, we could not rule out a global effect on protein export. To test this, we fractionated proteins from *mos7-1* and the wild type and examined the localization and relative protein abundance of the known nuclear proteins CDC5, HDA19, and TGA2 using respective antibodies. CDC5 is a myb-like transcription factor, containing a strong NES and belonging to a nuclear MOS4-associated complex (Palma et al., 2007). HDA19 is a histone deacetylase, and TGA2 is a transcription factor that interacts with NPR1 (Zhang et al., 1999). Neither HDA19 nor TGA2 contains a strong NES. As shown in Figure 2.10A, nuclear accumulation of these proteins (as well as histone H3) is unaffected in *mos7-1*. These data suggest that the defects we observe in *mos7-1* in nuclear retention of snc1, NPR1, and EDS1 are rather selective.

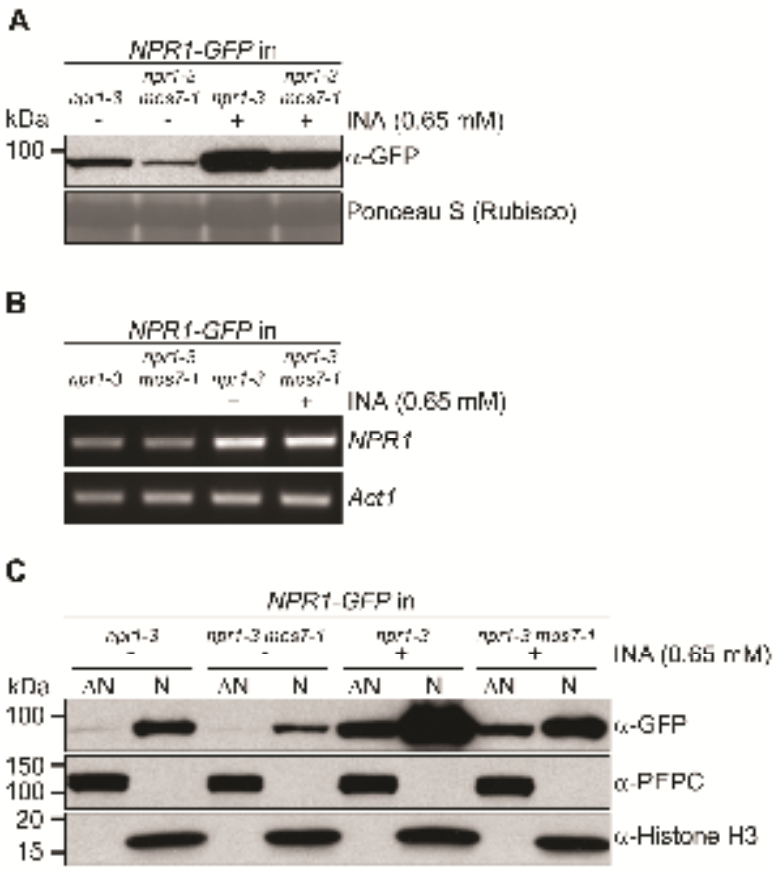

Figure 2.8: NPR1 protein abundance and subcellular localization in *mos7-1*.

(A) NPR1-GFP expressed by its native promoter in *mos7-1*. Immunoblot analysis of NPR1-GFP in total protein extracts of unchallenged leaf tissues (-) and leaf tissues harvested 24 h after spraying plants with 0.65 mM INA (+). Equal loading was monitored by staining the membrane with Ponceau S.
(B)RT-PCR for *NPR1* on RNA extracted from 4-week old plants of the indicated genotypes treated with or without INA. *Actin1* expression was used as control.
(C) Immunoblot analysis of NPR1-GFP in nuclei-depleted (ΔN) and nuclear (N) protein extracts of unchallenged (-) and INA treated (+) tissues of the indicated genotypes. Anti-PEPC was used as a cytosolic marker and anti-Histone H3 was used as a nuclear marker. Nuclear protein extracts (N) were 35x concentrated as compared to nuclei-depleted fractions (ΔN).

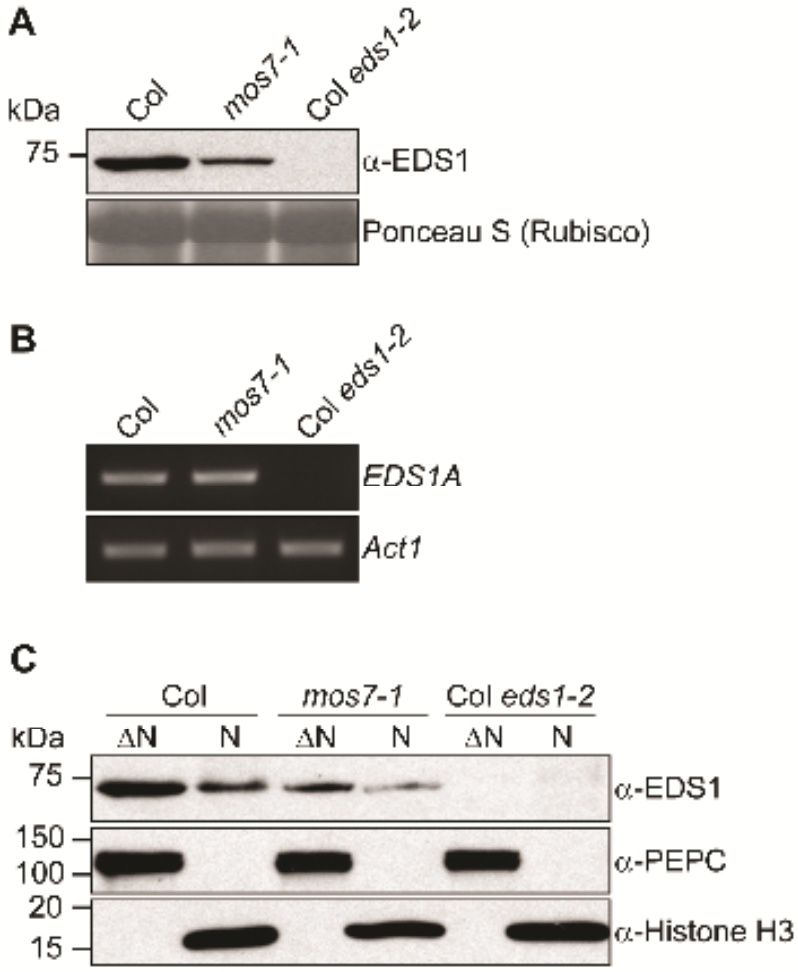

Figure 2.9: EDS1 protein abundance and subcellular localization in *mos7-1*.

(A) EDS1 in *mos7-1*. Immunoblot analysis of EDS1 in total protein extracts of unchallenged leaf tissues. Equal loading was monitored by staining the membrane with Ponceau S.
(B)RT-PCR for *EDS1A* on RNA extracted from 4-week old unchallenged plants of the indicated genotypes. *Actin1* expression was used as control.
(C) Immunoblot analysis of EDS1 in nuclei-depleted (ΔN) and nuclear (N) protein extracts of unchallenged leaf tissues. Anti-PEPC was used as a cytosolic marker and anti-Histone H3 was used as a nuclear marker. Nuclear protein extracts (N) were 35x concentrated as compared to nuclei-depleted fractions (ΔN).

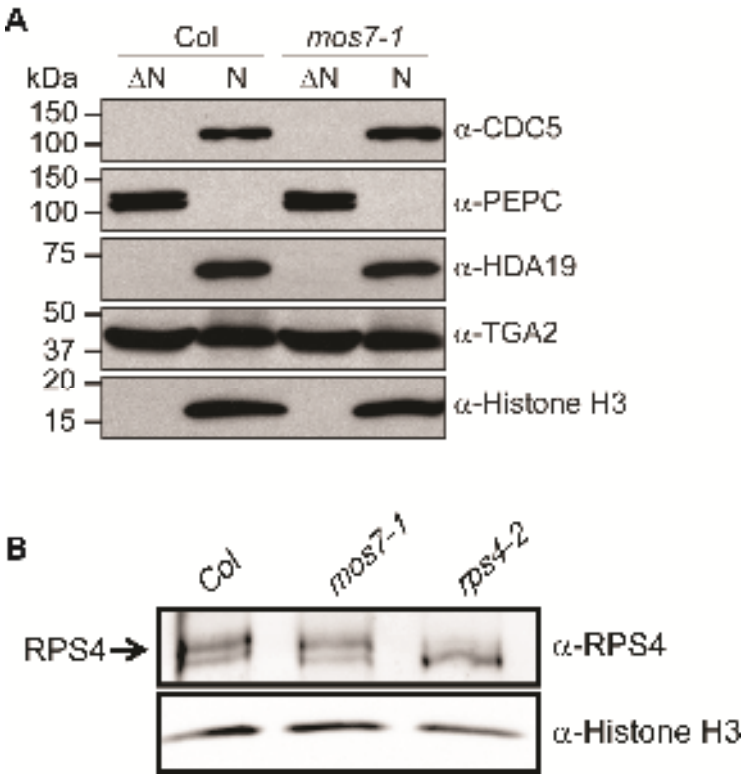

Figure 2.10: CDC5, PEPC, HDA19, TGA2 and Histone H3 protein abundance and subcellular localization, and RPS4 nuclear abundance are unaltered in *mos7-1*.

(A) Immunoblot analysis of CDC5, PEPC, HDA19, TGA2 and Histone H3 in nuclei-depleted (ΔN) and nuclear (N) protein extracts of unchallenged leaf tissues. Nuclear protein extracts (N) were 35x concentrated as compared to nuclei-depleted fractions (ΔN).
(B) Nuclear abundance of RPS4 is not altered in *mos7-1*. Immunoblot analysis of RPS4 in nuclear protein extracts of unchallenged leaf tissues. *rps4-2* is a transcriptional null allele; it contains a T-DNA insertion in the second exon of *RPS4*. Equal loading was monitored by probing the membrane with anti-Histone H3.

2.3 Discussion

Several recent lines of evidence suggest that nucleocytoplasmic trafficking pathways play important roles in plant innate immunity through dynamic partitioning of signalling regulators between the nucleus and cytosol. Studies of MOS3/SAR3 indicate that mRNA export, regulated by nucleoporins of the Nup107-160 complex, is required for both basal defense and R protein-mediated resistance (Zhang and Li, 2005; Dong et al., 2006; Parry et al., 2006). Also, a requirement for MOS6 and RanGAP2 in R protein-triggered resistance points to import to the nucleus of protein regulators that have NLSs as an important process in plant immunity (Palma et al., 2005; Sacco et al., 2007; Tameling and Baulcombe, 2007). However, contributions of other nucleocytoplasmic trafficking pathways or components controlling nuclear protein export and retention are unclear. In this study, we identified *mos7-1* as a genetic suppressor of the autoimmune mutant *snc1*. We isolated the *MOS7* gene and found it to encode a plant homolog of human and Drosophila Nup88. Our analysis reveals that MOS7 contributes to several aspects of plant immunity. Importantly, resistance defects of *mos7-1* mutants correlate specifically with reduced nuclear accumulation of the autoactivated TIR-NB-LRR immune receptor, snc1. Nuclear pools of the downstream signalling components NPR1 and EDS1 are also strongly depleted in *mos7-1*, although unlike snc1, reduced abundance in nuclei appears to reflect lower total steady state levels of these defence regulators.

While only limited studies have been performed on nucleoporins in plants, nuclear pore complexes seem to be conserved among eukaryotes, in both structure and functionality (Terry et al., 2007). For example, Nup107-160 complex components in yeast and animals are critical for mRNA export (Dockendorff et al., 1997; Emtage et al., 1997). In Arabidopsis, mutations in homologs of Nup160 and Nup96, both belonging to the corresponding Nup107-160 complex, similarly affect mRNA export (Dong et al., 2006; Parry et al., 2006). Mutations in Arabidopsis *MOS3/Nup96/SAR3* partially disable innate immunity (Zhang and Li, 2005). In mice, although a complete knockout of *Nup96* causes lethality, knockdown of Nup96 exhibits defects in both innate and adaptive immunity (Faria et al., 2006). Our studies on MOS7 suggest that the function of Nup88 is also conserved between plants and animals since Nup88s in Drosophila and human are critical for the regulation of innate immunity. Consistent with this idea, MOS7-GFP fusion protein resides mainly at the nuclear rim (Figures 2.6A and B). In animals, Nup88 interacts directly with CAN/Nup214 and Nup358/RanBP2. The major function of Nup88 is to anchor Nup214 and CRM1 on the nuclear envelope to attenuate NES-mediated nuclear export (Roth et al., 2003; Bernad et al., 2004; Xylourgidis et al., 2006). The lethality phenotype of null *mos7* mutations agrees with its potential function in general NES-mediated nuclear export. Partial loss-of-function mutations in Drosophila *mbo* or depletion of mammalian Nup88 lead to increased nuclear export, resulting in reduced retention of Drosophila Rel protein Dorsal and NF-κB, respectively (Uv et al., 2000; Xylourgidis et al., 2006; Takahashi et al., 2008). Our analysis suggests that nuclear accumulation of snc1, NPR1, and EDS1 is controlled in part by MOS7. *mos7-1* affects nuclear levels of all three proteins but did not affect the NES-containing CDC5, indicating that the partial loss-of-function mutation in *mos7-1* enhances NES-mediated nuclear export in plants with some degree of specificity.

Previous studies revealed nuclear pools of the plant NB-LRR proteins MLA, N, and RPS4 and showed that their nuclear accumulation is required for disease resistance (Burch-Smith et al., 2007; Shen et al., 2007; Wirthmueller et al., 2007). Future in-depth nuclear partitioning

analysis of wild-type SNC1 should resolve whether SNC1 has nuclear activity, and if so whether the nuclear activity of SNC1 is essential for activation of defense responses. We find that snc1 (an autoactivated NB-LRR protein) localizes to both the cytosol and the nucleus. Nuclear accumulation of snc1 is disproportionately reduced in *mos7-1*, and adding an NES to snc1-GFP abolishes its autoimmunity, suggesting that MOS7/Nup88 promoting retention of snc1 in the nucleus is a critical process in defence activation. It is notable that resistance mediated both by CC (RPM1 and RPS5) and TIR-NB-LRR (RPP4) proteins was strongly compromised in *mos7-1*, suggesting that some R proteins may require MOS7 for nuclear retention. Whether these tested NB-LRR receptors have a nuclear activity remains to be characterized. On the other hand, RPS4 resistance was only marginally compromised in *mos7-1*, and no detectable change in RPS4 nuclear accumulation was observed in *mos7-1* (Figure 2.10B). Further analysis should establish whether regulation of nucleocytoplasmic partitioning of NB-LRR proteins by MOS7 is a general phenomenon or whether MOS7 is selective for certain R proteins depending on their intracellular abundance, spatial dynamics, and activities.

One striking phenotype of *mos7-1* is its defect in SAR. Similar to the SAR-deficient *npr1* mutants, *mos7-1* plants had reduced *PR* gene expression and systemic resistance after SAR induction and exhibited reduced tolerance to high levels of SA. Since NPR1 nuclear accumulation is essential for SAR and lower NPR1 levels were observed in nuclei of *mos7-1* plants after SAR induction, the SAR defects in *mos7-1* are likely caused by the reduced nuclear NPR1 pool. Nuclear accumulation of EDS1 was also reduced in *mos7-1*. Reducing the nuclear EDS1 pool partially disables plant defences (A.V. García and J.E. Parker, unpublished data); therefore, lower amounts of nuclear EDS1 probably contribute to the enhanced disease susceptibility phenotype of *mos7-1*. For both EDS1 and NPR1, there is a general decrease in protein accumulation in both nonnuclear and nuclear compartments of the *mos7-1* mutant. Thus, the influence of *mos7-1* on these proteins is different to its effect on snc1. The data support selective retention of snc1 inside the nucleus by MOS7. By contrast, MOS7 may act more indirectly on EDS1 and NPR1. One scenario is that lower cellular accumulation of EDS1 and NPR1 reflects an indirect influence of MOS7 by lowering basal resistance and, thus, the flux through various positive feedback loops (Feys et al., 2001; Shah, 2003). However, *mos7-1* did not affect expression of *NPR1* or *EDS1* mRNAs, suggesting that such feedback mechanisms are not operating at the transcriptional level. Alternatively, MOS7 may act directly on these proteins, but they are subject to increased degradation after being exported from the nucleus, thereby reducing the amount in a cytosolic pool available for nuclear import.

Plant defence responses rely on dynamic translocation of signalling components across the nuclear envelope, and nucleocytoplasmic trafficking might constitute a central regulatory node for the integration of distinct signalling pathways. Although *mos7-1* exhibits strong immunity defects, overexpression of *MOS7* did not lead to enhanced disease resistance, indicating that MOS7 itself is probably not a rate-limiting defence signalling component. The identification of MOS7 reveals how the nuclear protein export pathway contributes to cellular innate immune responses and provides us with a system to test the relevance of different cellular compartments in plant pathogen recognition and defence activation.

2.4 Material and Methods

2.4.1 Plant Growth Conditions, Gene Expression Analysis, and Mutant Phenotypic Characterization

All plants were grown at 22°C under 16-hour light/8-hour night or 10-hour light/14-hour night cycles. The *snc1* suppressor screen was described previously (Zhang and Li, 2005). Gene expression analysis was done by extracting RNA from 3-week-old plate-grown or 4-week-old soil-grown plants using the Totally RNA kit (Ambion). The extracted RNA was then reverse transcribed using the RT-for-PCR kit (Clontech) or SuperScript II reverse transcriptase (Invitrogen). Expression analysis for *PR-1*, *PR-2*, and *Actin1* was as previously described by Zhang et al. (2003a) with cDNA samples being normalized by real-time PCR using *Actin1* and the QuantiTect SYBR Green PCR kit (Qiagen). For *EDS1* and *NPR1* expression analysis, 0.5 µg of total RNA were reverse transcribed using SuperScript II reverse transcriptase and 0.5 µg of oligo$(dT)_{18}$ primer at 42°C in a 20-µL reaction volume. Aliquots of 1 µL RT reaction products were subsequently used for PCR analysis with PCR conditions as follows: 94°C for 3 min and 29 cycles of 94°C for 30 s, 57°C for 30 s, and 72°C for 45 s. Single-band PCR products were analyzed by agarose gel electrophoresis and ethidium bromide staining. *Actin1* expression was used to standardize transcript levels in each sample. Gene-specific primers for RT-PCR analyses used in this study are as follows:
*PR-1*F, 5'-GTAGGTGCTCTTGTTCTTCCC-3',
*PR-1*R, 5'-CACATAATTCCCACGAGGATC-3';
*PR-2*F, 5'-GCTTCCTTCTTCAACCACACAGC-3',
*PR-2*R 5'-CGTTGATGTACCGGAATCTGAC-3';
Actin1-F, 5'-CGATGAAGCTCAATCCAAACGA-3',
Actin1-R, 5'-CAGAGTCGAGCACAATACCG-3';
Actin7-F, 5'-GGTGTCATGGTTGGTATGGGTC-3',
Actin7-R, 5'-CCTCTGTGAGTAGAACTGGGTGC-3';
EDS1A-F, 5'-ATCATCATAGCTATGAGGAACTGG-3',
EDS1A-R, 5'-CAGCTCTCTTGACGTTTGC-3'; and
NPR1-F, 5'-AGAAGACAAACGAGAACAAATTCC-3',
NPR1-R, 5'-TCAGCAGTGTCGTCTTCTCC-3'.
Infection experiments with *Pseudomonas syringae* and *Hyaloperonospora arabidopsidis* (previously *Hyaloperonospora parasitica*) were performed as described (Li et al., 2001; Feys et al., 2005). Endogenous SA levels were determined as described by Li et al. (1999).

2.4.2 Map-Based Cloning of *mos7-1*

Positional cloning of *mos7-1* was performed according to procedures described by Zhang and Li (2005). The markers used to map *mos7-1* were derived from insertion-deletion polymorphisms (Table 2.1) identified from the genomic sequences of Col and L*er* ecotypes provided by Monsanto on The Arabidopsis Information Resource homepage (Jander et al., 2002).

Table 2.1: Molecular markers used for map-based cloning of *mos7-1*.

BAC Name	Primer Name	Primer Sequence (5'→3')	Polymorphism (Col/L*er*)
K18I23	K18I23-F	AGATTCCAGCTCCGACGATG	172bp/205bp
	K18I23-R	ACGCGCCAAAAGTGCGTGTC	
MOP10	MOP10-F	CTACATGTCCATAGAACCTTC	118bp/129bp
	MOP10-R	CAGTTCTATCATGTATCCACC	
MJJ3	MJJ3-3F	TCTGACTCAATATGAGAGTCC	117bp/108bp
	MJJ3-3R	ATAACTTTATGGGCTGCAGTG	
K18J17	K18J17-F	CGCGATTAAAGATCCGGTA	119bp/107bp
	K18J17-R	TCGAGCAATAAGAGTGATTCC	
MHF15	MHF15-F	CAGAAAGGTCATGAAACCTAG	212bp/159bp
	MHF15-R	GAGCACCAATAAGGTTTCCTC	

2.4.3 Construction of Plasmids

The construct used to complement the *mos7-1* mutation was generated by PCR amplifying a genomic fragment containing the *MOS7* coding region and its promoter 1.1 kb upstream of the ATG start codon. The primers MOS7 pro-F (5'-ccaatacacaaaatactctggc-3') and MOS7-3' (5'-cgcGGATCCtgcgtccctgttacagtga-3') were used for PCR, and the fragment was subsequently cloned into *pGreen0229* (Hellens et al., 2000) to obtain *pG229-MOS7* for complementation analysis. To generate *35S*-driven *MOS7-GFP* construct, full-length *At5g05680* cDNA lacking a stop codon was cloned into the *pBS-GFP5* vector with *GFP* in frame at the C terminus (Haseloff et al., 1997). The resulting *MOS7-GFP* fusion construct was subsequently excised and cloned into *pBI1.4* containing the *35S* promoter to obtain *pBI-MOS7-GFP*. To localize mos7-1, a *35S*-driven *mos7-1-GFP* construct was generated by cloning full-length *At5g05680* cDNA lacking a stop codon from *mos7-1* using the following primers:
MOS7-CDS-F, 5'-CGGGGTACCATGAAATTTAACTTTAACGAGAC-3',
MOS7-CDS-R, 5'-CGCGGATCCCATGAAACTGCTTTCTTGC-3' into the binary vector *pCAMBIA-1300* (http://www.cambia.org.au) with *GFP* in frame at the C terminus. *NPR1-GFP* construct was generated by PCR amplifying *NPR1* cDNA without a stop codon and a 1.6-kb genomic region upstream of the *NPR1* ATG start codon. These two fragments were subsequently cloned into a modified *pGreen0229* vector that has a sequence encoding *GFP* in frame at the C terminus. To generate *promSNC1-snc1-GFP*, *pG229-snc1* (Zhang et al., 2003a) lacking a stop codon was used as the template for PCR amplification. The amplified fragment was subsequently cloned into *pGreen0229-GFP* vector with *GFP* in frame at the C terminus. All constructs were sequenced to ensure accuracy in PCR and cloning. All constructs were transformed into designated genotypes using the floral dip method (Clough and Bent, 1998) to generate transgenic lines for subsequent analysis.

2.4.4 Systemic Acquired Resistance Experiments

The infection experiment used to test SAR was performed as described by Cao et al. (1994) with minor modifications. In brief, two leaves of each 5-week-old soil-grown plant were infiltrated with *Psm* ES4326 expressing a*vrB* at an OD_{600} = 0.2 in 10 mM $MgCl_2$ to induce SAR or 10 mM $MgCl_2$ without bacteria (mock). Twenty-four hours after inoculation, the upper uninoculated leaves were challenged with *Psm* ES4326 at OD_{600} = 0.001. Leaf discs within the infiltrated systemic area were taken immediately (day 0) and 3 days after inoculation (day 3) to measure the bacterial growth in those leaves.

2.4.5 Cellular Distribution of snc1-GFP

Three-week-old plants (0.5 g) were harvested and ground to a fine powder in liquid nitrogen and mixed with 2 volumes of lysis buffer (20 mM Tris-HCl, pH 7.4, 25% glycerol, 20 mM KCl, 2 mM EDTA, 2.5 mM $MgCl_2$, 250 mM sucrose, and 1 mM PMSF). The homogenate was filtered through a 95- and 37-µm nylon netting successively. The flow-through was spun at 1500*g* for 10 min, and the supernatant consisting of the cytosolic fraction was collected and mixed with 5x Laemmli loading buffer and heated at 95°C for 5 min. The pellet was washed four times with 5 mL of nuclear resuspension buffer NRBT consisting of 20 mM Tris-HCl, pH 7.4, 25% glycerol, 2.5 mM $MgCl_2$, and 0.2% Triton X-100. The final pellet was mixed with 50 µL of 1x Laemmli buffer and heated at 95°C for 5 min. Fifty microliters of each fraction was loaded on an 8% SDS-PAGE gel for protein separation. Antibodies used for immunoblot analyses were as described: anti-Histone H3 (Feys et al., 2005), anti-GFP (Wirthmueller et al., 2007), and anti-PEPC (Noël et al., 2007). Band intensities were measured by Quantity One 4.6.1 software (Bio-Rad). The experiment was repeated five times; a figure representative of all repetitions is shown. Various exposure times on films were used to make sure that the exposure used was in the linear range.

2.4.6 NPR1 and EDS1 Protein Expression and Localization Analyses

For NPR1 protein extraction from INA-induced tissues, 4-week-old plants were sprayed to imminent runoff with an aqueous solution of 0.65 mM INA with 0.01% Silwett L-77 surfactant. Plants were harvested 24 h after being sprayed for the first time and 3 hour after being treated a second time with INA. Total protein extracts and preparation of nuclear/nuclei-depleted protein extracts were described previously (Feys et al., 2005). Anti-EDS1 antibody used for immunoblot analysis was described earlier (Feys et al., 2005).

2.4.7 Nuclear Protein Export Assay in Protoplast

Protoplast were prepared and transformed from 3- to 4-week-old Arabidopsis plants as previously described (Sheen, 2001; Yoo et al., 2007). Plasmid construct encoding NES, NLS variant of chalcone synthase were kindly provided by Thomas Merckle (Universitat Bielefeld, Germany; Haasen et al., 1999). Transformed protoplasts were kept in the dark overnight and observed using a confocal microscope the following day.

2.4.8 Accession Numbers

Sequence data from this article can be found in the GenBank/EMBL data libraries under the following accession numbers: At5g05680, NP_196187 (*MOS7*); NP_002523 (hNup88); NP_524330 (DNup88/Mbo); At4g16890 (*SNC1*); At2g14610 (*PR-1*); At3g57260 (*PR-2*); At2g37620 (*Actin1*); At5g09810 (*Actin7*); At3g48090 (*EDS1A*); and At1g64280 (*NPR1*).

2.5 Manuscript Acknowledgements

We thank the ABRC for seeds of *mos7-2* and *mos7-3* and Roger Innes for *Pst* DC3000 carrying *avrPphB*. We also thank Fred Sack and EunKyoung Lee for their help with confocal microscopy. The research is supported by funds to X.L. from the Natural Sciences and Engineering Research Council of Canada, the Canadian Foundation for Innovation, the British Columbia Knowledge Development Fund, the University of British Columbia Blusson Fund, and the University of British Columbia Michael Smith Laboratories. We are thankful for a Feodor Lynen research fellowship of the Alexander von Humboldt Foundation to M.W., and Le Fonds Québécois de la Recherche sur la Nature et les Technologies to H.G. J.E.P. is grateful for an International Max Planck Research School PhD fellowship supporting A.V.G. and Deutsche Forschungsgemeinschaft SFB 670 funding of L.W.

3 Regulation of Transcription of NB-LRR Encoding Genes SNC1 and RPP4 via H3K4 Tri-Methylation

3.1 Introduction

Plants are constantly threatened by pathogens, yet they are healthy most of the time. During their long evolutionary history, plants have developed elegant mechanisms to fend off pathogen infections. Conceptually, plants possess two layers of innate immunity (Chisholm et al., 2006; Jones and Dangl, 2006). The first layer is dependent on membrane residing pattern recognition receptors (PRRs), which recognize conserved pathogen-associated molecular patterns (PAMPs; or MAMPs, microbe-associated molecular patterns) to activate defence responses termed PAMP-triggered immunity (PTI) (Boller and Felix, 2009). Successful pathogens have evolved effectors to suppress PTI in order to promote pathogen virulence. During the arms race between plants and pathogens, plants have developed a second layer of immunity that is mediated by Resistance (R) proteins. R proteins can specifically recognize the activities of pathogen effectors and effector-triggered immunity (ETI). ETI is a robust defence response that usually results in the induction of the hypersensitive response (HR), a type of localized cell death that may contribute to restriction of pathogen proliferation. Most R proteins have a central nucleotide binding (NB) domain and C-terminal leucine-rich repeats (LRRs). These nucleotide-binding domain leucine-rich repeat-containing proteins (NLRs) share structural similarity with animal immune receptors such as Nod proteins, possibly due to convergent evolution (Ausubel, 2005). NB-LRR R proteins can be further grouped into the TIR-type (Toll/Interleukin-1-receptor-like) or the CC-type (coiled-coil) based on their different N-termini. Although resistance mediated by plant R proteins is rapid and robust, and effectively restricts pathogen growth, the molecular events surrounding R protein activation are largely unknown.

An Arabidopsis gain-of-function autoimmune mutant *snc1* (*suppressor of npr1-1, constitutive 1*) constitutively expresses defence marker *PR* genes and exhibits enhanced disease resistance against the virulent bacterial pathogen *Pseudomonas syringae* pv. *maculicola* (*Psm*) ES4326 and the oomycete pathogen *Hyaloperonospora arabidopsidis* (*H.a.*) Noco2 (Li et al., 2001). As a consequence, *snc1* plants are severely dwarfed. The autoimmune phenotypes in *snc1* are caused by a point mutation that results in a glutamic acid (E) to lysine (K) substitution in the linker region between the NB and LRR domains of a TIR-type NB-LRR protein (Zhang et al., 2003). This unique mutation renders the NLR protein more stable, leading to autoimmunity of the mutant plants (Cheng et al., 2011).

To identify components required for TIR-type NLR protein-mediated immunity, forward genetic screens were employed to identify mutants that can suppress the autoimmune phenotypes of *snc1*. From these *MOS* (*modifier of snc1*) screens, important cellular and molecular processes were found to be critical for R protein-mediated resistance. These include RNA processing, nucleo-cytoplasmic trafficking, transcriptional reprogramming and protein modifications (Palma et al., 2005; Zhang and Li, 2005; Zhang et al., 2005; Goritschnig et al., 2007; Palma et al., 2007; Goritschnig et al., 2008; Cheng et al., 2009; Germain et al., 2010; Li et al., 2010b; Zhu et al., 2010; Xu et al., 2011; Xu et al., 2012). The diverse components identified from the *MOS* screens suggest that NLR activities are regulated at multiple levels to achieve appropriate immune response.

R gene transcription is an early regulatory node in the modulation of NLR activities. The example of *SNC1* illustrates the importance and delicacy of transcriptional regulation of *R* genes. Less than two-fold increase or decrease in *SNC1/snc1* gene expression can dramatically alter the outcome of the immune response. The homozygous *snc1* mutant is severely dwarfed, while the heterozygous *snc1/SNC1* plant with 50% transcriptional activity of the *snc1* allele, is morphologically wild-type-like (Li et al., 2001). Conversely, a duplication of the *SNC1* locus in *bal* that leads to a one-fold increase in the transcriptional activity of *SNC1* results in autoimmunity (Yi and Richards, 2009). Adequate *R* gene transcription is required to mount an appropriate degree of resistance, whereas excessive *R* gene transcription results in an over-accumulation of R proteins leading to autoimmunity, which is detrimental to development and growth. Although the transcriptional regulation of *R* genes is a critical step in plant immunity, little is known about the details of the mechanisms controlling this process. Here we report the identification, characterization, and functional study of *mos9* (*modifier of snc1, 9*). MOS9 is a plant-specific nuclear protein that plays an important role in regulating the expression level of *SNC1* and *RPP4*, both TIR-type NLR-encoding genes. MOS9 was found to associate with Arabidopsis Trithorax-Related, 7 (ATXR7), a histone methyl transferase that activates *FLC* expression through tri-methylation of the fourth lysine of histone H3 (H3K4me3), close to the start codon of *FLC* (Tamada et al., 2009). We show that ATXR7 is also required for the regulation of *SNC1* and *RPP4* expression, suggesting that MOS9 functions together with ATXR7 to regulate the expression of these *R* genes.

3.2 Results

3.2.1 Identification of the *mos9* Mutant

The *mos9* (*modifier of snc1*, *9*) mutant was identified from a suppressor screen of *snc1* single mutant (Zhang and Li, 2005). The size of the *mos9 snc1* double mutant plant is much bigger than that of *snc1*, but still exhibits *snc1*-like twisted leaves (Figure 3.1A). Quantitative RT-PCR analysis showed that the elevated *PR1* and *PR2* expression in *snc1* is largely reduced by *mos9*, although not to wild-type levels (Figure 3.1B and 3.1C). The free and total salicylic acid (SA) content in *mos9 snc1* double mutant plants was noticeably lower when compared to that of *snc1* plants (Figure 3.1D and 3.1E), but still significantly higher than those of wild type. When *mos9 snc1* double mutant plants were challenged with the virulent oomycete pathogen *Ha* Noco2 or the bacterial pathogen *Psm* ES4326, they produced more spores and supported more bacterial growth than *snc1* plants but not to the level of wild-type (Figure 3.1F and 3.1G). Taken together, *mos9* partially suppresses all autoimmune phenotypes of *snc1*.

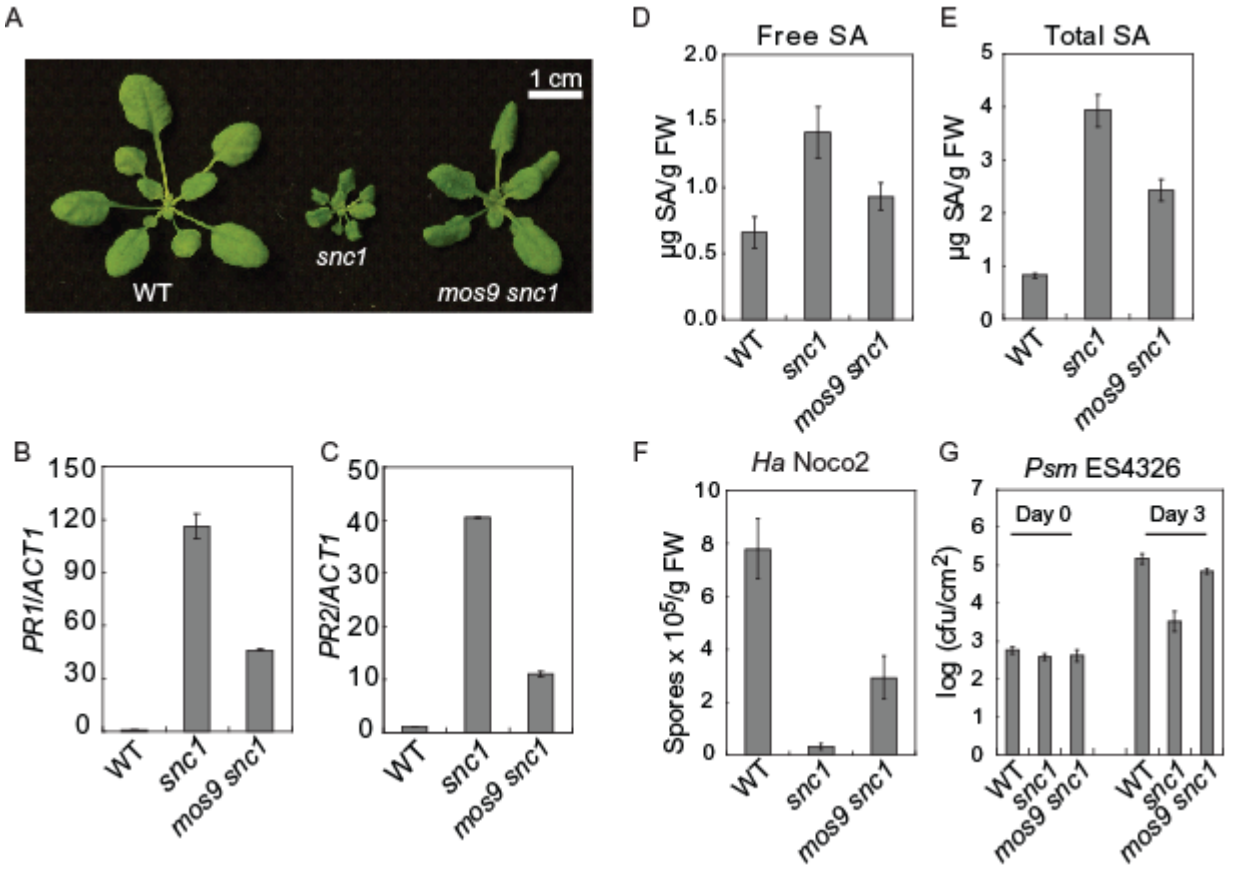

Figure 3.1: Mutation in *mos9* partially suppresses the autoimmune phenotypes of *snc1*.

(A) Morphology of four-week old soil-grown Col wild type (WT), *snc1* and *mos9 snc1* plants.
(B and C) Relative *PR1* (B) and *PR2* (C) expression in WT, *snc1* and *mos9 snc1* plants. Two-week-old seedlings grown on ½ MS were collected for total RNA extraction and reverse transcribed to obtain cDNA. The cDNA amounts were quantified with real-time PCR as described in Zhang et al., 2003.
(D and E) Free (D) and total (E) SA levels in leaves of WT, *snc1* and *mos9 snc1* plants. SA was extracted and measured from 4-week-old soil-grown plants using a previously described procedure (Li et al., 1999).
(F) Growth of *Ha* Noco2 on WT, *snc1* and *mos9 snc1* plants. Two-week-old seedlings were sprayed with *Ha* Noco2 at a concentration of 100,000 spores per ml of water. The infection was scored 7 days after inoculation. The values presented are averages of four replicates ± standard deviation.
(G) *Psm* ES4326 bacterial growth in WT, *snc1* and *mos9 snc1* plants. Leaves were infiltrated with a bacterial suspension at OD_{600} = 0.0001 (Day 0). Bacterial growth was measured 3 days after infiltration (Day 3) as previously described (Zhang et al., 2003).

3.2.2 Map-Based Cloning of *mos9*

To identify the molecular lesion in *mos9* that leads to the suppression of *snc1*, *mos9 snc1* (in Columbia [Col] accession) was crossed with Landsberg *erecta* (L*er*) with *snc1* introgressed (L*er-snc1*; (Zhang and Li, 2005)). Linkage analysis on 24 F_2 plants that had lost the *snc1* morphology revealed that the *mos9* locus is located on the top arm of chromosome 1 between markers T28P6 and F3F19 (Figure 3.2A). Further mapping with over 1,000 F_2 plants narrowed the *mos9* mutation to the region between markers T28K15 and T12C24. Unfortunately, with this population, we could not narrow the region beyond this 250 kb interval.

To further resolve the position of the *mos9* mutation, we transformed *mos9 snc1* plants with a set of overlapping TAC clones (JAtY, John Innes Center) covering the 250kb region. Only one clone, JAtY51H02, complemented the *mos9* phenotype (Figure 3.2B and Table 3.1). By subtracting the regions covered by the non-complementing clones from JAtY51H02, the *mos9* lesion could be confined to a small interval containing 6 candidate genes (Figure 3.2C). Since *mos9* was identified from a fast neutron-mutagenized population and fast neutron induces deletion mutations, the coding sequences of these candidate genes were amplified from *mos9 snc1* to test whether any of them has been deleted in the mutant. Two genes, *At1g12520* and *At1g12530*, could not be PCR-amplified from *mos9 snc1*, suggesting that *mos9* contains a deletion mutation affecting both genes. Direct transgenic complementation using the genomic region of *At1g12520* or *At1g12530* driven by their native promoters was used to test which gene is *MOS9* (Chu et al., 2005). As shown in Figures 3.2D and 3.2E, only *mos9 snc1* transgenic plants carrying *At1g12530* exhibited *snc1*-like morphology and enhanced resistance against *Ha* Noco2, indicating that *MOS9* is *At1g12530*.

Sequence analysis of *MOS9* revealed that it encodes a plant-specific protein of 193 amino acids with no discernible motifs or domains. In Arabidopsis, MOS9 has a remote paralog, At1g56420 (Figures 3.3A and 3.4). MOS9 and At1g56420 seem to have evolved at different rates (Figure 3.4). MOS9 homologs in other plant species, including *A. lyrata*, are more divergent, while those of At1g56420 are highly conserved. A survey of coding regions of MOS9 in 75 *A. thaliana* accessions revealed that there are at least 11 alleles present in the population containing 24 polymorphic sites, 15 of which are non-synonymous changes resulting in amino acid substitutions. In contrast, At1g56420 shows 7 alleles with 6 polymorphic sites, only two of which lead to amino acid substitutions. Codeml analysis (Yang, 2007) indicates that two of the individual amino acid residues (39D and 156 K) in MOS9 could be positively selected under Positive Selection Model 8 with posterior probabilities 0.703 and 0.707, respectively (Table 3.2). However, there was no indication of positive selection in At1g56420 (Table 3.3).

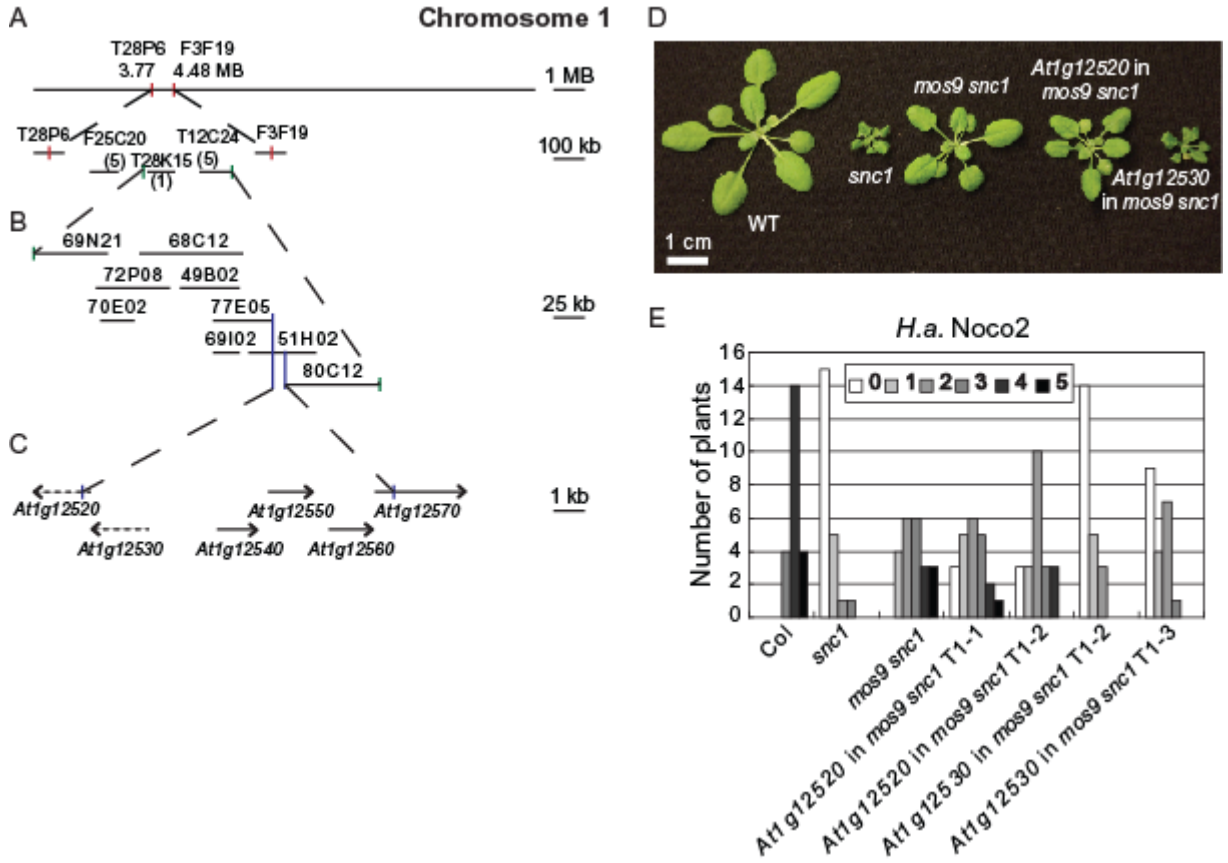

Figure 3.2: Positional cloning of *mos9*.

(A) The rough position of *mos9* locus on chromosome 1 between markers T28P6 (3.77 Mb) and F3F19 (4.48 Mb) determined by using a small mapping population. Positions of the markers used for mapping are indicated. The more defined position between markers T28K15 and T12C24 was achieved using a larger mapping population with over 1,000 plants.
(B) Overlapping JAtY clones used to transform *mos9 snc1* for complementation.
(C) Candidate genes in the final interval containing *mos9*. Arrows indicate transcription direction. Black arrows are genes that can be PCR-amplified whereas dashed arrows indicate genes which failed to be amplified using PCR.
(D) Morphology of WT, *snc1*, *mos9 snc1*, and *mos9 snc1* transformed with genomic sequences of *At1g12520* or *At1g12530* driven by their native promoters.
(E) Disease ratings of plants of the indicated genotypes infected with *Ha* Noco2. Two-week-old seedlings were sprayed with *Ha* Noco2 at a concentration of 100,000 spores per ml of water. The infection was scored 7 days after inoculation. A total of 20 plants were scored for each genotype. Disease rating scores are as follows: 0, no conidiophores on the plants; 1, one leaf infected with no more than five conidiophores; 2, one leaf infected with more than five conidiophores; 3, two leaves infected, but with no more than five conidiophores on each infected leaf; 4, two leaves infected with more than five conidiophores on each infected leaf; 5, more than two leaves infected with more than five conidiophores (Jing et al., 2011).

Table 3.1: Transgenic complementation of *mos9 snc1* using overlaying JAtY clones covering the final mapped region containing *mos9* mutation (see Figure 3.2B for details).

JAtY clones	Start (bp)	End (bp)	Number of transgenic plants	Number of *snc1*-like plants
69N21	4078012	4137095	34	2
72P08	4127703	4186821	50	1
70E02	4131084	4158419	40	0
68C12	4162550	4245243	41	2
49B02	4194672	4242296	23	0
69I02	4221297	4242295	14	0
77E05	4221297	4268656	24	4
51H02	4249648	4303405	31	26
80C12	4278603	4353946	17	0

A

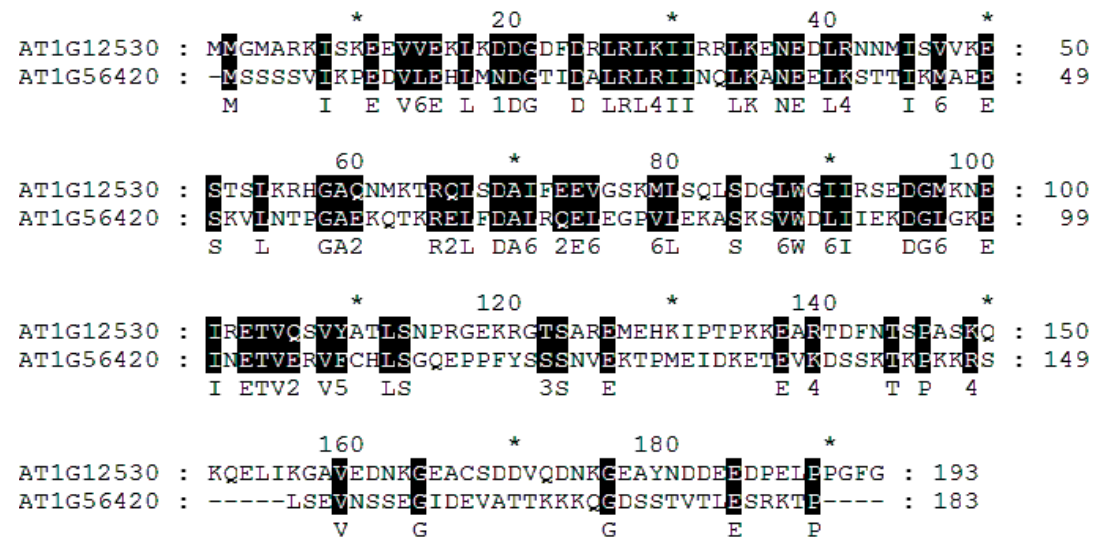

B

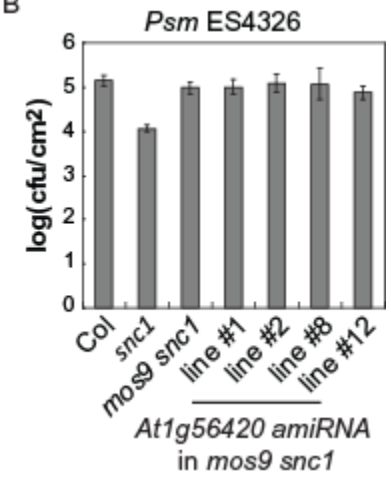

Figure 3.3: Protein sequence analysis between MOS9 and its paralog At1g56420 and contribution of At1g56420 in defence.

(A) Protein sequence alignment of MOS9 (At1g12530) and its paralog At1g56420. Similar amino acids are highlighted.
(B) *Psm* ES4326 bacterial growth in WT, *snc1* and *mos9 snc1* and four independent transgenic lines of *mos9 snc1* carrying artificial microRNA that targets *At1g56420* (*At1g56420* amiRNA).

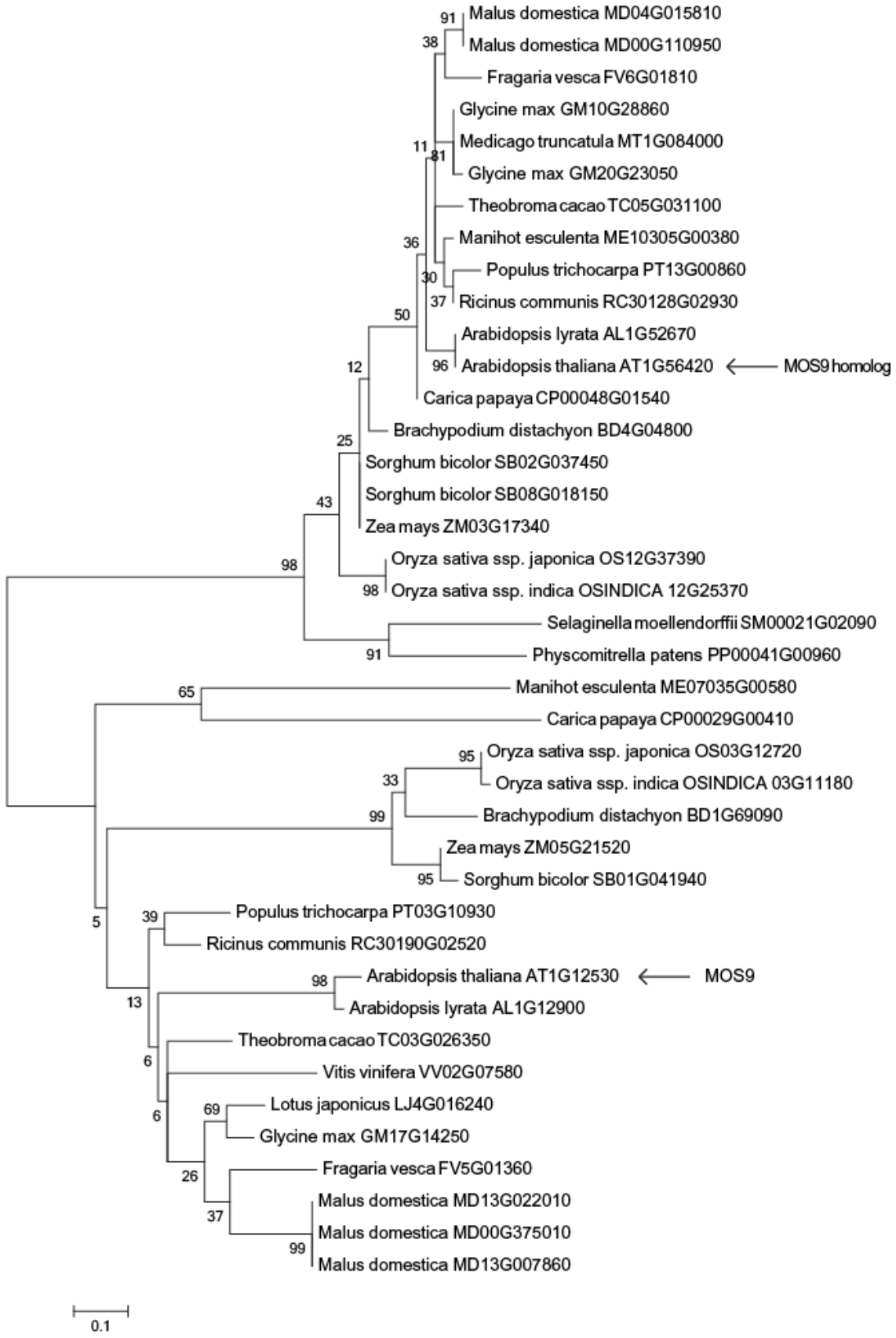
Malus domestica MD04G015810
Malus domestica MD00G110950
Fragaria vesca FV6G01810
Glycine max GM10G28860
Medicago truncatula MT1G084000
Glycine max GM20G23050
Theobroma cacao TC05G031100
Manihot esculenta ME10305G00380
Populus trichocarpa PT13G00860
Ricinus communis RC30128G02930
Arabidopsis lyrata AL1G52670
Arabidopsis thaliana AT1G56420
MOS9 homolog
Carica papaya CP00048G01540
Brachypodium distachyon BD4G04800
Sorghum bicolor SB02G037450
Sorghum bicolor SB08G018150
Zea mays ZM03G17340
Oryza sativa ssp. japonica OS12G37390
Oryza sativa ssp. indica OSINDICA 12G25370
Selaginella moellendorffii SM00021G02090
Physcomitrella patens PP00041G00960
Manihot esculenta ME07035G00580
Carica papaya CP00029G00410
Oryza sativa ssp. japonica OS03G12720
Oryza sativa ssp. indica OSINDICA 03G11180
Brachypodium distachyon BD1G69090
Zea mays ZM05G21520
Sorghum bicolor SB01G041940
Populus trichocarpa PT03G10930
Ricinus communis RC30190G02520
Arabidopsis thaliana AT1G12530
MOS9
Arabidopsis lyrata AL1G12900
Theobroma cacao TC03G026350
Vitis vinifera VV02G07580
Lotus japonicus LJ4G016240
Glycine max GM17G14250
Fragaria vesca FV5G01360
Malus domestica MD13G022010
Malus domestica MD00G375010
Malus domestica MD13G007860
0.1

Figure 3.4: Evolutionary tree of MOS9 (At1g12530) and its paralog At1g56420.

Amino acid sequences of the proteins were used to generate the tree (bootstrap = 1000).

Table 3.2: Codeml analysis of MOS9 sequences from 75 *Arabidopsis thaliana* accessions.

codeml (w = 0.4)	Model	LnL[3]	Positively selected sites (Bayes Empirical Bayes analysis)[4]	Model Comparison	2ΔL[5]	χ^2 Critical value	Degrees of freedom
75 seqs	M0	-976.52	Not allowed				
	M1	-974.70	Not allowed				
	M2	-974.63	39D (0.598); 156K (0.603)	M2 Vs. M1	0.139398	9.21	2
	M3	-975.23	N/A	M3 Vs. M0	2.582882	13.28	4
	M7	-975.35	Not allowed				
	M8	-974.63	39D (0.703); 156 K(0.707)	M8 Vs. M7	1.440424	9.21	2

Table 3.3: Codeml analysis of MOS9 paralog sequences from 74 *Arabidopsis thaliana* accessions.

codeml (w = 0.4)	Model	LnL	Positively selected sites (Bayes Empirical Bayes (BEB) analysis)	Model Comparison	2ΔL	χ2 Critical value	Degrees of freedom
74 seqs	M0	-784.39	Not allowed				
	M1	-784.70	Not allowed				
	M2	-784.39	None	M2 Vs. M1	0.605296	9.21	2
	M3	-784.39	N/A	M3 Vs. M0	0.000266	13.28	4
	M7	-785.00	Not allowed				
	M8	-784.70	None	M8 Vs. M7	0.606448	9.21	2

[3] InL 1/4 log likelihood value.
[4] Amino acid sites inferred to be under diversifying selection (Posterior probabilities are shown in parenthesis).
[5] Likelihood ratio test: 2ΔL 1/4 2(InL alternative hypothesis-InL null hypothesis).

3.2.3 Characterization of the *mos9* Single Mutant

To obtain the *mos9* single mutant, *mos9 snc1* was crossed with wild-type Col-0 plants. Lines homozygous for *mos9* and wild type for *SNC1* were selected as the *mos9* single mutant. As shown in Figure 3.5A, *mos9* is morphologically indistinguishable from wild-type plants.

To test whether *MOS9* contributes to basal defence against virulent pathogens, *mos9* plants were challenged with *Psm* ES4326 at a concentration of OD_{600} = 0.0001. Wild-type plants usually develop no disease symptoms at this low dose. Like wild-type plants, *mos9* plants support similar bacterial growth 3 days after inoculation, whereas the susceptible control, Col-*eds1*, carries 1000-time more bacteria (Figure 3.5B). Therefore, *MOS9* does not seem to contribute to basal resistance.

To determine whether *MOS9* is required for resistance mediated by other TIR-type R proteins, we challenged *mos9* single mutant plants with *H.a.* isolates Emwa1 and Cala2, and *P.s.tomato* (*Pst*) DC3000 carrying *avrRps4* that can be recognized by TIR-type RPP4 (van der Biezen et al., 2002), RPP2 (Sinapidou et al., 2004), and RPS4 (Hinsch and Staskawicz, 1996), respectively. Resistance mediated by RPP4 is compromised in *mos9* plants (Figure 3.5C). *mos9* supported growth of ~1500 spores per seedling, while less than 200 spores were observed on wild type. However, resistance mediated by RPS4 (Figure 3.5D) and RPP2 (data not shown) is not affected in *mos9* plants.

Another large class of plant NLRs is the CC-type. To test whether *MOS9* contributes to resistance mediated by CC-type NLRs, we challenged *mos9* single mutant plants with *Pst* DC3000 carrying the avirulent effectors, *avrRpt2*, *avrRpm1*, or *avrPphB* that can be recognized by plant CC-type NLRs RPS2 (Kunkel et al., 1993; Yu et al., 1993), RPM1 (Debener et al., 1991), and RPS5 (Simonich and Innes, 1995), respectively. As shown in Figures 3.5E to 3.5G, *mos9* single mutant plants were as resistant as wild-type Col-0 plants when challenged with bacterial pathogens carrying these avirulent effectors. These data suggest that *MOS9* does not contribute to resistance mediated by these CC-type NLR R proteins.

Because *mos9* only affects resistance responses mediated by *snc1* and *RPP4*, we tested whether the expression of *snc1* and *RPP4* is affected in the *mos9* mutant background. As shown in Figure 3.5H, the expression level of *snc1* is about half in the *mos9 snc1* double mutant as that in *snc1*. In addition, *RPP4* transcript is also similarly reduced in the *mos9* single mutant (Figure 3.5I). These data suggest that MOS9 affects the expression levels of *snc1* and *RPP4*.

3.2.4 Subcellular Localization of MOS9

Since protein sequence analysis of MOS9 yielded very little information, we first investigated its subcellular localization. MOS9 was expressed by its native promoter and with green fluorescent protein (GFP) fused to its C-terminus. *MOS9-GFP* fully complemented phenotypes associated with the *mos9* mutation, and *mos9* plants carrying the *MOS9-GFP* construct restored resistance against *Ha* Emwa1 (Figure 3.6A). This suggests that the construct expressing MOS9-GFP fusion protein localizes and functions as the wild-type MOS9 *in planta*. Very weak GFP signal was observed inside the nuclei in both root cells and leaf pavement cells (Figure 3.6B).

Because we could not exclude the possibility that MOS9 also localizes to other cellular compartments, we also carried out subcellular fractionation on complementing *mos9* mutant plants expressing *MOS9-GFP*. As shown in Figure 3.6C, MOS9-GFP signal can be detected in both nuclear and nuclei-depleted fractions. Taken together, MOS9 seems to be a protein predominantly localizing to the nucleus.

3.2.5 Identification of MOS9-Associated Proteins

To better understand how MOS9 affects the expression levels of *snc1* and *RPP4*, we searched for MOS9-associating proteins by affinity purification and mass spectrometry analysis. Because a large portion of MOS9-GFP protein is located inside the nucleus, the affinity purification experiments were carried out on the nuclear fractions of *MOS9-GFP* plants using anti-GFP microbeads. A nuclear fraction of wild type plants was used as negative control.

SDS-PAGE followed by silver staining showed that two proteins, one about 150 kD and the other about 65 kD co-purified with the MOS9-GFP bait protein (Figure 3.7A). Mass spectrometry analysis showed that the large protein is Arabidopsis Trithorax-Related 7 (ATXR7), a nuclear Set1 class H3K4 methylase of 159 kD and the smaller protein is High Chlorophyll Fluorescence Phenotype 173 (HCF173; 66 kD), a protein with weak similarities to the short-chain dehydrogenases/reductases (Figure 3.7B). Neither protein was detected in the wild type control sample. Because HCF173 localizes to the chloroplasts (Schult et al., 2007), it is likely a false positive interactor. We therefore focused our further analysis on ATXR7.

3.3.6 Suppression of *snc1* Mutant Phenotypes by *atxr7-1*

H3K4 methyl transferases ATXR7 and ATX1 are required for proper activation of *FLC* through H3K4 methylation (Tamada et al., 2009). The identification of ATXR7 as a protein associated with MOS9 prompted us to test whether ATXR7 is required for *snc1* mutant phenotypes. We first introduced *atxr7-1* into *snc1* to determine whether a mutation in *ATXR7* can suppress *snc1* like *mos9*. As shown in Figure 3.8, *atxr7-1* not only partially suppresses the stunted growth morphology of *snc1* (Figure 3.8A), but also suppresses the enhanced disease resistance of *snc1* against the virulent oomycete pathogen, *Ha* Noco2 (Figure 3.8B). The suppression of enhanced disease resistance of *snc1* is also reflected by reduced *SNC1* and *PR* gene expression in *atxr7-1 snc1* double mutant plants (Figure 3.8C to 3.8E). Unlike *mos9* and *atxr7*, a mutation in the *ATXR7* paralog, *ATX1*, cannot suppress the stunted growth morphology or the autoimmune phenotypes of *snc1* (Figure 3.9). These data suggest that both MOS9 and ATXR7 are required for full expression of *SNC1* and *snc1*-mediated autoimmunity. Consistent with reduced transcripts of *SNC1*, SNC1 protein levels were reduced in both *mos9* and *atxr7* single mutants when compared with that of wild type (Figure 3.8F).

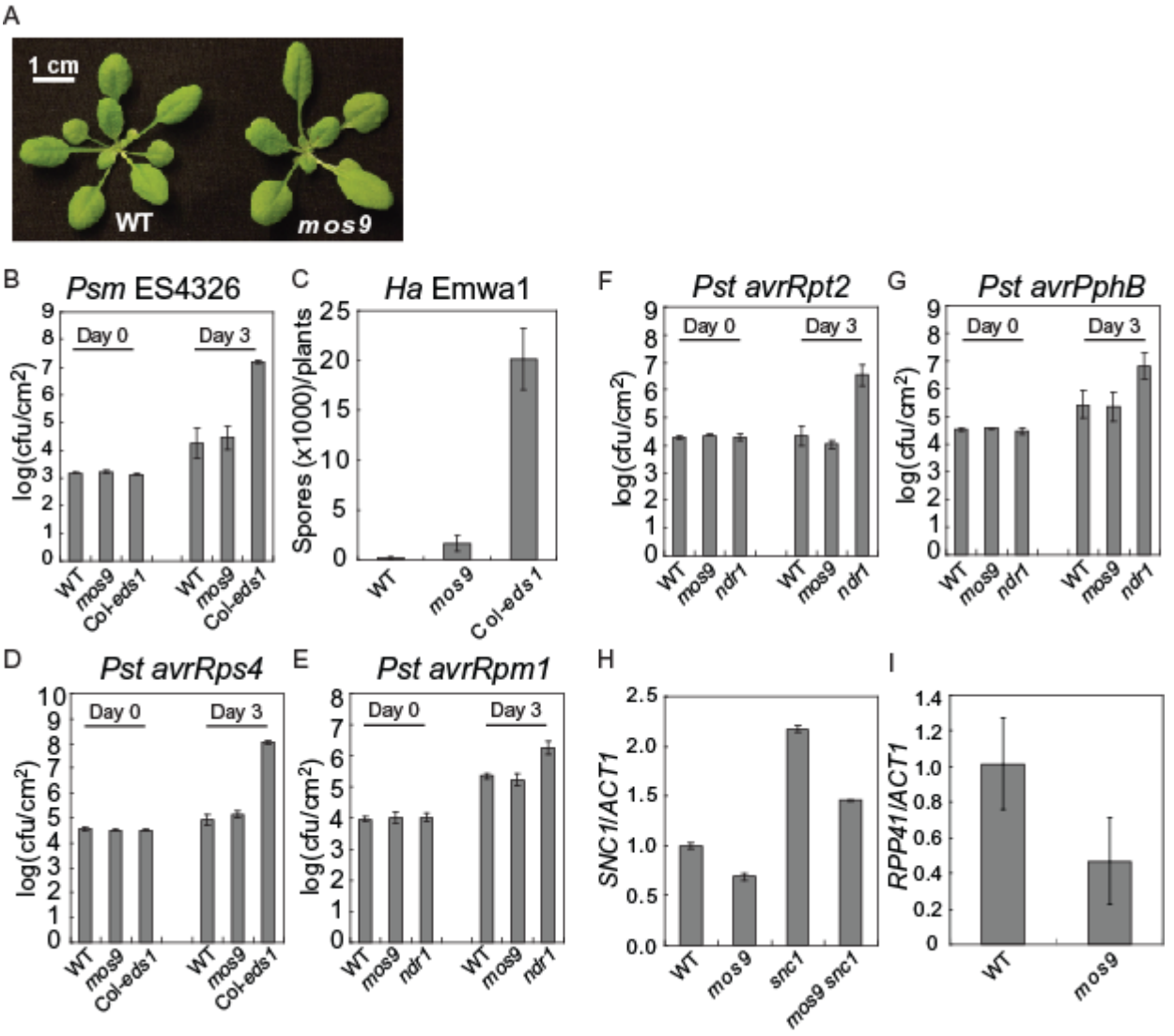

Figure 3.5: Characterization of the *mos9* single mutant.

(A) Morphology of four-week old soil-grown WT and *mos9* plants.
(B) *Psm* ES4326 bacterial growth in WT, *mos9*, and Col-*eds1* plants. Leaves were infiltrated with a bacterial suspension at OD_{600} = 0.0001 (Day 0). Bacterial growth was measured 3 days after infiltration (Day 3) as previously described in Zhang et al., 2003.
(C) Growth of *Ha* Emwa1 on seedlings of the indicated genotypes. Two-week-old soil-grown plants were sprayed with *Ha* Emwa1 at spore suspension 100,000 spores per ml of water. At least 20 plants were collected for spore counting 7 days after inoculation.
(D to G) Bacterial growth of *Pseudomonas* strains carrying avirulent effectors *avrRPS4* (D), *avrRpm1* (E), *avrRpt2* (F), and *avrPphB* (G) on the indicated genotypes. Plants from each genotype were infiltrated with a bacterial suspension at OD_{600} = 0.002. Wild type Col (WT) and Col-*eds1* or *ndr1* plants were used as controls.
(H) Relative *SNC1* and *snc1* expression level in the indicated genotypes.
(I) Relative *RPP4* expression levels in WT and *mos9*.

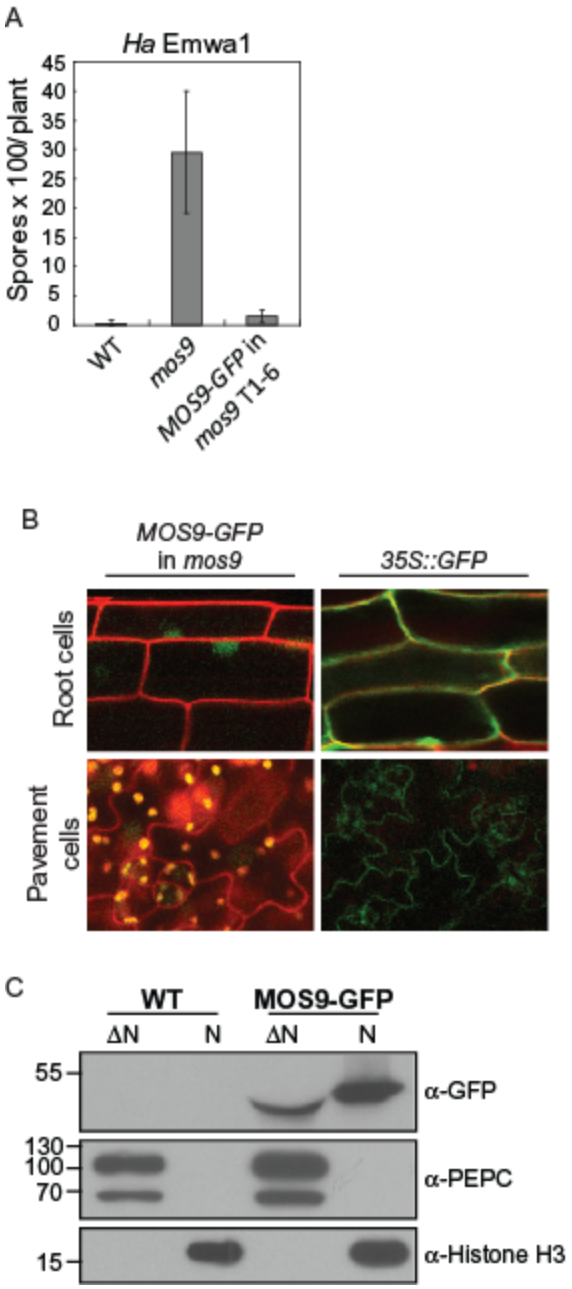

Figure 3.6: Nuclear localization of MOS9-GFP.

(A) Growth of *Ha* Emwa1 on seedlings of WT, *mos9*, and *mos9* transformed with *MOS9-GFP*. Two-week-old soil-grown plants were sprayed with *Ha* Emwa1 at a spore suspension 100,000 spores per ml of water. At least 20 plants were collected for spore counting 7 days after inoculation.
(B) Confocal microscopy images of MOS9-GFP localization in root and leaf pavement cells. Propidium iodide (PI) was used as cell wall stain.
(C) Western blot analysis of fractioned protein samples from WT and *MOS9-GFP* transgenic plants. PEPC and Histone H3 were used as cytosolic and nuclear protein markers, respectively. N: nuclear fraction; ΔN: nuclei-depleted fraction.

A

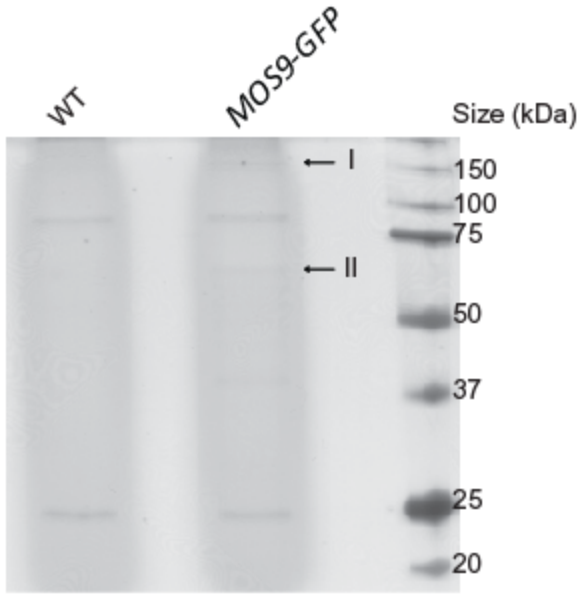

B

Band #	Identity	Predicticed localization
I	AT5G42400 (ATXR7)	Cytoplasm and nucleus
II	AT1G16720 (HCF173)	Chloroplast

Figure 3.7: Identification of proteins associated with MOS9-GFP.

(A) Silver-stained SDS-PAGE gel of the anti-GFP microbeads-immunoprecipitated protein samples from WT and MOS9-GFP transgenic plants. Two specific protein bands shown in MOS9-GFP IP sample are indicated with arrows.
(B) List of the specific proteins identified from the MOS9-GFP immuneprecipitated sample.

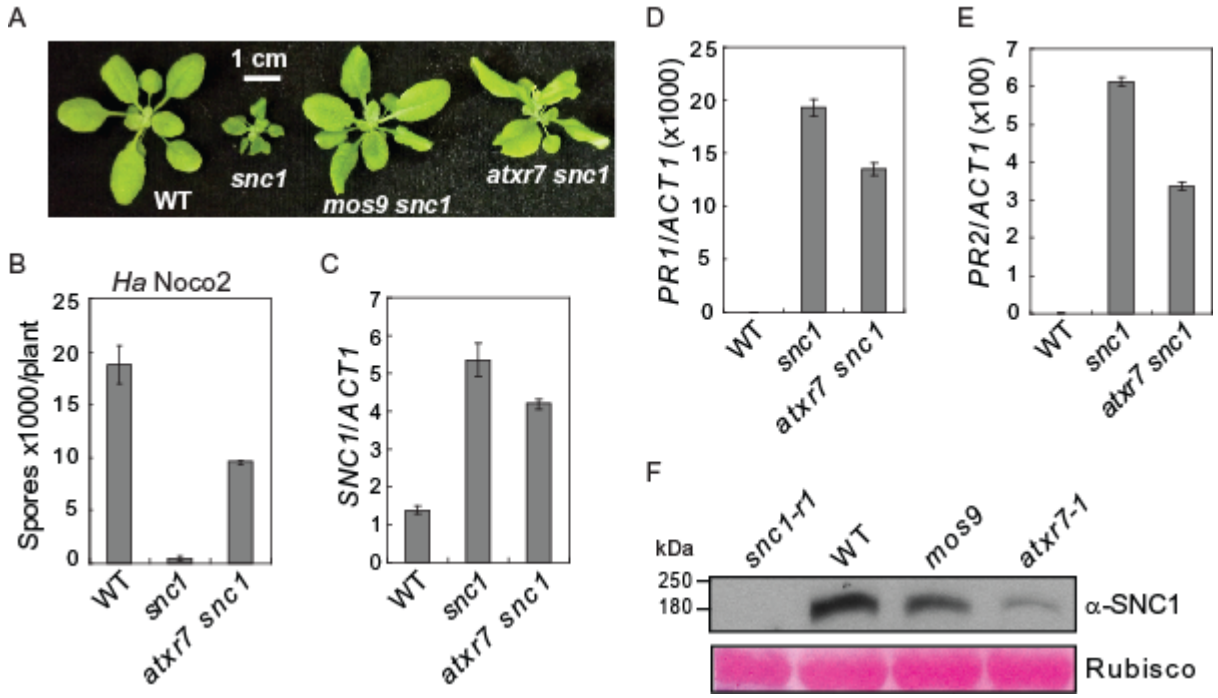

Figure 3.8: Mutation in *ATXR7* suppresses *snc1*.

(A) Morphology of WT, *snc1*, *mos9 snc1*, and *atxr7 snc1* plants. The picture shows four-week-old soil-grown plants.
(B) Growth of *H. a.* Noco2 on the indicated genotypes. Two-week-old seedlings were sprayed with *H. a.* Noco2 at a concentration of 100,000 spores per ml of water. The infection was scored 7 days after inoculation. The values presented are averages of four replicates ± standard deviation.
(C) Relative *SNC1* transcript levels in the indicated genotypes.
(D and E) Relative expression of *PR1* (D) and *PR2* (E) levels in the indicated genotypes.
(F) SNC1 protein levels in the indicated genotypes as detected by western blot analysis using a SNC1-specific antibody (Li et al., 2010a).

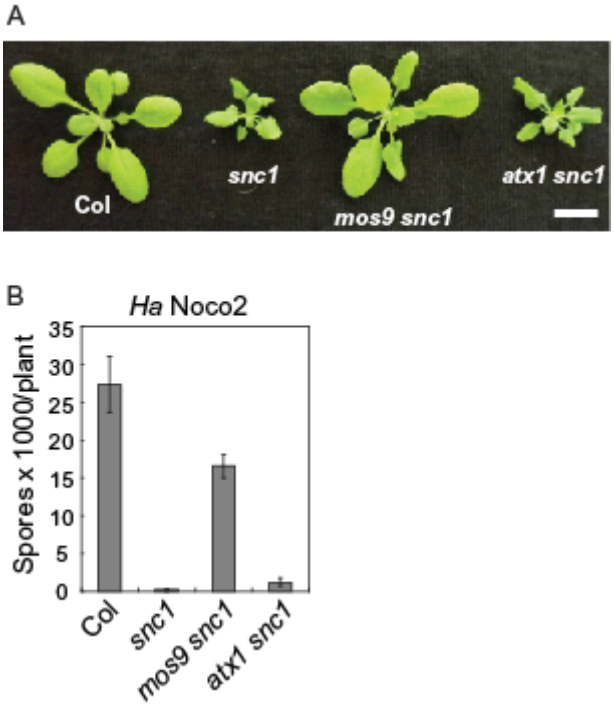

Figure 3.9: Mutation in *ATX1* does not affect *snc1*-mediated immunity.

(A) Morphology of WT, *snc1*, *mos9 snc1*, and *atx1 snc1* plants. The picture was taken on 4-week-old soil-grown plants.
(B) Growth of *H. a.* Noco2 on the above genotypes. Two-week-old seedlings were sprayed with *H. a.* Noco2 at a concentration of 100,000 spores per ml of water. The infection was scored 7 days after inoculation. The values presented are averages of four replicates ± standard deviation.

3.3.7 ATXR7 is Required for *RPP4* Expression and RPP4-Mediated Immunity

We further tested whether *ATXR7* is required for RPP4-mediated disease resistance toward *Ha* Emwa1. As shown in Figure 3.10A, *atxr7* mutant plants supported much higher growth of *Ha* Emwa1 than wild type. Similar as with *SNC1*, expression of *RPP4* is also reduced in *atxr7* (Figure 3.10B), suggesting that reduced expression of *RPP4* results in compromised resistance to *Ha* Emwa1 in *atxr7-1*.

3.3.8 Analysis of H3K4me3 Levels in the Promoter Regions of *SNC1* and *RPP4*

Because H3K4 methylation is correlated with transcriptional activation and ATXR7 functions as a H3K4 tri-methyl transferase, we further investigated whether MOS9 plays a role in the regulation of H3K4me3 levels in the promoter regions of *SNC1* and *RPP4* by chromatin immunoprecipitation (ChIP) assays using an antibody that specifically recognizes H3K4me3 marks. Real-time PCR was carried out on the DNA samples from the ChIP assays using primers specific to DNA close to the start codon of *SNC1* and *RPP4.* As shown in Figure 3.10C, *mos9* plants have reduced H3K4me3 levels in *RPP4* and *SNC1* compared to wild type, suggesting that MOS9 functions together with ATXR7 to regulate H3K4 tri-methylation.

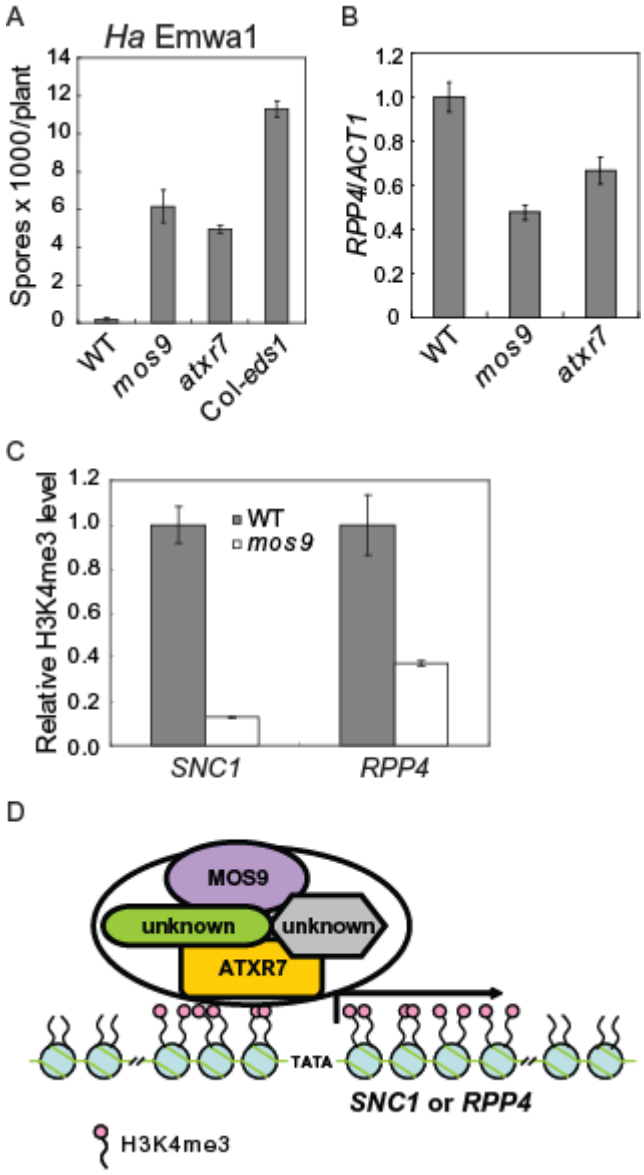

Figure 3.10: Compromised RPP4-mediated resistance in *atxr7* and *mos9* plants, and reduced H3K4me3 levels in *mos9* at *SNC1* and *RPP4* loci.

(A) Growth of *Ha* Emwa1 on WT, *mos9*, and *atxr7* mutant plants. Two-week-old soil-grown plants were sprayed with *Ha* Emwa1 at spore suspension 100,000 spores per ml of water. At least 20 plants were collected for spore counting 7 days after inoculation.
(B) Relative *RPP4* expression level in the indicated genotypes.
(C) Relative levels of H3K4me3 at *SNC1* and *RPP4* as determined by ChIP-PCR analysis in WT and *mos9* mutant seedlings. The y axis indicates relative levels of modifications. Each experiment was normalized to no antibody treatment. Bars indicate standard deviations.
(D) A conceptual model on the regulation of *SNC1* or *RPP4* expression by MOS9 and ATXR7. MOS9 associates with ATXR7 in a multi-protein complex. This association is probably responsible for the specificity of the target genes, such as *SNC1* and *RPP4*, for H3K4 bulk methylation by ATXR7.

3.4 Discussion

From the MOS forward genetics screens intended to isolate positive regulators of *snc1*-mediated immunity, we have identified *mos9*. This modifier partially suppresses the autoimmune phenotypes of *snc1*, including dwarfism, constitutive *PR* gene expression, elevated SA levels, and enhanced resistance against bacterial and oomycete pathogens. Positional cloning followed by transgene complementation revealed that *MOS9* encodes a small plant-specific protein with no known conserved domain or function. More detailed analysis on the *mos9* single mutant uncovered that MOS9 is not only required for *snc1*-mediated autoimmunity, it is also essential for *RPP4*-mediated resistance against the oomycete *Ha* Emwa1. MOS9 is not required for basal resistance. Further expression analysis of *SNC1* and *RPP4* in the *mos9* background revealed that, in *mos9* plants, the expression of both TIR-NB-LRR-encoding genes is significantly reduced, leading to attenuated resistance mediated by the encoded NLR proteins. Thus, MOS9 seems to be a nuclear regulator specifically required for proper transcription of *SNC1* and *RPP4*.

The regulation of R protein-mediated immunity is very complex. However, stringent control has to be imposed at *R* gene and R protein levels to ensure appropriate degree of immunity outcome conferred by these receptors. Despite the importance of *R* gene transcriptional regulation, its mechanisms are poorly understood. From past expression analysis and various microarray experiments, it has been taken for granted that most *R* genes are expressed at low level without pathogen interaction. Upon infection, many *R* genes, but not all, are moderately up-regulated, presumably to amplify immune signals and enhance immunity against pathogen attack (de Torres et al., 2003; Navarro et al., 2004). From the *RPP7* suppressor screen, EDM2 was identified as a transcriptional regulator of *RPP7* (Eulgem et al., 2007). EDM2 is a plant-specific nuclear protein with plant homeodomain (PHD)-finger-like domains. Loss of *EDM2* renders plants more susceptible to *Ha* Hiks1 due to reduced *RPP7* expression (Tsuchiya and Eulgem, 2010). *MOS1*, identified in the same screen as *MOS9*, encodes a conserved nuclear protein with a BAT2 domain of unknown function (Li et al., 2010b). Mutations in *MOS1* attenuate the expression of *SNC1*. The exact mechanism of how EDM2 and MOS1 regulate *R* gene transcription is unclear; however, regulation at the chromatin level is speculated for both proteins.

MOS9 is annotated as an unknown protein. Its only Arabidopsis paralog is At1g56420, which shares 39% identity and 60% similarity at amino acid level with MOS9 throughout the protein sequence (Figure 3.3A). As shown by phylogenetic analysis (Figure 3.4), MOS9 and At1g56420 are both plant-specific proteins although, curiously, they belong to two separate clades. The cluster including MOS9 exhibits longer branches, suggesting that MOS9 has evolved faster compared to its paralog. This was confirmed by the maximum likelihood analysis implemented in the CODEML package (Yang, 2007) which shows at least two amino acid residues in MOS9 may be positively selected whereas there is no indication of positive selection in the paralogs (Table 3.2 and 3.3). Faster evolving genes are often under positive selection such as biotic stresses. The evolution pattern of MOS9 somewhat mimics the fast-evolving NB-LRR-encoding *R* genes. It is possible that as a transcriptional regulator, MOS9 has coevolved with its target *R* genes to properly regulate their transcription.

The biological function of the MOS9 paralog At1g56420 is unclear. It seems to be highly conserved in higher plants (Figure 3.4). Unfortunately, there is no null knockout line available from the public resources. RNAi lines for *At1g56420* did not exhibit any obvious defects with

regards to plant morphology, growth or development. When the RNAi construct was transformed into the *mos9 snc1* double mutant, no enhanced or suppressed *snc1*-mediated autoimmunity was observed either (Figure 3.3B). These data suggest that At1g56420 does not share redundancy with MOS9. Conceivably, like MOS9, At1g56420 may be specifically involved in the regulation of proper transcription of unknown target genes.

MOS9 is a nuclear protein associating with SET domain-containing protein, ATXR7 (Figure 3.7). Although we did not detect direct protein-protein interaction between MOS9 and ATXR7 in our yeast-two-hybrid analysis (data not shown), it is possible that there exist additional intermediates between the two proteins in the same protein complex (Figure 3.10D). The SET domain was named after Drosophila *Su(var)3-9*, *Enhancer of zeste* [*E(z)*], and *Trithorax*. Highly conserved amongst eukaryotes, most of the SET domain-containing proteins exhibit histone lysine methyl transferase (HKMT) activity. In recent years, histone modifications, in particular histone methylation marks, have been shown to be associated with different transcriptional activities of their target genes. For example, H3K4, H3K36, and H3K79 methylation is correlated with transcriptional activation, whereas methylation at H3K9, H3K20 and H4K27 is associated with transcriptional silencing or repression. In addition, each lysine residue of H3 can be mono-, di-, or trimethylated, and each methylation status may have a different biological relevance (Liu et al., 2010). These add more complexity to fine-tune the expression of a target gene at various developmental stages or during different cellular responses such as an immune response.

Specifically, SET1/COMPASS/ATXR7 proteins are H3K4 methyl transferases, where H3K4me3 are most often histone marks for actively transcribed genes. There are three SET1/COMPASS orthologs in Drosophila and six in human. They serve diverse roles in regulating gene expression in various biological processes such as development, diseases including cancer, aging, and pathogenesis (Shilatifard, 2012). In Arabidopsis, *ATXR7* is the only homolog of yeast *SET1/COMPASS*, which regulates flowering time by modifying the methylation status of histones close to the ATG start codon of the master flowering time repressor *FLOWERING LOCUS C* (*FLC*) (Tamada et al., 2009). Like *mos9*, *atxr7* suppresses the stunted growth and autoimmune phenotypes of *snc1* (Figure 3.8). The expression level of *SNC1* and *RPP4* is also lower in both *mos9* and *atxr7* mutant backgrounds (Figure 3.5H, 3.8C and 3.10B). These data suggest that both MOS9 and ATXR7 are required for full expression of *SNC1* and *RPP4*, which is crucial for providing the appropriate level of immunity mediated by these TIR-NB-LRR-encoding genes. Such transcriptional control is probably brought about through ATXR7 by H3K4 bulk methylation. Since *mos9* does not exhibit any flowering time defects (data not shown), and MOS9 does not have obvious DNA-binding motifs, it is possible that MOS9 is responsible for directing ATXR7 specifically to its target genes such as *SNC1* and *RPP4*. Agreeing with this hypothesis, less H3K4me3 was detected around the promoter region of *SNC1* and *RPP4* in *mos9* mutant plants (Figure 3.10C).

One intriguing fact about *SNC1* and *RPP4* is that they are highly homologous TIR-type NLR-encoding genes residing in the *RPP4* cluster on chromosome 4 (Noel et al., 1999). We speculate that MOS9 could co-regulate these two *R* genes through histone modification due to close proximity. Such speculation is supported by an independent study of *LAZARUS 5* (*LAZ5*; (Palma et al., 2010)). While searching for mutations that can suppress the autoimmunity and spontaneous cell death phenotype of *acd11*, Palma et al. found that *acd11* is suppressed by mutations in *LAZ2* and *LAZ5*. Further studies revealed that the expression of *LAZ5*, a TIR-NB-LRR-encoding gene, is under the control of *LAZ2*, which encodes another SET domain protein,

SDG8. SDG8 is responsible for H3K36 di- and tri-methylation, also a histone mark for actively transcribing genes. Interestingly, it was found that not all *R* genes tested are affected by the *laz2* mutation. Besides *LAZ5*, the expression level of another TIR-NB-LRR-encoding gene, *At5g45230*, located very close to *LAZ5* (*At5g44870*), is also affected by the *laz2* mutation. Thus, co-expression regulation through histone modifications could be a common theme in regulating *R* gene activity, especially when they are in close proximity. This type of regulation shares resemblance with a phenomenon observed in cancer cells where tumor suppressor genes are coordinately silenced during carcinogenesis – a process called Long Range Epigenetic Silencing (LRES). LRES can affect megabases of DNA, and can result in heterochromatin formation and hypermethylation of contiguous CpG islands inside the region (Clark, 2007; Coolen et al., 2010). Recent cancer epigenomics studies revealed that LRES might be achieved through a combination of reinforcement of repressive histone marks in genomic regions that are normally silenced and gain of repressive marks in regions that are transcriptionally active in normal cells. In addition, exchange of repressive marks on genes that are inactive or expressed at low levels in normal cells was also observed. It can be speculated that co-activation of *R* genes in close proximity may be achieved through coordinated opposite types of histone modifications such as H3K4, H3K36, and H3K79 methylations that are associated with transcriptional activation. This type of coordination probably involves protein factors such as MOS9.

Due to the nature of R protein-mediated responses, it is essential that the proper level of *R* gene expression is achieved with or without pathogen infection. Without infection, *R* genes are expressed at low levels – presumably to be prepared for immunity and take part in basal defence. With pathogen attack, proper expression has to be maintained to ensure the production of enough R protein molecules to take care of pathogen recognition, defence activation, and defence amplification and maintenance. Excessive *R* gene expression would lead to autoimmunity while insufficient expression would lead to disease. Our study of MOS9 revealed that it is required for full expression of *SNC1* and *RPP4*. This positive regulation of expression likely involves H3K4me3 histone modifications by ATXR7, which associates with MOS9 (Figure 3.10D). We anticipate that there are other regulators in addition to H3K4 and H3K36 methylation events involved in *R* gene expression, and that there must also be repressive forces that hold the *R* genes under check to prevent autoimmunity. Future in-depth studies on these mechanisms will reveal the full picture of the intricate epigenetic regulation of expression of *R* genes.

3.5 Material and Methods

3.5.1 Plant Growth Conditions, Mutant Screen and Mutant Phenotypic Characterization

All plants were grown at 22°C under a 16-hour light/8-hour dark regime. *mos9 snc1* was identified from a fast neutron-treated *snc1* mutant population previously described (Zhang and Li, 2005). In brief, the M_2 population of fast neutron treated *snc1* (carrying *pPR2::GUS* reporter gene system) was first screened for suppression of *snc1*'s dwarf and stunted growth morphology. These putative mutants were further tested for suppression of constitutive defence phenotype of *snc1* by carrying out GUS staining. Mutants that showed reduced or no GUS staining were studied further.

Gene expression analysis was carried out by extracting RNA from 2-week-old plate-grown or 4-week-old soil-grown plants using the Totally RNA kit (Ambion). The extracted total RNA (~0.4μg) was then reverse transcribed using SuperScript II reverse transcriptase (Invitrogen). Expression analysis for *PR1*, *PR2*, and *Actin1* was performed as previously described by Zhang et al., 2003, with cDNA samples being normalized by real-time PCR using *Actin1* and the QuantiTect SYBR Green PCR kit (Qiagen). Gene-specific primers for RT-PCR analyses used in this study are listed in Table 3.4.

Infection experiments with *Pseudomonas* and *Hyaloperonospora* strains were performed as described (Li et al., 2001). In brief, infection of *Ha* Noco2 was performed on 2-week-old seedlings by spraying with an *Ha* Noco2 spore suspension at a concentration indicated in figure legends. Plants were maintained at 18°C under 12-hour light/12-hour dark cycles with 80% humidity, and the infection was scored 7 days after inoculation by counting the number of conidiospores per gram of tissue (when plants of different treatments are of different sizes) or per plant (when plants of different treatments are of similar sizes) using a haemocytometer or using a 0 to 5 disease rating system as previously described (Jing et al., 2011).

3.5.2 Map-Based Cloning

Positional cloning of *mos9* was performed as previously described (Zhang and Li, 2005). The markers used to map *mos9* were designed according to the insertion-deletion (InDel) polymorphisms between the genomic sequences of Col and L*er* ecotypes provided by Monsanto on The Arabidopsis Information Resource homepage (https://www.arabidopsis.org/Blast/cereon.jsp). Primer sequences for these markers are listed in Table 3.4.

3.5.3 Construction of Plasmids

For the construction of *pGreen0229-pMOS9::MOS9* which was used for transgene complementation of *mos9 snc1*, the genomic sequence covering the *MOS9* coding region plus 1.8 kb 5'-upstream and ~0.4 kb 3'-dowstream sequence was PCR amplified using primers
5'-CGCGGATCCGACGTGGAGACGATCGGGAG-3' and
5'-CCGGAATTCCATCCGACACTAGGTTCTTG-3'.
The amplified fragment was digested with BamHI and EcoRI and the digested fragment was cloned into *pGreen0229* vector.

For construction of *pCambia1305-pMOS9::MOS9-GFP* which was used for subcellular localization of MOS9-GFP and immunoprecipitation of MOS9-GFP experiments, the genomic sequence covering the *MOS9* coding region without the stop codon plus 1.8 kb 5'-upstream sequence was PCR-amplified using primers 5'-ccgGAATTCcatccgacactaggttcttg-3' and 5'-CGCggatccGCCAAAGCCAGGAGGGAGTTC-3'. The amplified fragment was digested with BamHI and EcoRI and the digested fragment was cloned into a modified *pCAMBIA1305* vector that contained a *GFP* tag.

All constructs were transformed into designated genotypes using the floral dip method (Clough and Bent, 1998) to generate transgenic lines for subsequent analysis.

3.5.4 Mutant Genotyping

Mutants described in this study were PCR genotyped using the following primers. For genotyping *mos9*, which was generated using fast neutron bombardment, primer pairs
4269391_F: GGCGTAGACGGATTGAACGG and
At1g12530_R: TGATGCATCATGAAGCCCTG were used. A fragment with ~1.4 kb can be amplified from wild-type *MOS9* but not from homozygous *mos9* mutant. Seeds of *ATX1* and *ATXR7* mutants were obtained from Dr. Amasino (Tamada et al., 2009); they are T-DNA insertional mutant alleles and were genotyped by using the primer pairs listed in Table 3.4.

3.5.5 Total Protein Extraction

For total protein extraction, 0.1 g leaf tissue of 4-week-old soil grown plants was harvested in liquid nitrogen and ground into fine powder. Samples were homogenized in extraction buffer (100mM Tris-HCl pH8, 0.2% SDS, 2% β-mercaptoethanol). After 5 min of centrifugation at 4°C at 13,200 rpm, the supernatant was transferred to a new tube containing 4x Laemmli loading buffer and heated at 95°C for 5 min. Protein samples were loaded onto SDS-PAGE and followed by western blot analysis.

3.5.6 Nuclear Fractionation

Approximately 3g of 2-week-old plate-grown plants were frozen in liquid nitrogen, ground to fine powder and homogenized in 1.5V of lysis buffer (20mM Tris-HCl, pH 7.4, 25% glycerol, 20mM KCl, 2mM EDTA, 2.5mM $MgCl_2$, 250mM sucrose) at 4°C. The homogenate was sequentially filtered through a 100- and 30-μm nylon mesh. The nuclei were pelleted by centrifugation at 1500 g for 10 minutes. The nuclei pellet was washed three times with nuclei resuspension buffer with Triton X-100 (NRBT; 20 mM Tris-HCl, pH 7.4, 25% glycerol, 2.5 mM $MgCl_2$, 0.2% Triton X-100) at 4°C, and then washed once with nuclei resuspension buffer without Triton X-100 (NRB). The final nuclei pellet was resuspended in 300μl 2x Laemmli loading buffer and heated at 95°C for 5 min. For western blot analysis, the nuclear fraction was loaded 20x more than the nuclei-depleted fraction.

3.5.7 Nuclear Extraction and Immunoprecipitation

Approximately 20 g of 2-week-old plate-grown plants were frozen in liquid nitrogen, ground to fine powder and homogenized in lysis buffer (20mM Tris-HCl, pH 7.4, 25% glycerol, 20mM KCl, 2mM EDTA, 2.5mM $MgCl_2$, 250mM sucrose) at 4°C. Two samples were prepared simultaneously. Wild-type Col plants were used as negative control, and *MOS9-GFP* transgenic plants were used for immunopurification. Nuclei were purified as above and then resuspended in 2 mL ice-cold buffer NE-2 (20mM HEPES-KOH, pH 7.9, 2.5mM $MgCl_2$, 250mM NaCl, 20% glycerol, 0.2% Triton X-100, 0.2mM EDTA, 1mM DTT and protease inhibitor cocktail (Sigma) and then subjected to sonication for 4 minutes with 5 seconds ON and 10 seconds OFF intervals to completely release nuclear proteins. The supernatant was mixed with 50 μL of anti-GFP MicroBeads (Miltenyi Biotec) and incubated at 4°C for one hour; the MicroBeads-bound target protein was magnetically precipitated on columns according to the manufacturer's instructions (μMACs; Miltenyi Biotec). The columns were then washed 8 times, each time with 1mL NE-3 buffer (20mM HEPES-KOH, pH 7.9, 2.5mM $MgCl_2$, 150mM NaCl, 20% glycerol, 0.2% Triton X-100, 0.2mM EDTA, 1mM DTT and protease inhibitors) before proteins were eluted with 60 μL 95°C pre-heated 1xSDS loading buffer. The samples were subsequently analyzed by SDS-PAGE followed by silver staining using ProteoSilver^{TM} Plus Silver Stain Kit (Sigma). The protein bands specific to MOS9-GFP were excised for MS analysis. Gel bands at the same positions of the Col treatment were also excised. The MS data from MOS9-GFP were compared with that of Col to rule out false-positive identifications.

3.5.8 Chromatin Immunoprecipitation (ChIP)

ChIP was performed as described previously (Lee et al., 2007) with some modifications. In brief, ~8g of two-week-old seedlings grown on MS plate were collected and cross-linked with 1% formaldehyde for 20 min and the cross-linking was terminated by adding 2M glycine to final concentration of 0.125M and vacuumed for 5 min. After rinsing seedlings with distilled water for 5 times, tissues were ground into fine power using liquid nitrogen and nuclei purified as described above. Nuclei pellet was re-suspended in 1mL ChIP lysis buffer (50 mM Tris-HCl, pH 8.0, 10mM EDTA, pH 8.0, 1% SDS, 1x Protease inhibitor, 1 mM PMSF) and sonicated with a Fisher 550 Sonic Dismembrator for 2 min (15 sec ON and 60 sec OFF , power 4.0) to yield DNA of an average fragment size of ~0.5 to 1.0kb. Sonicated chromatin was centrifuged at 13000 rpm at 4°C for 5 min to pellet the debris and the supernatant was collected into a new 1.5ml eppendorf tube. The soluble chromatin solution was diluted 10-fold with ChIP dilution buffer (16.7 mM Tris-HCl, pH8.0, 167mM NaCl, 1.1% Triton X-100, 1.2 mM EDTA, 1x Protease inhibitor, 1mM PMSF) to decrease the SDS concentration to 0.1%. Chromatin solution was pre-cleared with no antibody conjugated Protein A Sepharose (GE Healthcare ; 17-1279) at 4°C for 1 hour with gentle rotation and 1 µL of α-H3K4me3 (Abcam, ab8580) antibody was added to ~2.5 mL of diluted chromatin solution and incubated at 4°C overnight. 30µl pre-washed Protein A Sepharose beads (GE Healthcare; 17-1279) were added to each sample to pull down the antibody for 2 hours at 4 °C. After washing with different washing buffers, immunocomplex was eluted twice from the beads with 250 µL of elution buffer (0.1M $NaHCO_3$, 1% SDS). Eluted immunocomplex was reverse cross-linked by adding 5M NaCl to a final concentration of 200mM at 65°C overnight. Protein was removed by adding proteinase K and DNA was extracted using phenol/chloroform/isoamyl alcohol (25:24:1) followed by chloroform/isoamyl alcohol (24:1) extraction methods and precipitated by ethanol. The immunoprecipitated DNA was resuspended in TE buffer and subjected to real-time PCR analysis with primers listed in Table 3.4.

3.5.9 Phylogenetic Analyses of MOS9 and Its Homologs

To identify whether MOS9 or MOS9 paralogs have been positively selected due to selection pressure such as biotic stress, we used maximum likelihood models of codon substitution that allow for heterogeneous selection pressures among amino acid residues along the protein (Nielsen and Yang, 1998; Yang and Bielawski, 2000; Yang et al., 2000). Analyses were performed with the computer program ‘codeml’ in the PAML package (Yang, 2007).

Table 3.4: Primer sequences used in the study.

a) In/Del primers for map-based cloning of *mos9*

Primer Name	Sequence (5'→3')
T28P6_F	cgtggttttgacaacaaatgtc
T28P6_R	ggctacgtatggtatggaatgg
F3F19_F	tgaaaccctgccggaggaag
F3F19_R	tcatcccaaggtcatgctcg
T12C24_F	gcaaggcgtatgcaagtcag
T12C24_R	tcgagcacacttggctatgg
F25C20_F	gatgagaggcgagagagatg
F25C20_R	acacgaccactgcaaccacc
T28K15_F	gtcttccatcgtcccttctg
T28K15_R	atctccgccttgtgcaactc

b) Primers used for gene experssion analyses

Primer Name	Sequence (5'→3')
PR1_F	gtaggtgctcttgttcttccc
PR1_R	cacataattcccacgaggatc
PR2_F	gcttccttcttcaaccacacagc
PR2_R	cgttgatgtaccggaatctgac
SNC1_rt_F	ggtagcgacaatggaagaccacg
SNC1_rt_R	ttcagatgtccccgatgtcatccg
RPS2_rt_F	catatacagcatctccacgttg
RPS2_rt_R	tggttaagttgtgaaggctgtg
RPS4_rt_F	gctagaccatgtcttcattgga
RPS4_rt_R	tcttttcaacaggcataacgtac
RPS5_rt_F	aattggagacactacacctg
RPS5_rt_R	tcaacctttctatccattc
RPP2a_F	gttgtgggaaggaaagaaaaatc
RPP2a_R	cttcgcaaacgagaacagtc
RPP2b_F	gtacttagatgctcatgggt
RPP2b_R	tccagaagtagtcccttatg
RPP4_rt_F	gtcaacttgtcatctcttatc
RPP4_rt_R	gtcggcgaccattagacttg
Actin1_F	cgatgaagctcaatccaaacga
Actin1_R	cagagtcgagcacaataccg

c) Primers used to genotype atx1-2 and atxr7-1 mutations

Primer Name	Sequence (5'→3')
SALK_149002 (atx1-2)_LP	ggtgcacattaatttccaacg
SALK_149002 (atx1-2)_RP	gtctacacttaatatgtgtctc
SALK_149692 (atxr7-1)_LP	actgtatcttccgcttgttgc
SALK_149692 (atxr7-1)_RP	acatttcaccctccatacacc

d) Primers used in ChIP-PCR analysis

Primer Name	Sequence (5'→3')
RPP4_intron_1_F	cactcgacattgatctaatgcg
RPP4_intron_1_R	gaagctcaattctcagcctc
SNC1_chip_10C_F	cctggtgcctgaatgaattg
SNC1_chip_10C_R	atcatccgatggtgtcatag

3.6 Acknowledgements

We thank Dr. Richard M. Amasino (University of Wisconsin, Madison) for seeds of *atxr7* and *atx1*, and Dr. Kristoffer Palma and Ms. Kaeli Johnson for careful reading of the manuscript. The work described here was funded by the Canadian National Science and Engineering Research Council (NSERC) Discovery grant program, Michael Smith Laboratories, and the UBC Department of Botany William Cooper Endowment Fund.

4 Stability of Plant Immune Receptor Resistance Proteins is Controlled by SCF-Mediated Protein Degradation[6]

4.1 Introduction

Plants and animals rely on innate immunity to defend against microbial pathogen infections. Although plant surface-residing receptors often recognize common features of the microbes, intracellular receptors detect specific effectors from pathogens to initiate a downstream defense cascade (Jones and Dangl, 2006). Remarkably, plants and animals use immune sensors with similar structural features, such as nucleotide-binding (NB) and leucine rich repeats (LRR) domains (Eitas and Dangl, 2010). These immune receptors are commonly named Nod-like Receptors (NLRs; or nucleotide binding and leucine-rich repeat-containing) after the human innate immunity receptor Nod1 and Nod2 (Magalhaes et al., 2011). In plants, they are designated as NB-LRR resistance proteins (NLR R proteins). Upon detection of specific pathogen effectors, R proteins mount a quick and robust reaction, usually culminating in a hypersensitive response, a type of programmed cell death, to defend against and restrict further spread of the pathogen (Jones and Dangl, 2006). Because of the detrimental effects of R protein activation on plant cell growth and development, normally R protein-mediated immunity has to be under multiple levels of tight negative control. Overaccumulation of R proteins often leads to autoimmunity, implying the importance of stability control of R protein levels. In addition, gain-of-function mutants of NLRs, such as *snc1* (*suppressor of npr1-1, constitutive 1*) and *ssi4* (*suppressor of salicylic acid insensitivity of npr1-5, 4*), can render the NLR proteins constitutively active without pathogen interaction (Li et al., 2001; Shirano et al., 2002). These mutations are speculated to enhance the stability or activities of the NLRs. Constitutive expression of defense marker *Pathogenesis Related* (*PR*) genes, enhanced pathogen resistance, and altered plant development, such as dwarfism, are general features of plant autoimmunity.

The Arabidopsis genome contains about 170 genes encoding NLRs (Tan et al., 2007), with either Toll/IL-1 receptor (TIR) or coiled-coil (CC) domains at their N terminus. The detailed activation mechanism of NLR R proteins is unclear. During the past decade, intensive studies on RAR1, SGT1, and HSP90 using genetic and biochemical approaches established these components as members of fold and stabilize NLR R proteins (Shirasu, 2009; Zhang et al., 2010). Interestingly, mammalian SGT1 and HSP90 were also shown to be required for NLR mediated immune responses. Some NLRs, including Nod1 and Nod2, form complexes with HSP90 and SGT1 (Mayor et al., 2007).

Aside from the positive roles SGT1 plays in R protein folding, it is also involved in the negative regulation of R protein stability. A loss-of-function mutation in SGT1b restores reduced accumulation of CC-type NLR RPS5 in *rar1* mutant plants (Holt et al., 2005). In addition, level of SNC1 is increased in *sgt1b* mutant plants. Recently, the evolutionarily conserved SRFR1 was shown to interact directly with SGT1 (Li et al., 2010). Loss-of-function of *SRFR1* results in increased accumulation of SNC1 and activation of SNC1-mediated defence responses (Kim et al.,

[6] A version of this chapter has been published. Yu Ti Cheng, Yingzhong Li, Shuai Huang, Yan Huang, Xinnian Dong, Yuelin Zhang and Xin Li. (2011) *Proceedings of the National Academy of Sciences USA* 108(35):14694-9.

2010; Li et al., 2010). However, the mechanism on how SGT1 and SRFR1 negatively regulate the accumulation of R proteins is unclear.

Besides interactions with HSP90 and RAR1, SGT1 was also shown to associate with SKP1 and CULLIN1 (CUL1) (Azevedo et al., 2002; Shirasu, 2009), members of the SCF (SKP1-CUL1-F-box protein) E3 ubiquitin ligase complex that targets specific substrate proteins for ubiquitination and most often subsequent protein degradation. The F-box protein usually interacts directly with the protein substrate and serves as the substrate determinant of SCF. The association between SGT1 and SCF suggests potential connections between SCF and R protein-mediated immunity. Here we provide experimental evidence that Arabidopsis F-box protein CPR30/CPR1 targets NLR proteins SNC1 and RPS2 for degradation, revealing how some NLR R protein levels are controlled mechanistically.

4.2 Results

4.2.1 *snc1* Mutation Affects the Stability of SNC1

The gain-of-function mutant *snc1* carries a mutation in *SNC1*, an NLR *R*-like gene that leads to constitutive activation of defense responses in Arabidopsis (Li et al., 2001; Zhang et al., 2003). Like other TIR-type R proteins, *snc1* signals through *PAD4* (Wiermer et al., 2005). Mutations in *PAD4* can completely suppress the dwarfism of *snc1* caused by autoimmunity (Figure 4.1A). To investigate how the E552 to K552 change in the linker region causes constitutive activation of SNC1, we first examined the *snc1* transcript level in the mutant and found only a moderate increase (Figure 4.1B). This increase is fully suppressed when *PAD4*, an essential signaling component downstream of *SNC1*, is mutated (Figure 4.1B), indicating that the increased *snc1* transcription is caused by feedback up-regulation from downstream defense signaling. With the availability of an antibody specific to the endogenous SNC1 protein (Li et al., 2010), we analyzed snc1 protein levels in *snc1* and *snc1 pad4* plants. To our surprise, snc1 protein levels are still considerably higher in the *snc1 pad4* double mutant plants than in the wild-type (Figure 4.1C), suggesting that the *snc1* mutation renders the R protein more stable.

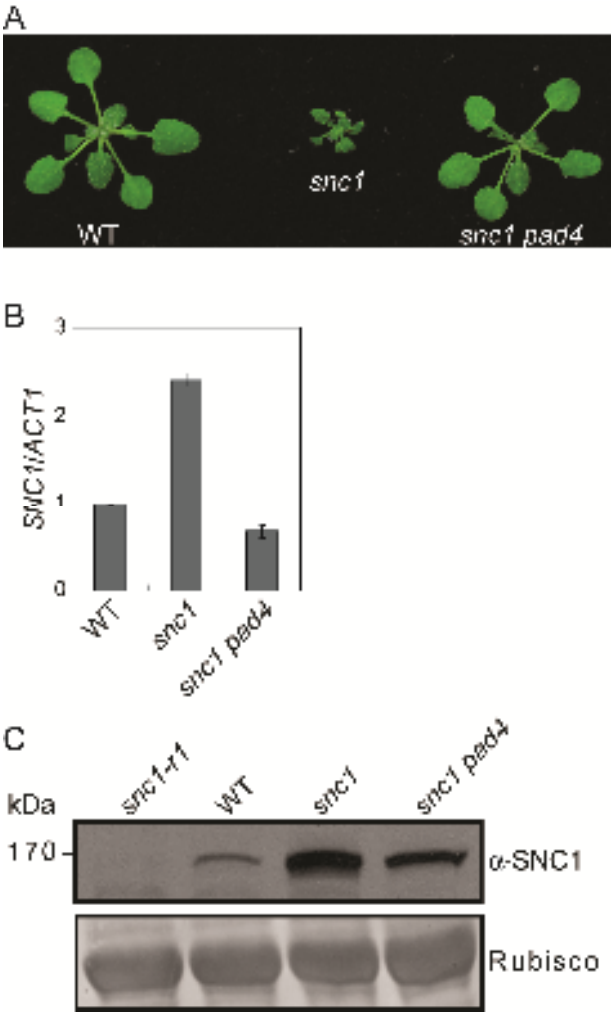

Figure 4.1: Increased snc1 protein levels in *snc1* and *snc1 pad4* double mutant.

(A) Morphology of wild-type Col (WT), *snc1* (gain-of-function allele of *SNC1*), and *snc1 pad4* double-mutant plants (Zhang et al., 2003). The picture was taken with 4-week-old soil-grown plants. (B) qRT-PCR analysis of SNC1 transcript levels in WT, *snc1*, and *snc1 pad4* plants. (C) Western blot analysis of SNC1/snc1 protein levels in *snc1-r1* (a loss-of-function deletion allele of *SNC1*), WT, *snc1*, and *snc1 pad4* plants (Zhang et al., 2003). Rubisco levels serve as loading control.

4.2.2 *cul1-7* Exhibits Increased SNC1 Level and Constitutive Defence Responses

Because a mutation in *SGT1b* also results in increased SNC1 protein level and SGT1 associates with SKP1 and CUL1 (Azevedo et al., 2002; Shirasu, 2009; Li et al., 2010), two shared members of the SCF E3 ubiquitin ligase complex, we asked whether the stability of SNC1 could be controlled by SCF-mediated protein degradation. In Arabidopsis, null mutations in *CUL1* are lethal (Shen et al., 2002). A partial loss-of-function allele of *CUL1*, *cul1-7*, was found to exhibit a dwarf phenotype similar to *snc1* (Gilkerson et al., 2009) (Figure 4.2A). In *cul1-7*, the T510 to I510 substitution seems to affects the C terminus of the protein, as well as the stability of CUL1, thus resulting in the misregulation of SCFs. The mutant exhibited accumulation of target proteins of many known SCF complexes, including AUS/IAA1 and RGA1 for auxin and gibberellic acid signaling, respectively (Gilkerson et al., 2009). Additionally, *cul1-7* plants express high levels of defence-marker *PR* genes, *PR1* and *PR2* (Figure 4.2B and C), suggesting that the mutation causes activation of defence responses. The dwarfism of *cul1-7* is more severe than that of *snc1* and can be partially complemented by a transgene expressing the CUL1-FLAG fusion protein (Gilkerson et al., 2009) (Figure 4.2A). Although the transcript level of *SNC1* in *cul1-7* is not significantly different from that of wild-type (Figure 4.2D), Western blot analysis showed that the SNC1 protein level in *cul1-7* was much higher than that in wild-type and this increased accumulation of SNC1 can be partially complemented by the *CUL1-FLAG* transgene (Figure 4.2E), indicating that CUL1 contributes to the control of SNC1 levels.

4.2.3 SNC1 Protein Levels are Increased in *cpr1* and *cpr30* Mutants

The substrate specificity of the SCF complexes is most often determined by the F-box proteins. Previously it was shown that mutations in the F-box protein, CPR30 [At4g12560; Constitutive *PR* gene expression, 30 (*cpr30*)], lead to constitutive activation of *PR* genes, accumulation of the defence hormone salicylic acid, and a dwarf phenotype strikingly similar to that of *snc1* (Gou et al., 2009) (Figure 4.3A). Western blot analysis revealed that SNC1 overaccumulates in the *cpr30* mutant plants (Figure 4.3B). Another well-known mutant with constitutive defence responses and *snc1*-like morphology is *cpr1* (Bowling et al., 1994) (Figure 4.3A). Although *cpr1* was isolated over 15 years ago, its identity was unknown. Interestingly, similar to the *cpr30* alleles, the SNC1 protein level in *cpr1* was much higher than that in wild type (Figure 4.3B). The levels of SNC1 in *cpr1* and two alleles of *cpr30* are very similar.

4.2.4 *cpr1* and *cpr30* are Allelic Mutations

Because *cpr1* and *cpr30* are both recessive mutations mapped to chromosome 4 (Bowling et al., 1994; Gou et al., 2009), we crossed *cpr1* and *cpr30-2* to test for allelism. As shown in Figure 4.3C, *cpr1* and *cpr30-2* failed to complement in F1, indicating that they are allelic to each other. Because *cpr1* was identified as the founding member of the *cpr*-type mutants, for simplicity and to avoid confusion in the literature, we renamed *cpr1* as *cpr1-1*, the allele obtained by Gou et al.

(Gou et al., 2009) (previously named *cpr30-1*) as *cpr1-2*, and the T-DNA allele (SALK_045148; previously named *cpr30-2*) as *cpr1-3*. Further sequence analysis of *cpr1-1* revealed a G to A point mutation in *At4g12560*. This mutation is located at an intron-exon junction (Figure 4.4), leading to a shift of the splicing site which results in a reading frame change in the gene. When a construct expressing *At4g12560* under the control of a *35S* promoter was transformed into *cpr1-1*, all transgenic plants exhibited wild-type morphology (Figure 4.3D); this confirms that the *cpr1-1* mutant phenotype was caused by the mutation in *At4g12560*.

4.2.5 Constitutive Defence Responses in *cpr1-3* Are Largely Suppressed by Knocking Out *SNC1*

To test whether the increased SNC1 protein accumulation contributes to the activation of defence responses in the *cpr1* mutants, we crossed *snc1-r1*, a loss-of-function deletion allele of *SNC1* (Zhang et al., 2003), into *cpr1-3*. As shown in Figure 4.5A, the *snc1-r1* mutation reverted *cpr1-3* to wild-type morphology. Analysis of *PR* gene expression showed that constitutive expression of both *PR1* and *PR2* was reduced in *snc1-r1 cpr1-3* (Figure 4.5B and C). In addition, enhanced resistance against the virulent oomycete pathogen *Hyaloperonospora arabidopsidis* Noco2 in *cpr1-3* was also attenuated by the *snc1-r1* mutation (Figure 4.5D). These data suggest that overaccumulation of SNC1 in *cpr1-3* is one of the main factors leading to the *cpr1* autoimmune mutant phenotypes.

4.2.6 Overexpression of *CPR1* Results in Reduced snc1 Protein Levels and Suppression of *snc1* Mutant Phenotypes

Increased accumulation of SNC1 protein in *cpr1* mutants and suppression of *cpr1-3* phenotypes by *snc1-r1* suggest that CPR1 might target SNC1 for degradation. Because the F-box proteins are usually the limiting factor in SCF-mediated target protein degradation, we tested whether overexpression of *CPR1* would reduce the accumulation of SNC1 by overexpressing *CPR1* in the *snc1* mutant background. As shown in Figure 4.6A, *snc1* transgenic lines T1-5 and T1-6 carrying *35S::CPR1* exhibit wild type-like morphology. Both lines expressed high levels of *CPR1* (Figure 4.6B) and modestly reduced level of *SNC1* (Figure 4.6C) because of reduced feedback up-regulation in *snc1*. In addition, enhanced resistance against *H. arabidopsidis* Noco2 (Figure 4.6E) and constitutive *PR* gene expression (Figure 4.6F and G) in *snc1* were completely suppressed in the *CPR1* overexpression lines. Western blot analysis revealed that snc1 protein accumulation was clearly reduced even below the wild-type level in the two *CPR1* overexpression lines (Figure 4.6D). These data support that CPR1 is the F-box protein targeting SNC1 for degradation.

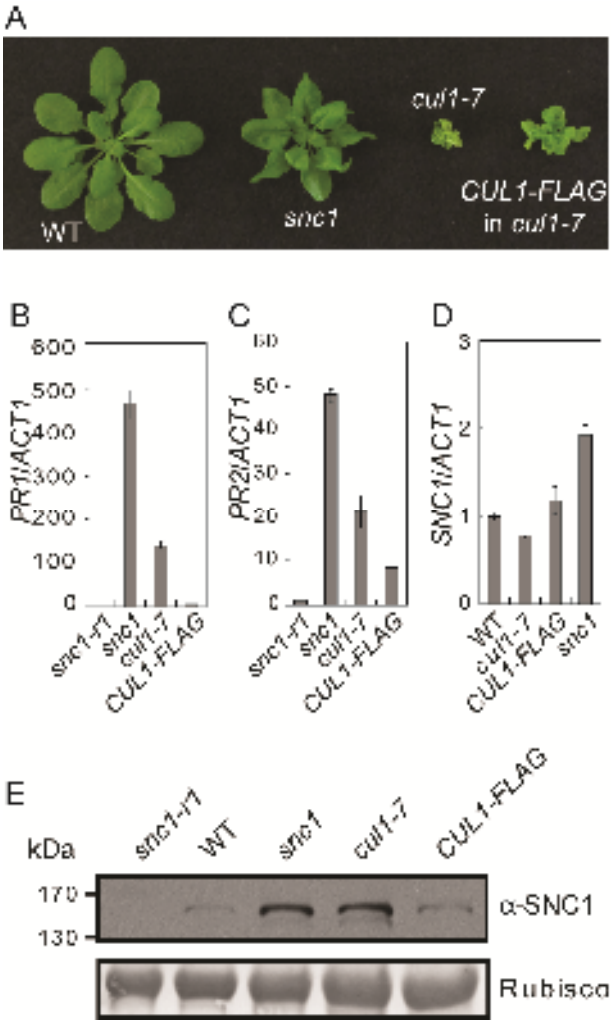

Figure 4.2: Increased accumulation of SNC1 proteins in *cul1-7* mutant.

(A) Morphology of WT, *snc1*, *cul1-7* and *cul1-7* carrying the partially complementing transgene *CUL1-FLAG*. The picture was taken with five-week-old soil-grown plants.
(B-C) qRT-PCR analysis of the expression of *PR1* (B) and *PR2* (C) in the indicated genotypes.
(D) Western blot analysis of SNC1/snc1 protein levels in *snc1-r1*, wild type (WT), *snc1*, *cul1-7* and a transgenic line expressing *CUL1-FLAG* in *cul1-7* (*CUL1-FLAG* in *cul1-7*) (Gilkerson et al., 2009).

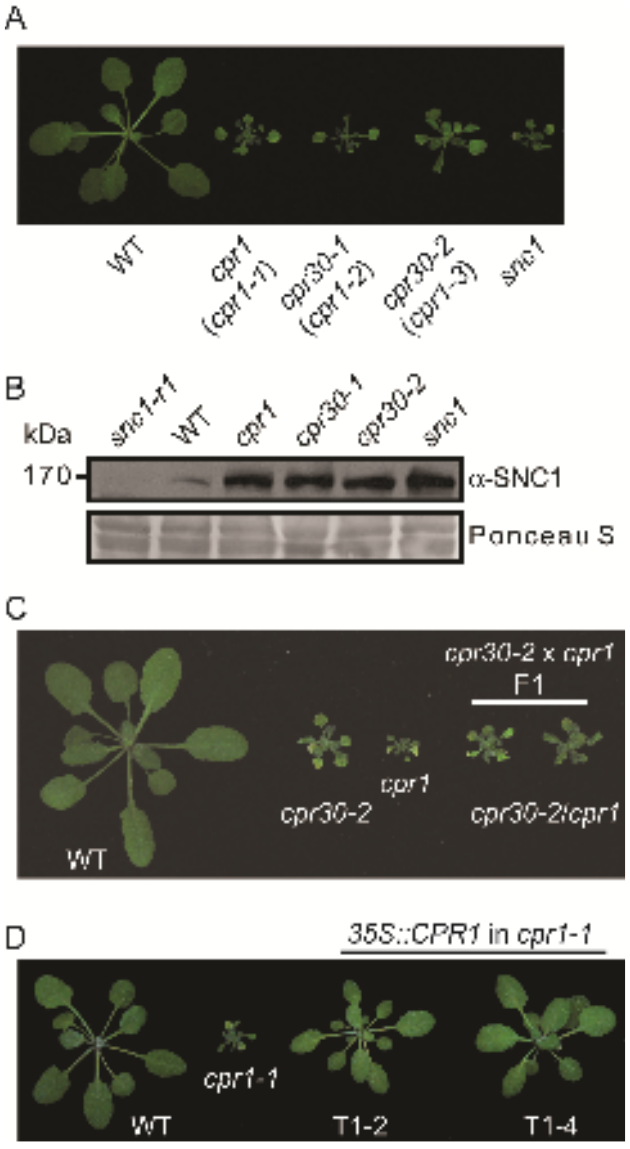

Figure 4.3: *cpr1* and *cpr30* are alleles of *At4g12560*.

(A) Morphology of WT, *cpr1* (later renamed to *cpr1-1*), *cpr30-1* (renamed to *cpr1-2*), *cpr30-2* (renamed to *cpr1-3*), and *snc1*.
(B) Western blot analysis of SNC1 protein levels in *cpr1* (renamed *cpr1-1*), *cpr30-1* (renamed *cpr1-2*) and *cpr30-2* (renamed *cpr1-3*). *snc1-r1*, wild type (WT) and *snc1* plants were used as controls.
(C) Allelism test between *cpr30-2* and *cpr1*. Morphology of two F1 plants from the cross between *cpr30-2* and *cpr1*, with WT, *cpr30-2* and *cpr1* plants as controls.
(D) Complementation of *cpr1-1* by the *CPR1* transgene under *35S* promoter. Morphologies of two independent transgenic lines (T1-2 and T1-4) are shown.

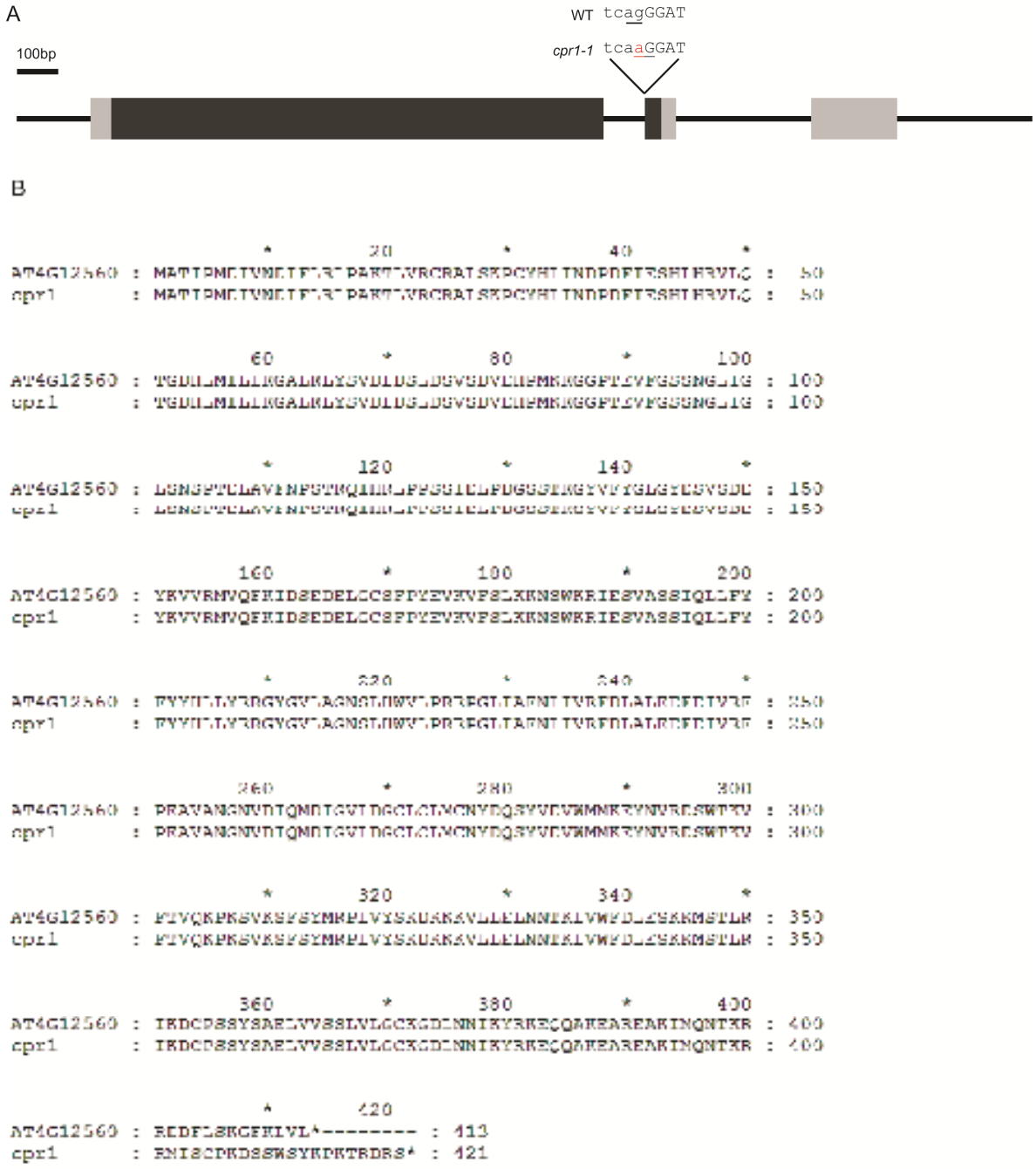

Figure 4.4: Sequence analysis of cpr1.

(A) Gene structure of At4g12560. Gray boxes indicate untranslated regions, black boxes are exons, and black lines are either intergenic region or introns. Uppercase letters are exons and lowercase letters are introns. Letters with underline are predicted splicing acceptor sites. (B) Protein alignment of wild-type CPR1 and cpr1-1. The asterisks at the end of the amino acid sequences indicate stop codons.

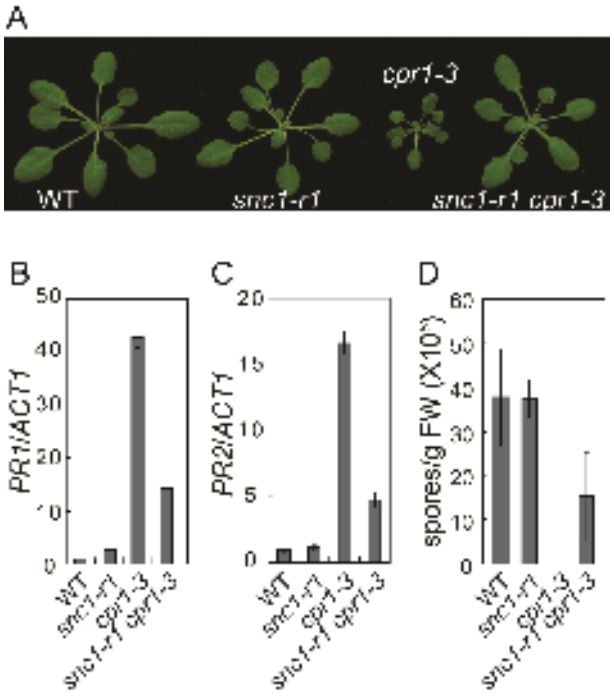

Figure 4.5: CPR1 regulates SNC1-mediated defense responses.

(A) Morphology of WT, *snc1-r1*, *cpr1-3* and *snc1-r1 cpr1-3* mutant plants.
(B-C) qRT-PCR analysis of *PR1* (B) and *PR2* (C) expression in *snc1-r1*, *cpr1-3* and *snc1-r1 cpr1-3*.
(D) Growth of *H. a.* Noco2 spores on the indicated genotypes.

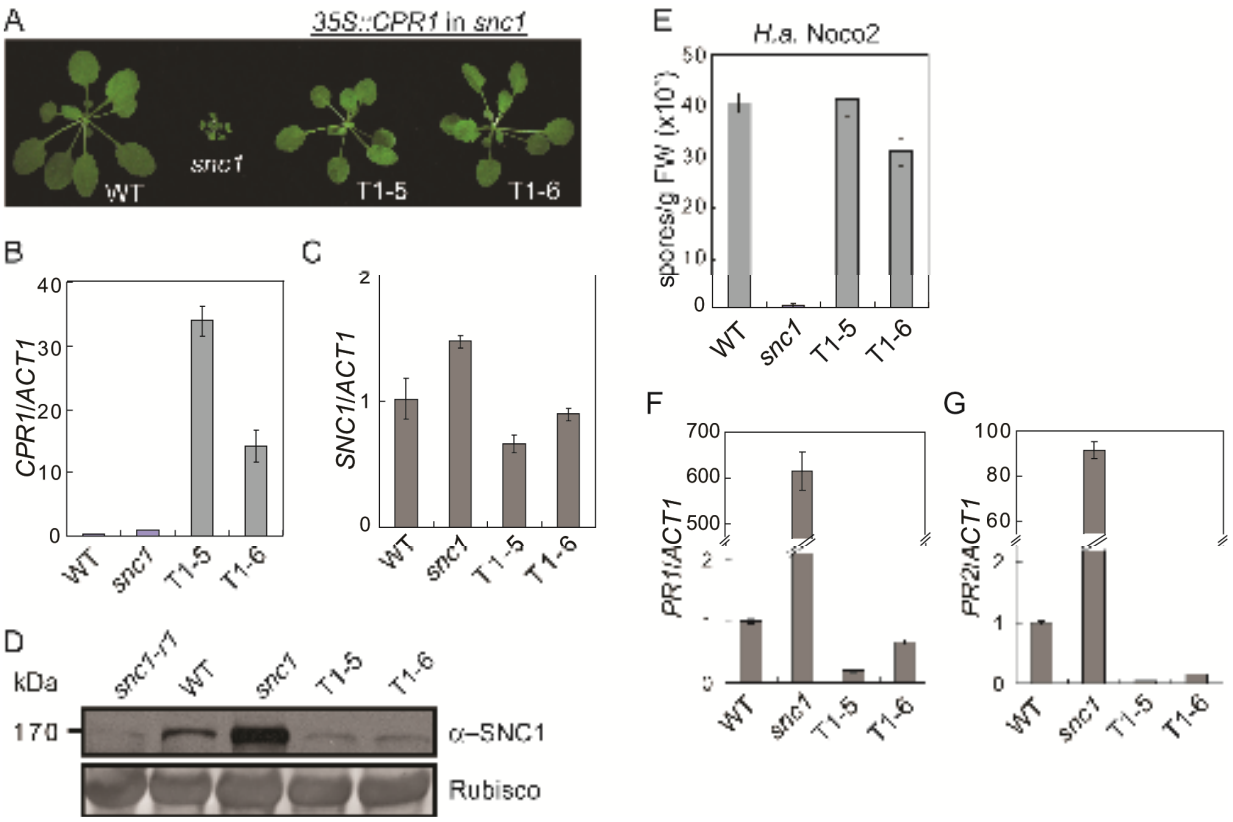

Figure 4.6: Overexpression of *CPR1* in *snc1* alleviates the enhanced disease resistance phenotypes of *snc1* and reduces the protein levels of snc1.

(A) Morphology of WT, *snc1* and two independent transgenic lines (T1-5 and T1-6) overexpressing *CPR1* in the *snc1* mutant background.
(B) Expression levels of *CPR1* in the indicated genotypes.
(C) Expression levels of *SNC1* in the indicated genotypes
(D) Western blot analysis of snc1/SNC1 protein levels in the transgenic lines overexpressing *CPR1*. *snc1-r1*, wild type (WT) and *snc1* plants were used as controls.
(E) Growth of oomycete *H. a.* Noco2 spores on the indicated genotypes.
(F-G) Expression levels of *PR1* (F) and *PR2* (G) in *snc1* transgenic lines overexpressing *CPR1*.

4.2.7 Overexpression of *CPR1* Affects R Protein-Mediated Resistance

Although *snc1-r1* completely suppresses the dwarfism of *cpr1-3*, constitutive *PR* gene expression and enhanced resistance against *H. arabidopsidis* Noco2 in *cpr1-3* is only partially attenuated by *snc1-r1* (Figure 4.5), suggesting that CPR1 may also target R proteins other than SNC1 for degradation. The residual enhanced resistance in *snc1-r1 cpr1-3* is probably caused by increased accumulation of the other R proteins. To test this hypothesis, we generated transgenic lines overexpressing *CPR1* in the wild-type Columbia (WT) background (Figure 4.7A) and challenged the transgenic plants with pathogens carrying different effectors that activate specific R protein-mediated resistance. The two *CPR1* overexpression lines were slightly more susceptible to the virulent bacterial pathogen *Pseudomonas syringae* pv. *tomato* DC3000 (Figure 4.7B). Overexpression of *CPR1* also has modest effects on resistance mediated by RPS5, RPS4, RPP2, and RPP4 (Figure 4.7C to F). In contrast, resistance mediated by RPS2 and RPM1 is severely compromised when *CPR1* is expressed at high levels (Figure 4.8A and B), suggesting that CPR1 may also target R proteins, such as RPS2 and RPM1, for degradation. Because the expression levels of *RPS2* and *RPM1* are not significantly affected in these transgenic plants, the defects in RPS2- and RPM1-mediated resistance in *CRP1* overexpressing lines are not likely caused by reduced *RPS2* and *RPM1* transcription (Figure 4.8C and D).

4.2.8 CPR1 Regulates the Stability of RPS2

RPS2 and RPM1 are both CC-type NLR R proteins. RPS2 was chosen for further testing because the *RPS2-HA* transgenic line was available to us (Axtell and Staskawicz, 2003) (a kind gift of B. Staskawicz, University of California at Berkeley). To test whether over-expression of *CPR1* affects the accumulation of RPS2, we transformed plants expressing the RPS2-HA fusion protein with a construct expressing CPR1 with a C-terminal 3×FLAG tag, under its own promoter. As shown in Figure 4.8E, increased expression of CPR1-FLAG protein correlated with reduced accumulation of RPS2-HA. Next we tested whether loss of *CPR1* function leads to increased accumulation of RPS2 by crossing *cpr1-3* into the *RPS2-HA* transgenic line. Western blot analysis showed that RPS2-HA protein level dramatically increased in *cpr1-3* (Figure 4.8F). Because *RPS2* transcript level in *cpr1-3* was only moderately higher than in wild-type (Figure 4.8G), the increase in RPS2-HA protein level is most likely due to increased stability of RPS2-HA in *cpr1-3*. A similar approach was used to test for the correlation between CPR1 and RPS4, where minor effect was observed for RPS4-mediated immunity in *CPR1* overexpression lines (Figure 4.7D). When we transformed the *RPS4-HA* transgenic line (Wirthmueller et al., 2007) (a gift of Jane Parker, MPI, Köln) with the same *CPR1-3×FLAG* construct. As shown in Figure 4.9, the RPS4-HA level remains the same in *cpr1* and *CPR1* overexpression backgrounds as in wild type. In contrast, when the same samples were probed with anti-SNC1 antibody, reverse correlation between CPR1 and SNC1 levels was observed (Figure 4.9). Thus CPR1 does not seem to regulate RPS4 stability.

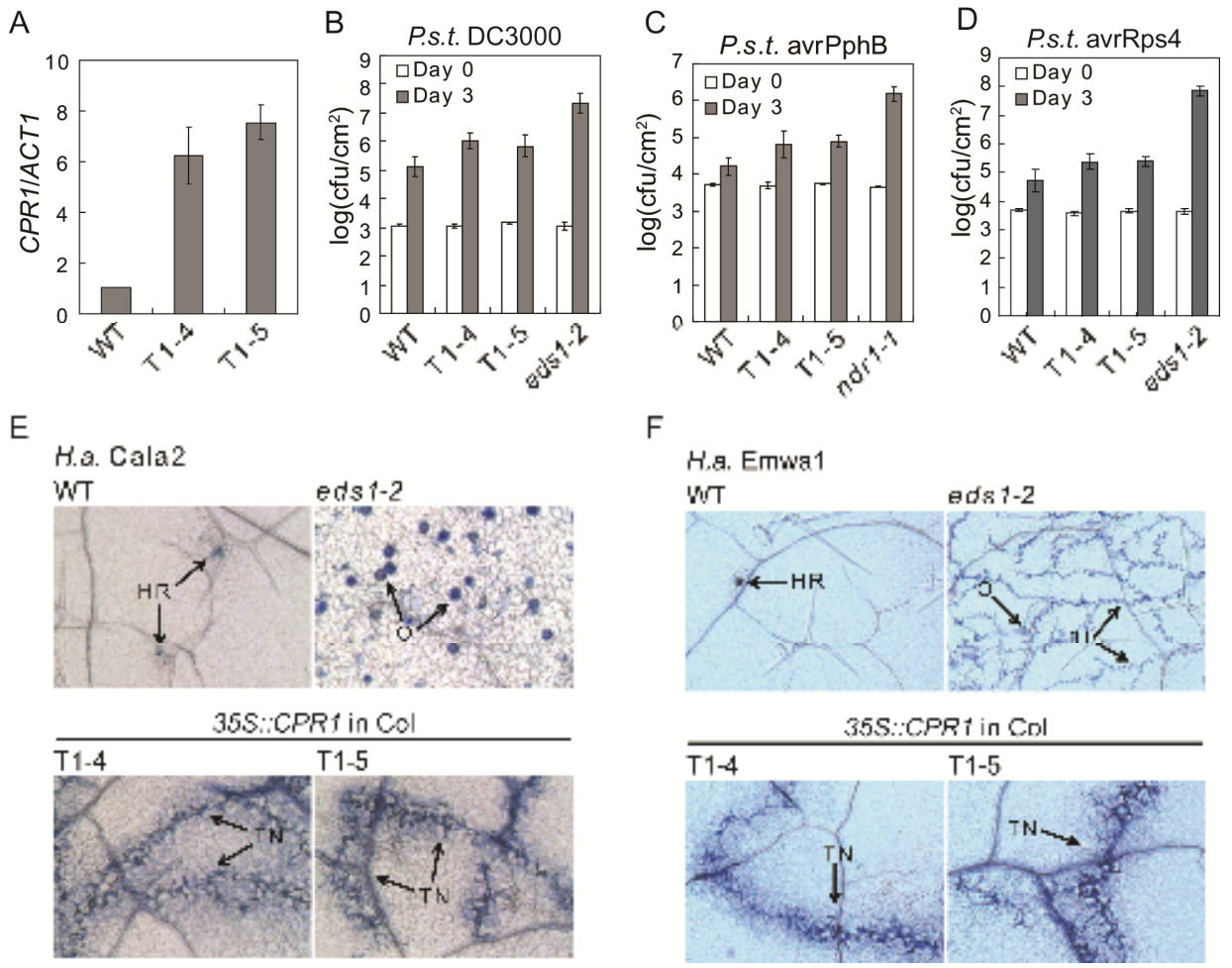

Figure 4.7: Analysis of basal resistance and resistance mediated by RPS5, RPS4, RPP2, and RPP4 in two independent transgenic lines (T1-4 and T1-5) overexpressing CPR1 in wild type Col background.

(A) qRT-PCR analysis of the transcript levels of *CPR1* in WT, T1-4 and T1-5.
(B) Growth of *Pseudomonas syringae* pv. *tomato* DC3000 in WT, T1-4 and T1-5; *eds1-2* plants were used as susceptible controls.
(C-D) Growth of *Pseudomonas syringae* pv. *tomato* DC3000 carrying *avrPphB* (C), and *avrRps4* (D) in T1-4 and T1-5. WT, *eds1-2*, and *ndr1-1* plants were used as controls. (E and F) Growth of *Hyaloperonospora arabidopsidis* Cala2 (E) and *H. arabidopsidis* Emwa1 (F) on T1-4 and T1-5 plants. WT and *eds1-2* plants were used as controls. fH, free hyphae; HR, hypersensitive response; O, oospores; and TN, trailing necrosis.

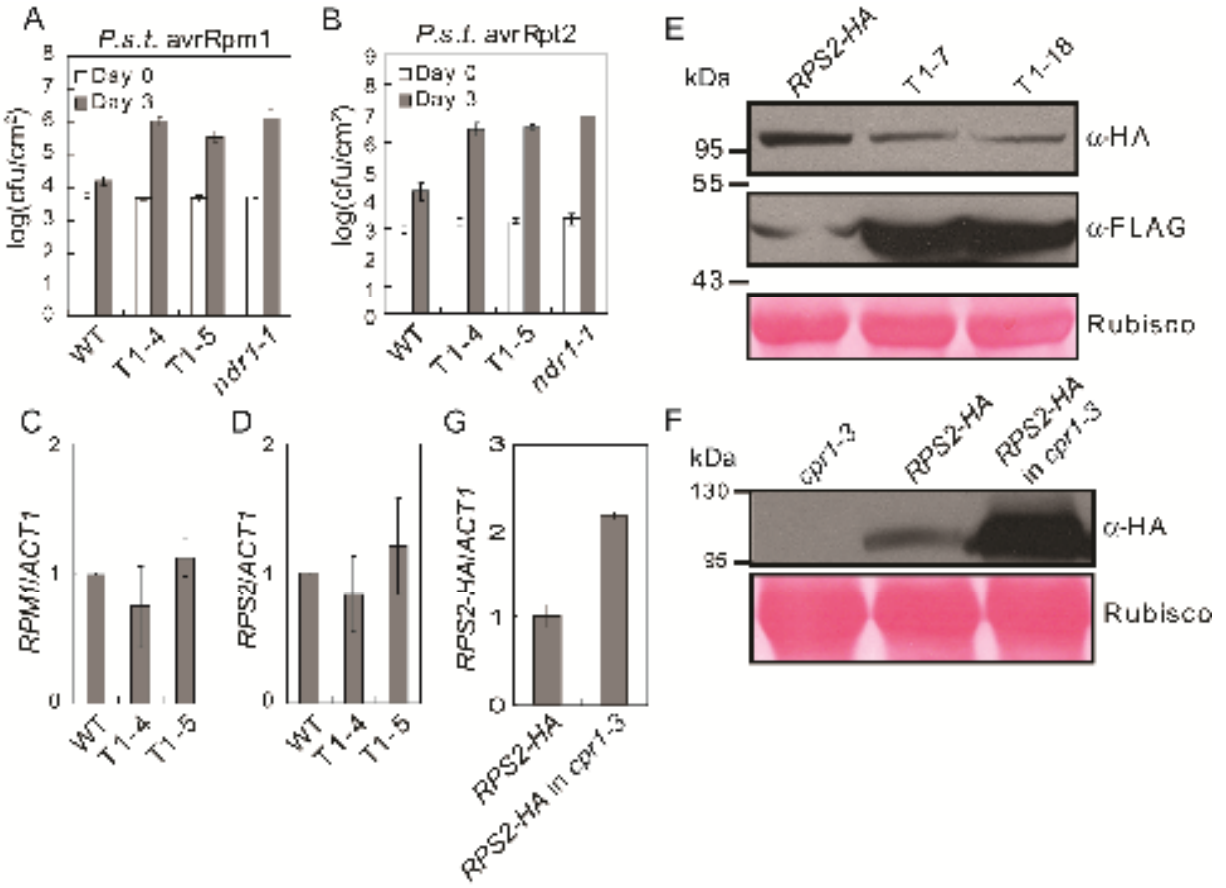

Figure 4.8: Regulation of RPS2-mediated resistance and RPS2 protein accumulation by CPR1.

(A-B) Growth of *Pst* DC3000 carrying *avrRpm1* (A) and *avrRpt2* (B) that is recognized by RPM1 and RPS2, respectively, in two independent transgenic lines (T1-4 and T1-5) overexpressing *CPR1* in wild type Col background. Wild type (WT) and *ndr1-1* plants were used as controls.
(C-D) Expression analysis of *RPM1* and *RPS2* in the indicated genotypes using qRT-PCR
(E) Western blot analysis of RPS2-HA protein levels in two *CPR1-FLAG* transgenic lines (T1-7 and T1-18) expressing CPR1-FLAG under its own promoter.
(F) Western blot analysis of RSP2-HA protein levels in *cpr1-3*. The *RPS2-HA* transgene was crossed into *cpr1-3* from a previously described *RPS2-HA* transgenic line (Axtell and Staskawicz, 2003).
(G) Expression analysis of *RPS2-HA* in the indicated genotypes using qRT-PCR

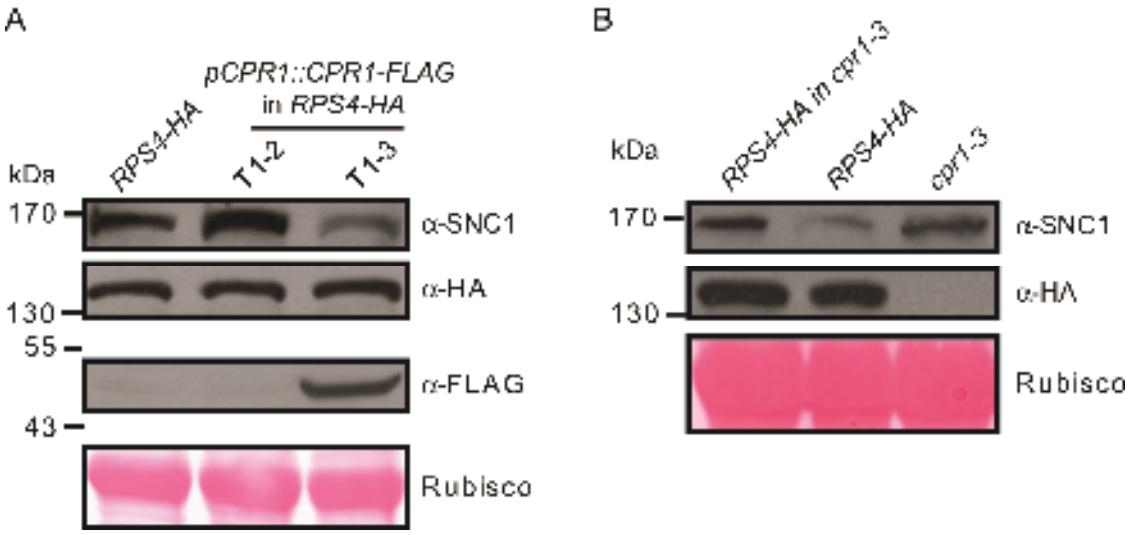

Figure 4.9: RPS4 protein level is not affected by CPR1.

RPS4-HA and SNC1 levels in two independent RPS4-HA lines (T1-2 and T1-3) transformed with CPR1-FLAG (A) and in cpr1-3 with RPS4-HA transgene (Wirthmueller et al., 2007) crossed into it (B). Total proteins were extracted from the indicated genotypes and probed with the specific antibodies to detect levels of CPR1-FLAG, RPS4-HA, and SNC1. Rubisco bands were used as loading controls.

4.2.9 CPR1 Interacts with SNC1 and RPS2 *in vivo*

F-box proteins are known to form SCF complexes with their substrates. The genetic interaction between *CPR1* and *SNC1*, plus the negative correlations between CPR1 protein level and accumulation of SNC1 and RPS2, prompted us to test whether CPR1 associates with SNC1 and RPS2 in vivo. Constructs expressing SNC1-HA and CPR1-FLAG fusion proteins were cotransformed into Arabidopsis mesophyll protoplasts and immunoprecipitation was subsequently performed on the protein extracts using anti-FLAG agarose beads. As shown in Figure 4.10A, SNC1-HA coimmunoprecipitated with the CPR1-FLAG protein. When RPS2-HA and CPR1-FLAG were coexpressed in Arabidopsis mesophyll protoplasts, RPS2-HA also coimmunoprecipitated with CPR1-FLAG (Figure 4.10B). These data suggest that CPR1 does associate with SNC1 and RPS2 in vivo, probably in SCF complexes, to target SNC1 and RPS2 for degradation. Because the point mutation in *snc1* stabilizes the SNC1 protein, we asked whether it caused a reduction of affinity with CPR1. As shown in Figure 4.10C, in Arabidopsis mesophyll protoplasts coexpressing CPR1-FLAG and SNC1-HA or snc1-HA, when immunoprecipitation was performed on the protein extracts using anti-HA microbeads, SNC1-HA and snc1-HA are both able to pull down CPR1. The snc1 mutation does not seem to have any obvious effect on interactions between CPR1 and SNC1 in this assay. However, when the immunoprecipitated samples were probed with an anti-ubiquitin (Ub) antibody, much less ubiquitination was observed in the immunoprecipitated snc1-HA, suggesting that SNC1 is a better substrate for ubiquitination than snc1.

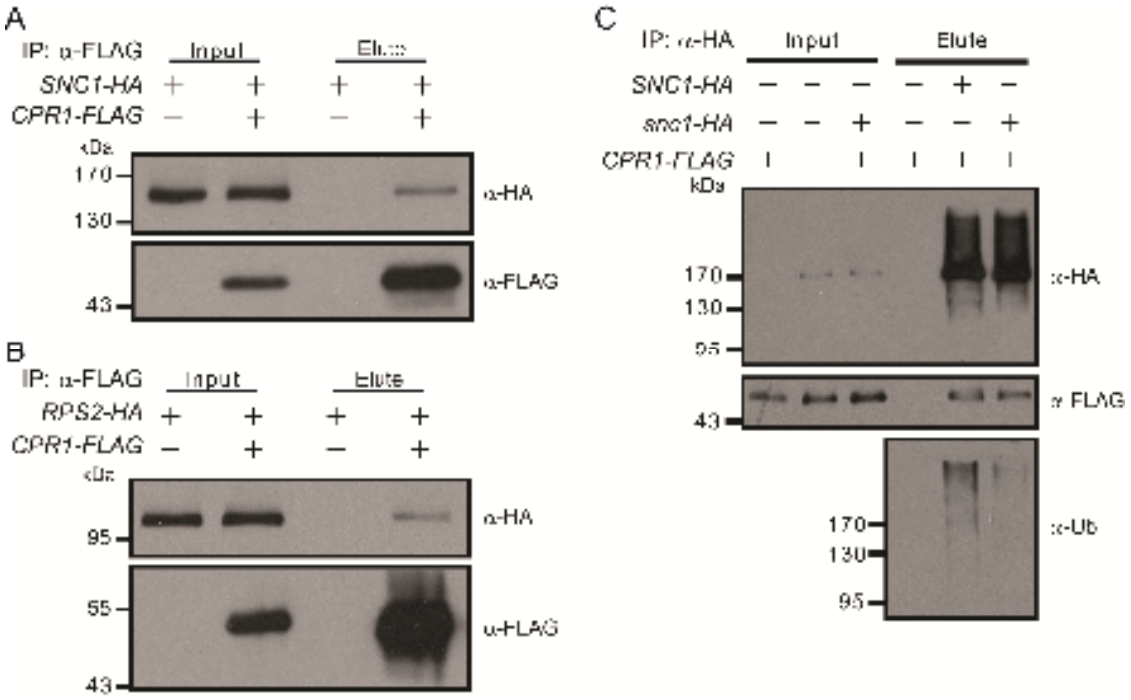

Figure 4.10: Interactions between CPR1 and SNC1 (A) or RPS2 (B).

(A) *In vivo* pull-down of SNC1-HA by CPR1-FLAG.
(B) *In vivo* pull-down of RPS2-HA by CPR1-FLAG.
(C) Immunoprecipitation of SNC1-HA or snc1-HA and ubiquitination levels of SNC1-HA or snc1-HA proteins.
Arabidopsis mesophyll protoplasts were transfected with the indicated constructs. Total protein extracts were subjected to immunoprecipitation with anti-FLAG agarose beads. Crude lysates (Input) and immunoprecipitated proteins (Elute) were detected with anti-FLAG or anti-HA antibodies.

4.3 Discussion

In plants, SCF-mediated protein degradation is involved in the regulation of diverse biological processes. The most well studied examples are from auxin signaling. SCF^{TIR1} and its homologous F-box proteins serve as auxin receptors and modulate Aux/IAA proteins for degradation (Santner and Estelle, 2009). There is evidence that SCFs are also involved in the regulation of plant immunity. In tobacco, N mediated resistance response to TMV was compromised when SKP1 was silenced (Liu et al., 2002). In addition, the tobacco F-box protein ACIF1 is required for the Cf-9- and Cf-4-mediated hypersensitive response, whereas the Arabidopsis F-box protein SON1 plays a negative role in defence (Kim and Delaney, 2002; van den Burg et al., 2008).

Recently it was shown that mutations in the F-box protein CPR30/CPR1 lead to constitutive expression of *PR* genes and enhanced pathogen resistance (Gou et al., 2009), but the mechanism of how CPR1 regulates plant defence responses was unclear. In this study, we provide strong evidence that SCF^{CPR1} targets the NLR R-like protein SNC1 for degradation to prevent overaccumulation of SNC1 and autoimmunity. Loss-of-function mutations in *CPR1* result in increased SNC1 accumulation, and the constitutive defence responses in *cpr1* are largely dependent on *SNC1*. In addition, overexpression of *CPR1* reduces the accumulation of SNC1 protein and suppresses the autoimmunity phenotype in *snc1*. Previously it was shown that SRFR1 and SGT1b are also involved in the negative regulation of SNC1 accumulation (Li et al., 2010). Because SRFR1 interacts with SGT1 and SGT1 associates with SKP1 and CUL1 in vivo (Azevedo et al., 2002; Shirasu, 2009; Li et al., 2010), SRFR1 and SGT1b may regulate the stability of SNC1 through modulating the activity of SCF^{CPR1}. In support of this hypothesis, association of SNC1 and SRFR1 was detected from coimmunoprecipitation experiments in transient expression system in tobacco (Kim et al., 2010).

In addition to SNC1, SCF^{CPR1} also negatively regulates the stability of RPS2. Loss of *CPR1* function leads to increased RPS2 levels, whereas overexpression of *CPR1* reduces the accumulation of RPS2 and severely compromises RPS2-mediated immunity. Furthermore, overexpression of *CPR1* abolishes immunity mediated by RPM1 and slightly compromises resistance specified by several other R proteins, such as RPP2 and RPP4, suggesting that SCF^{CPR1} may also target these R proteins for degradation. In contrast, overexpression of *CPR1* hardly affects the resistance mediated by RPS4 and RPS5. Whether the stability of these R proteins is controlled by other F-box proteins remains to be determined. It was surprising to us that CPR1 targets SNC1 and RPS2, two quite different NLR proteins, yet doesn't target RPS4, which is more closely related to SNC1. It is possible that CPR1 may recognize a common feature shared between SNC1 and RPS2, but not with RPS4.

Previous studies on RAR1-SGT1-HSP90 demonstrated that correct folding and maintaining NLR R proteins above a threshold level are required for quick induction of defence responses when under pathogen attack. Meanwhile, the activities and protein levels of NLR R proteins need to be tightly controlled to prevent activation of defence responses without the presence of pathogens because constitutive activation of defence responses is detrimental to growth and development (Shirasu, 2009). Our study identified SCF-mediated protein degradation as a critical mechanism for regulating the stability of plant NLR R proteins, suggesting that NLR R proteins are maintained at proper levels by balanced activities from the RAR1-SGT1-HSP90-mediated assembly and proteasome-mediated degradation. Because overexpression of NLR

immune receptors also results in autoactivation of immune responses in animals, and plant and animal NLRs are structurally similar, it will be interesting to test whether the stability of NLR proteins in animals is also controlled by a similar SCF-mediated mechanism.

4.4 Material and Methods

4.4.1 Plant Growth Conditions and Mutant Phenotypic Characterization

All plants were grown at 22 °C under a long-day (16-hour light/8-hour night) regime. Gene expression analysis was carried out by extracting total RNA from 2-week-old plate-grown plants. The extracted RNA was then reverse-transcribed to obtain cDNA. Real-time PCR was performed and the expression levels of *Actin1*, *PR1*, and *PR2* were determined as described previously (Zhang et al., 2003). Infection experiments with *P. syringae* and *H. arabidopsidis* (previously *Hyaloperonospora parasitica*) were performed as previously described (Li et al., 2001). *H. arabidopsidis* infection details were visualized under a light microscope after staining leaves with lactophenol Trypan blue (Koch and Slusarenko, 1990).

4.4.2 Construction of Plasmids and Arabidopsis Transformation

The coding sequence of *At4g12560* (*CPR1*/*CPR30*) was PCR-amplified using primers
5’ cggGGTACCATGGCGACGATTCCAATGGA 3’ and
5’ CGCggatccTTATAAGACCAGCTTGAATC 3’ from wild-type Col cDNA. The amplified fragment was then digested with KpnI and BamHI and cloned into *pHAN-35S* to generate *pHAN-35S::CPR1*. For the construction of *pCAMBIA1305-pCPR1::CPR1-3×FLAG*, the fragment containing 1,914 bp upstream of the start codon of *CPR1* and the CPR1 genomic sequence was amplified by using primers
5’ cggGGTACCaaatcacaagtcacctgacc 3’ and
5’ CGCggatccTAAGACCAGCTTGAATCCTTTGG 3’ from wild-type Col genomic DNA. The fragment was digested with KpnI and BamHI and cloned into *pCAMBIA-3×FLAG* to generate *pCAMBIA1305-pCPR1::CPR1-3×FLAG*. The above plasmids were electroporated into Agrobacterium and subsequently transformed into the appropriate Arabidopsis genotypes by floral dipping method (Clough and Bent, 1998).

Transient expression vectors *pUC19-35S-FLAG-RBS* and *pUC19-35S-HA-RBS* (kindly provided by Dr. Jian-Min Zhou, National Institute of Biological Sciences, Beijing, People’s Republic of China) containing the cauliflower mosaic virus *35S* promoter, 3×FLAG or 3×HA, and a Rubisco Small Subunit terminator were used for transient expression of *CPR1* and R protein-coding genes in protoplasts. *CPR1*, *SNC1*, and *RPS2* coding sequences were PCR-amplified using primers listed in Table 4.1. The amplified fragments were digested with restriction enzymes indicated in the same table and ligated into *pUC19-35SFLAG-RBS* or *pUC19-35S-HA-RBS*. The resulting constructs were used in the Arabidopsis mesophyll protoplasts transient expression system (Yoo et al., 2007).

Table 4.1: List of primers used in constructing protoplast transient expression constructs

Primer Name	primer sequence (5'-->3')	restriction enzyme used for cloning
CPR1-KpnI-F	cggGGTACCaaatcacaagtcacctgacc	KpnI and BstBI
CPR1-BstBI-R	gccGGATCCTTCGAATAAGACCAGCTTGAATCCTTT	
SNC1-KpnI-F	ccgGGTACCATGGAGATAGCTTCTTCTTC	KpnI and SalI
SNC1-SalI-R	gccGGATCCgtcgacGTTACCAGAAACAGGAAACA	
RPS2-KpnI-F	ccgGGTACCATGGATTTCATCTCATCTCTTAT	KpnI and SalI
RPS2-SalI-R	gccGGATCCgtcgacATTTGGAACAAAGCGCGGTA	

4.4.3 Generation of Arabidopsis Protoplasts

Arabidopsis mesophyll protoplasts were generated by following the protocol from Yoo et al. (Yoo et al., 2007), with minor modifications. Leaf strips were digested in enzyme solution (0.4 M mannitol, 20 mM KCl, 20 mM Mes pH 5.7, 10 mM $CaCl_2$ and 0.1% BSA) with 1.3% cellulose R10 (Yakult Pharmaceutical Ind. Co., Ltd.) and 0.3% Macerozyme R10 (Yakult Pharmaceutical Ind. Co., Ltd.) for 2.5 hours with gentle shaking. The protoplast solution was filtered through a 100 μm nylon mesh and washed once with W5 solution (154 mM NaCl, 125 mM $CaCl_2$, 5 mM KCl, and 2 mM Mes pH 5.7). Isolated protoplasts were resuspended in W5 solution and incubated on ice for 30 minutes. After incubation, protoplasts were pelleted down and resuspended in MMG solution (0.4 Mmannitol, 15 mM MgCl2, and 4 mM Mes pH 5.7). For coimmunoprecipitation, we used 2 mL of protoplasts (in MMG solution), 100 μL of plasmid A (1 μg/μL), 100 μL of plasmid B (1 μg/μL; or H_2O for controls), and 2.2 mL PEG solution [40% PEG4000 (Fluka; cat. no. 81240), 0.2 M mannitol and 100 mM CaCl2]. The resulting transfection mix was well mixed and allowed to react for 10 minutes. The mix was then diluted with 8 mL W5 solution to stop the reaction.

4.4.4 Plant Total Protein Extraction, Protein Immunoprecipitation, and Western Blot Analyses

Plant total protein was extracted from 100 mg of 12-day-old plate-grown plants using extraction buffer (100 mM Tris-HCl pH 8.0, 0.2% SDS and 2% β-mercaptoethanol). Laemmli buffer (4×) was added to each protein sample and boiled for 5 to 10 minutes. The resulting protein samples were subjected to Western blot analyses.

For protein immunoprecipitation, proteins in the tranfected protoplasts were extracted using 1.5 mL grinding buffer [50 mM Tris-HCl pH 7.5, 10 mM MgCl2, 150 mM NaCl, 0.1% Nonidet P-40, 1 mM PMSF, 1× Protease Inhibitor Coctail (Roche; Cat. #11873580001), and 100 μM MG132]. The sample was spun at 16,000 × g for 10 min at 4 °C to remove cellular debris. 40μL of the supernatant was saved as input. The rest of the supernatant was transferred to a tube containing 35 μL anti-FLAG M2 beads (Sigma; Cat. #A2220) and incubated for 2 hours at 4 °C with gentle rotation. After incubation, the beads were spun down at 1,500 × g for 30 seconds at 4

°C. The beads were washed thoroughly with 1 mL of grinding buffer three times before immunoprecipitated proteins were eluted with 60 μL 3 × FLAG peptide (150 μg/mL; Sigma, Cat. #F4799).

The anti-SNC1 antibody was generated against a SNC1-specific peptide in rabbit (Li et al., 2010). The anti-HA antibody was from Roche (Cat. #11867423001). The anti-FLAG antibody and the anti-Ubiquitin antibody were both from Sigma (Cat. # F1804 and U0508, respectively).

4.5 Manuscript Acknowledgements

We thank our colleagues around the globe who kindly provided us with materials: Dr. Judy Callis for seeds of the cul1-7 and transgenic CUL1-FLAG in cul1-7; Dr. Jian-Min Zhou for pUC19-35S-FLAG-RBS and pUC19-35S-HA-RBS; Dr. Brian Staskawitz for seeds of the RPS2-HA transgenic line; Dr. Jane Parker for seeds of the RPS4-HA transgenic line; Dr. Guoying Wang for seeds of cpr1-2 (previously cpr30-1) and cpr1-2 pad4; Dr. Mary Berbee and Dr. Sean Graham for their help with phylogenetic analysis of CPR1 and its homologs; Kaeli Johnson and Virginia Woloshen for careful reading of the manuscript; and Yan Li for assistance with making figures. Work described is supported by funds from Natural Sciences and Engineering Research Council of Canada (to X.L.) and the Chinese Ministry of Science and Technology (to Y.Z.).

5 Final Summary and Future Perspectives

Land plants, which are sessile organisms, rely entirely on the innate immune system to protect themselves against pathogen invasions. Among host-pathogen interactions, the R protein-mediated resistance is the most effective defence mechanism. Most of the R proteins are intracellular nuclear-binding (NB) and leucine-rich repeat (LRR) containing proteins (Chisholm et al., 2006; DeYoung and Innes, 2006; Jones and Dangl, 2006). These NB-LRR proteins often recognize the presence of pathogen effectors and activate a series of defence responses that usually culminate in localized programmed cell death, hypersensitive response (HR), to restrict spreading of pathogens to unaffected tissues (Nurnberger and Scheel, 2001; Greenberg and Yao, 2004).

snc1, which carries a gain-of-function mutation in a TIR-type NB-LRR R protein, exhibits constitutive defence responses in the absence of pathogens (Li et al., 2001; Zhang et al., 2003). Interestingly, unlike other gain-of-function R protein mutants, which often show uncontrollable cell death/HR (Hwang et al., 2000; Bendahmane et al., 2002; Shirano et al., 2002; Palma et al., 2010), *snc1* plants do not exhibit any macroscopic or microscopic HR (Li et al., 2001). Beside autoimmune phenotypes, *snc1* mutant plants also show very distinctive morphological phenotypes, including stunted growth and curled leaves. The autoimmune phenotypes of *snc1* with no HR and its distinctive morphological phenotypes make *snc1* a unique tool for identifying signalling components downstream of the R protein. To search for these signalling components, *snc1* suppressor screens were conducted. From the screens, fifteen extragenic *mos* (*modifier of snc1*) mutants were found. The *MOS* genes identified by *mos* mutations encode proteins that participate in various cellular functions including epigenetic regulation (MOS1 [Li et al., 2010; Li et al., 2011]), transcriptional repression (MOS10 [Zhu et al., 2010]), nucleo-cytoplasmic trafficking (MOS6 [Palma et al., 2005] and MOS14 [Xu et al., 2011]), protein modifications (MOS5 [Goritschnig et al., 2007] and MOS8 [Goritschnig et al., 2008]), and a large class of MOS proteins involved in RNA processing/metabolism (MOS2 [Zhang et al., 2005], MOS3 [Zhang and Li, 2005], MOS4 [Palma et al., 2007], MOS11 [Germain et al., 2010], and MOS12 [Xu et al., 2012]).

5.1 Nuclear-Cytoplasmic Trafficking and Plant Immunity – MOS7

mos7-1, a mutant generated by fast neutron bombardment, partially suppresses all *snc1* associated defence and morphological phenotypes (Figure 2.1). Positional cloning followed by direct single gene sequencing identified an in-frame twelve-base-pair deletion in the fourth exon of *At5g05680* in *mos7-1* (Figure 2.2). The predicted MOS7 protein shows amino acid sequence homology to human and Drosophila nuclear porin 88 (Nup88 or Mbo [members only]; Figure 2.3). In humans and Drosophila, Nup88 is required for binding and sequestering the exportin CRM1/XPO1, which is an export receptor for proteins with leucine-rich nuclear export signals (NES), at the nuclear rim. Failure to sequester CRM1/XPO1 would result in insufficient retention of nuclear proteins bearing NES (Roth et al., 2003; Bernad et al., 2004; Xylourgidis et al., 2006). While knock-out of Nup88 results in lethality, knock-down studies in these two

systems showed that NFκB, a key immune regulator in animal cells, failed to accumulate inside the nucleus and resulted in impaired defence activation (Uv et al., 2000).

Consistent with its homology with Nup88, MOS7 localizes to the nuclear rim (Figure 2.6). Like its animal homologs, null mutations in *MOS7* are lethal; the partial loss-of-function allele *mos7-1* showed compromised basal resistance and resistance mediated by several R proteins (Figure 2.4). Further investigation of nuclear-cytoplasmic distribution of EDS1 and NPR1, two important plant immune receptors, revealed that in *mos7-1* mutant background, the overall levels of EDS1 and NPR1 are markedly reduced (Figure 2.8 and 2.9). Interestingly, while studying the mechanistic function that MOS7 plays in plant innate immunity, we found that the majority of SNC1 localizes in the cytoplasm, whereas a small portion (~5-10%) of SNC1 protein resides in the nucleus. In *mos7-1*, this nuclear-cytoplasmic distribution of SNC1 is altered (Figure 2.7). The suppression of *snc1* autoimmune and morphological phenotypes by *mos7-1* is likely a combined effect of altered SNC1 nuclear-cytoplasmic distribution and markedly reduced protein levels of EDS1 and NPR1.

Nuclear-cytoplasmic trafficking plays essential roles in immunity in animals (Ting et al., 2006). However, its roles in plant immunity remain elusive. This study highlights NES-mediated nuclear export as a component in regulating defence outputs. Identification of MOS7, together with previous studies on MOS6, from the same *snc1* suppressor screen, reveals the importance of nuclear-cytoplasmic trafficking in plant innate immunity. The striking similarity of the roles that nuclear-cytoplasmic trafficking plays in plant and animal immunity suggests a conserved function of Nup88/MOS7 in regulating innate immunity in both kingdoms.

The intracellular NB-LRR R proteins serve as immune receptors to recognize pathogens and activate disease resistance. However, the site of pathogen effector recognition and the signaling transducing mechanisms employed by R proteins are largely unknown. Several recent studies suggested that the nuclear pool of numerous plant NB-LRR R proteins are important in defence activation, including the TIR-type RPS4 (Wirthmueller et al., 2007), RRS1 (Tasset et al., 2010) and N (Burch-Smith et al., 2007), and the CC-type MLA10 (Shen et al., 2007) and Rx (Sacco et al., 2007; Tameling and Baulcombe, 2007); however, the exact role that these NB-LRR immune receptors play inside the nucleus is not clear. Besides RRS1, which is predicted to have the ability to bind to DNA molecules because of its C-terminal WRKY domain, none of the above mentioned NB-LRR R proteins are annotated to have the ability to bind to DNA (Meyers et al., 2003).

Although a number of studies suggested that nucleo-cytoplamisic trafficking is important for R protein function, this is not to restrict the cellular compartment of where NB-LRR proteins function. A recent study on the CC-type NB-LRR R protein RPM1 suggested that RPM1 is activated on the plasma membrane and does not relocalize to the nucleus (Gao et al., 2011). This study adds the diversity of the sites of R protein recognition and signaling transduction mechanisms to achieve the final outcome as immunity.

During the investigation of MOS7, we found that a sub-pool of snc1 also localizes inside the nucleus (Figure 2.7). Similar to most of the nuclear localized R proteins, SNC1 lacks DNA binding ability judging by its predicted protein sequence. Like its name suggests, MOS7/Mbo (members only) acts as the doorkeeper controlling the molecular traffic across the nuclear pore. It would be interesting to know how the NB-LRR proteins gain access to the nucleus, and what the dynamics of these R proteins in response to pathogen invasion is. Do they travel alone or are they shuttled in as a complex, and what are their functions inside the nucleus? A combination of

genetic and biochemical approaches may help to decipher the molecular functions of SNC1 inside the nucleus, and enhance our understanding on how plants achieve immunity.

5.2 Epigenetic Regulation of R Genes – MOS9

Like *mos7-1*, *mos9* was identified from the same *snc1* suppressor screen generated using fast neutron bombardment. *mos9* partially suppresses all *snc1*-associated autoimmune and morphological phenotypes (Figure 3.1). Crude mapping followed by Agrobacteria-mediated transformation of overlapping TAC clones covering the region of interest suggested that *mos9* mutation is in an interval containing six genes on the top arm of chromosome I (Figure 3.2). Direct single gene complementation indicated that *MOS9* is *At1g12530*. *MOS9* encodes a plant specific protein with no known domains and previously unknown function. Subcellular localization of MOS9 using MOS9-GFP fusion protein construct revealed that it localizes to both nucleus and cytoplasm (Figure 3.6).

Immunoprecipitation using *MOS9-GFP* complemented transgenic plants, followed by mass spectrometric analysis showed that one of the MOS9 interacting proteins is a SET domain containing protein, ATXR7 (Arabidopsis trithorax-related protein 7). Like *mos9*, mutation in *ATXR7* partially suppresses all *snc1*-associated autoimmune and morphological phenotypes (Figure 3.8). Studies of ATXR7 showed that it is required for tri-methylation of lysine 4 of histone H3 (H3K4me3) and for transcriptional activation of Flowering locus C (FLC; Tamada et al., 2009). Identification of ATXR7 as an interacting partner of MOS9 led us to ask whether MOS9 role in plant immunity is to regulate methylation status of histone proteins. Supporting our hypothesis, the transcription levels of *SNC1* and a neighbouring R protein-encoding gene *RPP4* are reduced in *mos9* and *atxr7* mutant backgrounds (Figure 3.5H, 3.8C and 3.10). The reduced *RPP4* expression level in *mos9* and *atxr7* is associated with compromised RPP4-mediated resistance against *Ha* Emwa1 (Figure 3.10). A chromatin immunoprecipitation (ChIP) experiment using specific antibodies against H3K4me3 revealed that H3K4me3 levels around the *SNC1* and *RPP4* genes are remarkably reduced (Figure 3.10).

MOS1, the first *MOS* gene cloned from the *snc1* suppressor screen, encodes a protein with a BAT2 domain at its N terminus. Studies of MOS1 found that it is involved in epigenetic transcriptional regulation of *SNC1* (Li et al., 2010). In the absence of pathogen infections, *R* genes are expressed at low levels (Tan et al., 2007), presumably to maintain plants' competency to prepare for immunity and take part in basal defence. When they encounter pathogens, plants must achieve and maintain proper *R* gene expression to ensure the production of enough R protein molecules in the battle for pathogen recognition, defence activation, and defence amplification and maintenance. Excessive *R* gene expression would lead to autoimmunity and fitness loss, while insufficient expression would lead to disease. Hitherto, little was known on how epigenetic regulation plays a role in plant immunity (Berr et al., 2012; Gutzat and Mittelsten Scheid, 2012).

The identification of two MOS proteins, MOS1 and MOS9, from *snc1* suppressor screens that function in epigenetic regulation of *SNC1* transcription emphasizes the importance of epigenetic regulation in plant immunity. It would be interesting to know if MOS1 and MOS9 function co-ordinately in regulating *R* gene expression. MOS9 localizes both in the cytoplasm and in the nucleus. MOS9 interactor ATXR7 functions as chromatin remodelling protein and it is

believed that ATXR7 is a nuclear-localized protein; however, there is no experimental evidence that the subcellular localization of ATXR7 is solely nuclear. It would also be interesting to know the dynamics of MOS9 and ATXR7 during defence responses. Do they stably associate as a protein complex, or do they form a "defensome" in response to pathogenic cues? Future in-depth studies should reveal the complete picture of the intricate epigenetic regulation of expression of *R* genes.

5.3 Regulation of R Protein Stability – SCF^{CPR1}

The activity of R proteins, how R proteins are structurally regulated, and how danger signals are transduced from activated R proteins to downstream components have been the focus of R protein-mediated resistance studies in the past decade. Detailed studies in the HSP90-SGT1-RAR1 complex suggested that these three highly conserved eukaryotic proteins are involved in the following three aspects of NB-LRR R protein quality control: 1) assembly/folding of R proteins, 2) preparing R proteins in the effector recognition competent state and 3) regulating the stability/turnover of these proteins (Kadota et al., 2010; Kadota and Shirasu, 2012). However, negative regulation of NB-LRR immune sensors through disassembly/degradation has long been the missing piece in both animal and plant immunity (Coll and O'Neill, 2010). Serendipitously, we came across the data published by Dr. Guoying Wang's group on CPR1 (previously named CPR30 [Gou et al., 2009]). This publication describes positional cloning and genetic characterization of the mutant *cpr1-2*. *CPR1* encodes an F-box containing protein, a member of the SCF E3 ubiquitin ligase that functions in recognizing protein substrates for 26S proteasome-mediated degradation (Ho et al., 2006; Hua and Vierstra, 2011). *cpr1-2* phenocopies *snc1* in all aspects. Also, like *snc1*, the phenotypes of *cpr1-2* depend on *EDS1* and *PAD4* (Gou et al., 2009). While mapping the *cpr1-2* locus, the recombinant frequencies flanking the mapping region (chromosome IV; 7.4-7.5Mb) were skewed, suggesting that a locus close to *cpr1-2* is affecting the mutant phenotype. Indeed, *SNC1* (chromosome IV; 9.5Mb) is located very close to *cpr1-2* locus. These interesting data led us to hypothesize that SNC1 may be a target of the F-box protein, CPR1. Supporting our hypothesis, overexpression of *CPR1* is able to suppress all *snc1*-associated phenotypes (Figure 4.6), whereas *cpr1* autoimmune phenotypes can be largely suppressed by *SNC1* loss-of-function mutation (Figure 4.5). In addition to our genetic data, we were able to demonstrate that CPR1 physically associates with SNC1 (Figure 4.10). Our study on CPR1 was the first to report how plant NB-LRR immune receptors are negatively regulated by the ubiquitin-26S proteasome.

The identification of RPS2, a CC-type NB-LRR R protein, as another target of CPR1 but not RPP4 or RPS4, which are TIR-type NB-LRR proteins highly homologous to SNC1, was unexpected. This finding led us to ask what determines substrate specificity of CPR1 for NB-LRR proteins. Future in-depth mutational analysis on SNC1 and RPS2 may help us pinpoint the domain/consensus amino acid sequence of NB-LRR proteins being recognized by CPR1. Knowing how substrate specificity is determined by CPR1 could also help us identify other NB-LRR proteins that are potential substrates of CPR1.

Overall, my studies on MOS7, MOS9 and CPR1 have increased our understanding of the importance of nucleo-cytoplasmic trafficking, epigenetic regulation and protein stability in SNC1-mediated immunity. By using the autoimmune mutant, *snc1*, in the model plant

Arabidopsis thaliana, my thesis work provides new insights and a starting point for dissecting the intricate and sophisticated regulatory mechanisms plants employ in protecting themselves against diverse pathogenic attacks.

References

Aarts N., Metz M., Holub E., Staskawicz B.J., Daniels M.J., and Parker J.E. (1998). Different requirements for *EDS1* and *NDR1* by disease resistance genes define at least two *R* gene-mediated signaling pathways in *Arabidopsis*. Proc Natl Acad Sci **95,** 10306-11.

Aravind L. and Koonin E.V. (1999). G-patch: a new conserved domain in eukaryotic RNA-processing proteins and type D retroviral polyproteins. Trends Biochem. Sci. **24,** 342-344.

Austin M.J., Muskett P., Kahn K., Feys B.J., Jones J.D., and Parker J.E. (2002). Regulatory role of *SGT1* in early *R* gene-mediated plant defenses. Science **295,** 2077-80.

Ausubel F.M. (2005). Are innate immune signaling pathways in plants and animals conserved? Nat. Immunol. **6,** 973-979.

Axtell, M.J., and Staskawicz, B.J. (2003). Initiation of *RPS2*-specified disease resistance in *Arabidopsis* is coupled to the AvrRpt2-directed elimination of RIN4. Cell **112:** 369–377.

Azevedo C., Sadanandom A., Kitagawa K., Freialdenhoven A., Shirasu K., and Schulze-Lefert P. (2002). The RAR1 interactor SGT1, an essential component of R gene-triggered disease resistance. Science **295,** 2073-6.

Baumberger N., Tsai C.H., Lie M., Havecker E., and Baulcombe D.C. (2007). The Polerovirus silencing suppressor P0 targets ARGONAUTE proteins for degradation. Curr. Biol. **17,** 1609-1614.

Bednarek P., Pislewska-Bednarek M., Svatos A., Schneider B., Doubsky J., Mansurova M., Humphry M., Consonni C., Panstruga R., Sanchez-Vallet A., Molina A., and Schulze-Lefert P. (2009). A glucosinolate metabolism pathway in living plant cells mediates broad-spectrum antifungal defense. Science **323,** 101-106.

Belkhadir, Y., Subramaniam, R., and Dangl, J.L. (2004). Plant disease resistance protein signaling: NBS-LRR proteins and their partners. Curr. Opin. Plant Biol. **7:** 391–399.

Bendahmane A., Farnham G., Moffett P., and Baulcombe D.C. (2002). Constitutive gain-of-function mutants in a nucleotide binding site-leucine rich repeat protein encoded at the Rx locus of potato. Plant J. **32,** 195-204.

Bergelson J., Kreitman M., Stahl E.A., and Tian D. (2001). Evolutionary dynamics of plant R-genes. Science **292,** 2281-2285.

Bernad, R., van der Velde, H., Fornerod, M., and Pickersgill, H. (2004). Nup358/RanBP2 attaches to the nuclear pore complex via association with Nup88 and Nup214/CAN and plays a supporting role in CRM1-mediated nuclear protein export. Mol. Cell. Biol. **24:** 2373–2384.

Bernoux M., Ve T., Williams S., Warren C., Hatters D., Valkov E., Zhang X., Ellis J.G., Kobe B., and Dodds P.N. (2011). Structural and functional analysis of a plant resistance protein TIR domain reveals interfaces for self-association, signaling, and autoregulation. Cell. Host Microbe **9,** 200-211.

Berr A., Menard R., Heitz T., and Shen W.H. (2012). Chromatin modification and remodelling: a regulatory landscape for the control of Arabidopsis defence responses upon pathogen attack. Cell. Microbiol. **14,** 829-839.

Berrocal-Lobo M., Stone S., Yang X., Antico J., Callis J., Ramonell K.M., and Somerville S. (2010). ATL9, a RING zinc finger protein with E3 ubiquitin ligase activity implicated in chitin- and NADPH oxidase-mediated defense responses. PLoS One **5,** e14426.

Bhattacharjee S., Halane M.K., Kim S.H., and Gassmann W. (2011). Pathogen effectors target Arabidopsis EDS1 and alter its interactions with immune regulators. Science **334,** 1405-1408.

Bittel P. and Robatzek S. (2007). Microbe-associated molecular patterns (MAMPs) probe plant immunity. Curr. Opin. Plant Biol. **10,** 335-341.

Block A. and Alfano J.R. (2011). Plant targets for Pseudomonas syringae type III effectors: virulence targets or guarded decoys? Curr. Opin. Microbiol. **14,** 39-46.

Boller T. and Felix G. (2009). A renaissance of elicitors: perception of microbe-associated molecular patterns and danger signals by pattern-recognition receptors. Annu. Rev. Plant. Biol. **60,** 379-406.

Bos J.I., Armstrong M.R., Gilroy E.M., Boevink P.C., Hein I., Taylor R.M., Zhendong T., Engelhardt S., Vetukuri R.R., Harrower B., Dixelius C., Bryan G., Sadanandom A., Whisson S.C., Kamoun S., and Birch P.R. (2010). Phytophthora infestans effector AVR3a is essential for virulence and manipulates plant immunity by stabilizing host E3 ligase CMPG1. Proc Natl Acad Sci **107,** 9909-9914.

Bowling S.A., Guo A., Cao H., Gordon A.S., Klessig D.F., and Dong X. (1994). A mutation in Arabidopsis that leads to constitutive expression of systemic acquired resistance. Plant Cell **6,** 1845-1857.

Burch-Smith, T.M., Schiff, M., Caplan, J.L., Tsao, J., Czymmek, K., and Dinesh-Kumar, S.P. (2007). A novel role for the TIR domain in association with pathogen-derived elicitors. PLoS Biol. **5:** e68.

Cao H., Bowling S.A., Gordon A.S., and Dong X. (1994). Characterization of an Arabidopsis Mutant That Is Nonresponsive to Inducers of Systemic Acquired-Resistance. Plant Cell **6,** 1583-1592.

Cao H., Glazebrook J., Clarke J.D., Volko S., and Dong X. (1997). The Arabidopsis *NPR1* gene that controls systemic acquired resistance encodes a novel protein containing ankyrin repeats. Cell **88,** 57-63.

Cao H., Li X., and Dong X. (1998). Generation of broad-spectrum disease resistance by overexpression of an essential regulatory gene in systemic acquired resistance. Proc Natl Acad Sci **95,** 6531-6.

Cao Y., Yang Y., Zhang H., Li D., Zheng Z., and Song F. (2008). Overexpression of a rice defense-related F-box protein gene OsDRF1 in tobacco improves disease resistance through potentiation of defense gene expression. Physiol. Plant. **134,** 440-452.

Capron A., Okresz L., and Genschik P. (2003). First glance at the plant APC/C, a highly conserved ubiquitin-protein ligase. Trends Plant Sci. **8,** 83-89.

Century K.S., Shapiro A.D., Repetti P.P., Dahlbeck D., Holub E., and Staskawicz B.J. (1997). *NDR1*, a pathogen-induced component required for *Arabidopsis* disease resistance. Science **278,** 1963-1965.

Chan S.L., Mukasa T., Santelli E., Low L.Y., and Pascual J. (2010). The crystal structure of a TIR domain from Arabidopsis thaliana reveals a conserved helical region unique to plants. Protein Sci. **19,** 155-161.

Cheng Y.T., Germain H., Wiermer M., Bi D., Xu F., Garcia A.V., Wirthmueller L., Despres C., Parker J.E., Zhang Y., and Li X. (2009). Nuclear pore complex component MOS7/Nup88 is required for innate immunity and nuclear accumulation of defense regulators in Arabidopsis. Plant Cell **21,** 2503-2516.

Cheng Y.T., Li Y., Huang S., Huang Y., Dong X., Zhang Y., and Li X. (2011). Stability of plant immune-receptor resistance proteins is controlled by SKP1-CULLIN1-F-box (SCF)-mediated protein degradation. Proc. Natl. Acad. Sci. U. S. A. **108,** 14694-14699.

Cheung M.Y., Zeng N.Y., Tong S.W., Li F.W., Zhao K.J., Zhang Q., Sun S.S., and Lam H.M. (2007). Expression of a RING-HC protein from rice improves resistance to Pseudomonas syringae pv. tomato DC3000 in transgenic Arabidopsis thaliana. J. Exp. Bot. **58,** 4147-4159.

Chinnusamy V., Gong Z., and Zhu J.K. (2008). Nuclear RNA export and its importance in abiotic stress responses of plants. Curr. Top. Microbiol. Immunol. **326,** 235-255.

Chisholm S.T., Coaker G., Day B., and Staskawicz B.J. (2006). Host-microbe interactions: shaping the evolution of the plant immune response. Cell **124,** 803-814.

Chu C.C., Lee W.C., Guo W.Y., Pan S.M., Chen L.J., Li H.M., and Jinn T.L. (2005). A copper chaperone for superoxide dismutase that confers three types of copper/zinc superoxide dismutase activity in Arabidopsis. Plant Physiol. **139,** 425-436.

Clark S.J. (2007). Action at a distance: epigenetic silencing of large chromosomal regions in carcinogenesis. Hum. Mol. Genet. **16 Spec No 1,** R88-95.

Clough, S.J., and Bent, A.F. (1998). Floral dip: A simplified method for *Agrobacterium*-mediated transformation of *Arabidopsis thaliana.* Plant J. **16:** 735–743.

Coll R.C. and O'Neill L.A. (2010). New insights into the regulation of signalling by toll-like receptors and nod-like receptors. J. Innate Immun. **2,** 406-421.

Collins N.C., Thordal-Christensen H., V L., Bau S., Kombrink E., Qiu J.L., Huckelhoven R., Stein M., Freialdenhoven A., Somerville S.C., and Schulze-Lefert P. (2003). SNARE-protein-mediated disease resistance at the plant cell wall. Nature **425,** 973-977.

Coolen M.W., Stirzaker C., Song J.Z., Statham A.L., Kassir Z., Moreno C.S., Young A.N., Varma V., Speed T.P., Cowley M., Lacaze P., Kaplan W., Robinson M.D., and Clark S.J. (2010). Consolidation of the cancer genome into domains of repressive chromatin by long-range epigenetic silencing (LRES) reduces transcriptional plasticity. Nat. Cell Biol. **12,** 235-246.

Coppinger, P., Repetti, P.P., Day, B., Dahlbeck, D., Mehlert, A., and Staskawicz, B.J. (2004). Overexpression of the plasma membrane-localized NDR1 protein results in enhanced bacterial disease resistance in *Arabidopsis thaliana.* Plant J. **40:** 225–237.

Cutler S., Ghassemian M., Bonetta D., Cooney S., and McCourt P. (1996). A protein farnesyl transferase involved in abscisic acid signal transduction in Arabidopsis. Science **273,** 1239-1241.

Danot O., Marquenet E., Vidal-Ingigliardi D., and Richet E. (2009). Wheel of Life, Wheel of Death: A Mechanistic Insight into Signaling by STAND Proteins. Structure **17,** 172-182.

de Torres M., Sanchez P., Fernandez-Delmond I., and Grant M. (2003). Expression profiling of the host response to bacterial infection: the transition from basal to induced defence responses in *RPM1*-mediated resistance. Plant J **33,** 665-676.

Debener T., Lehnackers H., Arnold M., and Dangl J.L. (1991). Identification and molecular mapping of a single Arabidopsis thaliana locus determining resistance to a phytopathogenic Pseudomonas syringae isolate. Plant J. **1,** 289-302.

DeYoung B.J. and Innes R.W. (2006). Plant NBS-LRR proteins in pathogen sensing and host defense. Nat. Immunol. **7,** 1243-1249.

Dhawan R., Luo H., Foerster A.M., Abuqamar S., Du H.N., Briggs S.D., Mittelsten Scheid O., and Mengiste T. (2009). HISTONE MONOUBIQUITINATION1 interacts with a subunit of the mediator complex and regulates defense against necrotrophic fungal pathogens in Arabidopsis. Plant Cell **21,** 1000-1019.

Dockendorff T.C., Heath C.V., Goldstein A.L., Snay C.A., and Cole C.N. (1997). C-terminal truncations of the yeast nucleoporin Nup145p produce a rapid temperature-conditional mRNA export defect and alterations to nuclear structure. Mol. Cell. Biol. **17,** 906-920.

Dong, C.H., Hu, X., Tang, W., Zheng, X., Kim, Y.S., Lee, B.H., and Zhu, J.K. (2006). A putative *Arabidopsis* nucleoporin, AtNUP160, is critical for RNA export and required for plant tolerance to cold stress. Mol. Cell. Biol. **26:** 9533–9543.

Downes B.P., Stupar R.M., Gingerich D.J., and Vierstra R.D. (2003). The HECT ubiquitin-protein ligase (UPL) family in Arabidopsis: UPL3 has a specific role in trichome development. Plant J. **35,** 729-742.

Du X., Miao M., Ma X., Liu Y., Kuhl J.C., Martin G.B., and Xiao F. (2012). Plant programmed cell death caused by an autoactive form of Prf is suppressed by co-expression of the Prf LRR domain. Mol. Plant. **5,** 1058-1067.

Dufu K., Livingstone M.J., Seebacher J., Gygi S.P., Wilson S.A., and Reed R. (2010). ATP is required for interactions between UAP56 and two conserved mRNA export proteins, Aly and CIP29, to assemble the TREX complex. Genes Dev. **24,** 2043-2053.

Dunning F.M., Sun W., Jansen K.L., Helft L., and Bent A.F. (2007). Identification and mutational analysis of Arabidopsis FLS2 leucine-rich repeat domain residues that contribute to flagellin perception. Plant Cell **19,** 3297-3313.

Durrant W.E. and Dong X. (2004). Systemic acquired resistance. Annu Rev Phytopathol **42,** 185-209.

Eitas T.K. and Dangl J.L. (2010). NB-LRR proteins: pairs, pieces, perception, partners, and pathways. Curr. Opin. Plant Biol. **13,** 472-477.

Emtage, J.L., Bucci, M., Watkins, J.L., and Wente, S.R. (1997). Defining the essential functional regions of the nucleoporin Nup145p. J. Cell Sci. **110:** 911–925.

Eulgem T., Tsuchiya T., Wang X.J., Beasley B., Cuzick A., Tor M., Zhu T., McDowell J.M., Holub E., and Dangl J.L. (2007). EDM2 is required for RPP7-dependent disease resistance in Arabidopsis and affects RPP7 transcript levels. Plant J. **49,** 829-839.

Ewan R., Pangestuti R., Thornber S., Craig A., Carr C., O'Donnell L., Zhang C., and Sadanandom A. (2011). Deubiquitinating enzymes AtUBP12 and AtUBP13 and their tobacco homologue NtUBP12 are negative regulators of plant immunity. New Phytol. **191,** 92-106.

Fabre E., Boelens W.C., Wimmer C., Mattaj I.W., and Hurt E.C. (1994). Nup145p is required for nuclear export of mRNA and binds homopolymeric RNA in vitro via a novel conserved motif. Cell **78,** 275-289.

Falk A., Feys B.J., Frost L.N., Jones J.D.G., Daniels M.J., and Parker J.E. (1999). *EDS1*, an essential component of *R* gene-mediated disease resistance in *Arabidopsis* has homology to eukaryotic lipases. Proc Natl Acad Sci **96,** 3292-3297.

Fan J. and Doerner P. (2012). Genetic and molecular basis of nonhost disease resistance: complex, yes; silver bullet, no. Curr. Opin. Plant Biol. **15,** 400-406.

Faria, A.M., Levay, A., Wang, Y., Kamphorst, A.O., Rosa, M.L., Nussenzveig, D.R., Balkan, W., Chook, Y.M., Levy, D.E., and Fontoura, B.M. (2006). The nucleoporin Nup96 is required for proper expression of interferon-regulated proteins and functions. Immunity **24:** 295–304.

Feys B.J., Moisan L.J., Newman M.A., and Parker J.E. (2001). Direct interaction between the *Arabidopsis* disease resistance signaling proteins, EDS1 and PAD4. Embo J **20,** 5400-5411.

Feys, B.J., Wiermer, M., Bhat, R.A., Moisan, L.J., Medina-Escobar, N., Neu, C., Cabral, A., and Parker, J.E. (2005). *Arabidopsis* SENESCENCE-ASSOCIATED GENE101 stabilizes and signals within an ENHANCED DISEASE SUSCEPTIBILITY1 complex in plant innate immunity. Plant Cell **17:** 2601–2613.

Gao Z., Chung E., Eitas T., and Dangl J. (2011). Plant intracellular innate immune receptor Resistance to Pseudomonas syringae pv. maculicola 1 (RPM1) is activated at, and functions on, the plasma membrane. Proc Natl Acad Sci **108**, 7619-7624

Gendrel A.V., Lippman Z., Yordan C., Colot V., and Martienssen R.A. (2002). Dependence of heterochromatic histone H3 methylation patterns on the Arabidopsis gene DDM1. Science **297,** 1871-1873.

Germain H., Qu N., Cheng Y.T., Lee E., Huang Y., Dong O.X., Gannon P., Huang S., Ding P., Li Y., Sack F., Zhang Y., and Li X. (2010). MOS11: a new component in the mRNA export pathway. PLoS Genet. **6,** e1001250.

Gilkerson J., Hu J., Brown J., Jones A., Sun T.P., and Callis J. (2009). Isolation and characterization of cul1-7, a recessive allele of CULLIN1 that disrupts SCF function at the C terminus of CUL1 in Arabidopsis thaliana. Genetics **181,** 945-963.

Gimenez-Ibanez S., Hann D.R., Ntoukakis V., Petutschnig E., Lipka V., and Rathjen J.P. (2009). AvrPtoB targets the LysM receptor kinase CERK1 to promote bacterial virulence on plants. Curr. Biol. **19,** 423-429.

Gingerich D.J., Gagne J.M., Salter D.W., Hellmann H., Estelle M., Ma L., and Vierstra R.D. (2005). Cullins 3a and 3b assemble with members of the broad complex/tramtrack/bric-a-brac (BTB) protein family to form essential ubiquitin-protein ligases (E3s) in Arabidopsis. J. Biol. Chem. **280,** 18810-18821.

Gohre V., Spallek T., Haweker H., Mersmann S., Mentzel T., Boller T., de Torres M., Mansfield J.W., and Robatzek S. (2008). Plant pattern-recognition receptor FLS2 is directed for degradation by the bacterial ubiquitin ligase AvrPtoB. Curr. Biol. **18,** 1824-1832.

Gomez-Gomez L., Bauer Z., and Boller T. (2001). Both the extracellular leucine-rich repeat domain and the kinase activity of FSL2 are required for flagellin binding and signaling in Arabidopsis. Plant Cell **13,** 1155-1163.

Gonzalez-Lamothe R., Tsitsigiannis D.I., Ludwig A.A., Panicot M., Shirasu K., and Jones J.D. (2006). The U-box protein CMPG1 is required for efficient activation of defense mechanisms triggered by multiple resistance genes in tobacco and tomato. Plant Cell **18,** 1067-1083.

Goritschnig S., Zhang Y., and Li X. (2007). The ubiquitin pathway is required for innate immunity in Arabidopsis. Plant J. **49,** 540-551.

Goritschnig S., Weihmann T., Zhang Y., Fobert P., McCourt P., and Li X. (2008). A novel role for protein farnesylation in plant innate immunity. Plant Physiol. **148,** 348-357.

Gou M., Su N., Zheng J., Huai J., Wu G., Zhao J., He J., Tang D., Yang S., and Wang G. (2009). An F-box gene, CPR30, functions as a negative regulator of the defense response in Arabidopsis. Plant J. **60,** 757-770.

Grant, M.R., Godiard, L., Straube, E., Ashfield, T., Lewald, J., Sattler, A., Innes, R.W., and Dangl, J.L. (1995). Structure of the *Arabidopsis RPM1* gene enabling dual specificity disease resistance. Science **269:** 843–846.

Greenberg J.T. and Yao N. (2004). The role and regulation of programmed cell death in plant-pathogen interactions. Cell. Microbiol. **6,** 201-211.

Gu Y. and Innes R.W. (2011). The KEEP ON GOING protein of Arabidopsis recruits the ENHANCED DISEASE RESISTANCE1 protein to trans-Golgi network/early endosome vesicles. Plant Physiol. **155,** 1827-1838.

Gutzat R. and Mittelsten Scheid O. (2012). Epigenetic responses to stress: triple defense? Curr. Opin. Plant Biol. **15,** 568-573.

Haasen, D., Kohler, C., Neuhaus, G., and Merkle, T. (1999). Nuclear export of proteins in plants: AtXPO1 is the export receptor for leucine-rich nuclear export signals in *Arabidopsis thaliana.* Plant J. **20:** 695–705.

Han S.W., Sriariyanun M., Lee S.W., Sharma M., Bahar O., Bower Z., and Ronald P.C. (2011). Small protein-mediated quorum sensing in a Gram-negative bacterium. PLoS One **6,** e29192.

Hardham A.R., Jones D.A., and Takemoto D. (2007). Cytoskeleton and cell wall function in penetration resistance. Curr. Opin. Plant Biol. **10,** 342-348.

Harton J.A., Linhoff M.W., Zhang J., and Ting J.P. (2002). Cutting edge: CATERPILLER: a large family of mammalian genes containing CARD, pyrin, nucleotide-binding, and leucine-rich repeat domains. J. Immunol. **169,** 4088-4093.

Haseloff, J., Siemering, K.R., Prasher, D.C., and Hodge, S. (1997). Removal of a cryptic intron and subcellular localization of green fluorescent protein are required to mark transgenic *Arabidopsis* plants brightly. Proc. Natl. Acad. Sci. USA **94:** 2122–2127.

Heidel A.J., Clarke J.D., Antonovics J., and Dong X. (2004). Fitness costs of mutations affecting the systemic acquired resistance pathway in *Arabidopsis thaliana*. Genetics **168,** 2197-2206.

Heil M. and Baldwin I.T. (2002). Fitness costs of induced resistance: emerging experimental support for a slippery concept. Trends Plant Sci. **7,** 61-67.

Hellens, R.P., Edwards, E.A., Leyland, N.R., Bean, S., and Mullineaux, P.M. (2000). pGreen: A versatile and flexible binary Ti vector for *Agrobacterium*-mediated plant transformation. Plant Mol. Biol. **42:** 819–832.

Hinsch, M., and Staskawicz, B. (1996). Identification of a new *Arabidopsis* disease resistance locus, *RPS4*, and cloning of the corresponding avirulence gene, *avrRps4*, from *Pseudomonas syringae* pv. *pisi.* Mol. Plant Microbe Interact. **9:** 55–61.

Ho M.S., Tsai P.I., and Chien C.T. (2006). F-box proteins: the key to protein degradation. J. Biomed. Sci. **13,** 181-191.

Holt B.F.,3rd, Belkhadir Y., and Dangl J.L. (2005). Antagonistic control of disease resistance protein stability in the plant immune system. Science **309,** 929-32.

Hua Z. and Vierstra R.D. (2011). The cullin-RING ubiquitin-protein ligases. Annu. Rev. Plant. Biol. **62,** 299-334.

Hua Z., Zou C., Shiu S.H., and Vierstra R.D. (2011). Phylogenetic comparison of F-Box (FBX) gene superfamily within the plant kingdom reveals divergent evolutionary histories indicative of genomic drift. PLoS One **6,** e16219.

Hubert D.A., Tornero P., Belkhadir Y., Krishna P., Takahashi A., Shirasu K., and Dangl J.L. (2003). Cytosolic HSP90 associates with and modulates the *Arabidopsis* RPM1 disease resistance protein. Embo J **22,** 5679-5689.

Hwang C.F., Bhakta A.V., Truesdell G.M., Pudlo W.M., and Williamson V.M. (2000). Evidence for a role of the N terminus and leucine-rich repeat region of the Mi gene product in regulation of localized cell death. Plant Cell **12,** 1319-1329.

Ingle R.A., Carstens M., and Denby K.J. (2006). PAMP recognition and the plant-pathogen arms race. Bioessays **28,** 880-889.

Inohara, Chamaillard, McDonald C., and Nunez G. (2005). NOD-LRR proteins: role in host-microbial interactions and inflammatory disease. Annu. Rev. Biochem. **74,** 355-383.

Jander, G., Norris, S.R., Rounsley, S.D., Bush, D.F., Levin, I.M., and Last, R.L. (2002). Arabidopsis map-based cloning in the post-genome era. Plant Physiol. **129:** 440–450.

Jebanathirajah J.A., Peri S., and Pandey A. (2002). Toll and interleukin-1 receptor (TIR) domain-containing proteins in plants: a genomic perspective. Trends Plant Sci. **7,** 388-391.

Jeong R.D., Chandra-Shekara A.C., Barman S.R., Navarre D., Klessig D.F., Kachroo A., and Kachroo P. (2010). Cryptochrome 2 and phototropin 2 regulate resistance protein-mediated viral defense by negatively regulating an E3 ubiquitin ligase. Proc Natl Acad Sci **107,** 13538-13543.

Jiang X. and Wang X. (2000). Cytochrome c promotes caspase-9 activation by inducing nucleotide binding to Apaf-1. J. Biol. Chem. **275,** 31199-31203.

Jing B., Xu S., Xu M., Li Y., Li S., Ding J., and Zhang Y. (2011). Brush and spray: a high-throughput systemic acquired resistance assay suitable for large-scale genetic screening. Plant Physiol. **157,** 973-980.

Jirage D., Tootle T.L., Reuber T.L., Frost L.N., Feys B.J., Parker J.E., Ausubel F.M., and Glazebrook J. (1999). *Arabidopsis thaliana* PAD4 encodes a lipase-like gene that is important for salicylic acid signaling. Proc Natl Acad Sci **96,** 13583-13588.

Johal G. and Briggs S. (1992). Reductase activity encoded by the HM1 disease resistance gene in maize. Science **258**, 985-987.

Jones J.D. and Dangl J.L. (2006). The plant immune system. Nature **444,** 323-9.

Kadota Y., Shirasu K., and Guerois R. (2010). NLR sensors meet at the SGT1-HSP90 crossroad. Trends Biochem. Sci. **35,** 199-207.

Kadota Y. and Shirasu K. (2012). The HSP90 complex of plants. Biochim. Biophys. Acta **1823,** 689-697.

Kawasaki T., Nam J., Boyes D.C., Holt B.F.,3rd, Hubert D.A., Wiig A., and Dangl J.L. (2005). A duplicated pair of Arabidopsis RING-finger E3 ligases contribute to the RPM1- and RPS2-mediated hypersensitive response. Plant J. **44,** 258-270.

Kelemen O., Convertini P., Zhang Z., Wen Y., Shen M., Falaleeva M., and Stamm S. (2013). Function of alternative splicing. Gene **514,** 1-30.

Kim H.S. and Delaney T.P. (2002). Arabidopsis SON1 is an F-box protein that regulates a novel induced defense response independent of both salicylic acid and systemic acquired resistance. Plant Cell **14,** 1469-1482.

Kim M.G., da Cunha L., McFall A.J., Belkhadir Y., DebRoy, S., Dangl, J.L., and Mackey, D. (2005). Two *Pseudomonas syringae* type III effectors inhibit RIN4-regulated basal defense in *Arabidopsis.* Cell **121:** 749–759.

Kim S.H., Gao F., Bhattacharjee S., Adiasor J.A., Nam J.C., and Gassmann W. (2010). The Arabidopsis resistance-like gene SNC1 is activated by mutations in SRFR1 and contributes to resistance to the bacterial effector AvrRps4. PLoS Pathog. **6,** e1001172.

Kitagawa K., Skowyra D., Elledge S.J., Harper J.W., and Hieter P. (1999). SGT1 encodes an essential component of the yeast kinetochore assembly pathway and a novel subunit of the SCF ubiquitin ligase complex. Mol. Cell **4,** 21-33.

Knepper C., Savory E.A., and Day B. (2011). Arabidopsis NDR1 is an integrin-like protein with a role in fluid loss and plasma membrane-cell wall adhesion. Plant Physiol. **156,** 286-300.

Kobe B. and Kajava A.V. (2001). The leucine-rich repeat as a protein recognition motif. Curr. Opin. Struct. Biol. **11,** 725-732.

Koch E. and Slusarenko A. (1990). Arabidopsis is susceptible to infection by a downy mildew fungus. Plant Cell **2,** 437-445.

Komander D., Clague M.J., and Urbe S. (2009). Breaking the chains: structure and function of the deubiquitinases. Nat. Rev. Mol. Cell Biol. **10,** 550-563.

Kraft E., Stone S.L., Ma L., Su N., Gao Y., Lau O.S., Deng X.W., and Callis J. (2005). Genome analysis and functional characterization of the E2 and RING-type E3 ligase ubiquitination enzymes of Arabidopsis. Plant Physiol. **139,** 1597-1611.

Kunkel B.N., Bent A.F., Dahlbeck D., Innes R.W., and Staskawicz B.J. (1993). RPS2, an Arabidopsis disease resistance locus specifying recognition of Pseudomonas syringae strains expressing the avirulence gene avrRpt2. Plant Cell **5,** 865-875.

Lange A., Mills R.E., Lange C.J., Stewart M., Devine S.E., and Corbett A.H. (2007). Classical nuclear localization signals: definition, function, and interaction with importin alpha. J. Biol. Chem. **282,** 5101-5105.

Lee D.H., Choi H.W., and Hwang B.K. (2011). The pepper E3 ubiquitin ligase RING1 gene, CaRING1, is required for cell death and the salicylic acid-dependent defense response. Plant Physiol. **156,** 2011-2025.

Lee J., He K., Stolc V., Lee H., Figueroa P., Gao Y., Tongprasit W., Zhao H., Lee I., and Deng X.W. (2007). Analysis of transcription factor HY5 genomic binding sites revealed its hierarchical role in light regulation of development. Plant Cell **19,** 731-749.

Lee J.H., Terzaghi W., Gusmaroli G., Charron J.B., Yoon H.J., Chen H., He Y.J., Xiong Y., and Deng X.W. (2008). Characterization of Arabidopsis and rice DWD proteins and their roles as substrate receptors for CUL4-RING E3 ubiquitin ligases. Plant Cell **20,** 152-167.

Lee S.W., Han S.W., Sririyanum M., Park C.J., Seo Y.S., and Ronald P.C. (2009). A type I-secreted, sulfated peptide triggers XA21-mediated innate immunity. Science **326,** 850-853.

Li W., Zhong S., Li G., Li Q., Mao B., Deng Y., Zhang H., Zeng L., Song F., and He Z. (2011). Rice RING protein OsBBI1 with E3 ligase activity confers broad-spectrum resistance against Magnaporthe oryzae by modifying the cell wall defence. Cell Res. **21,** 835-848.

Li, X., Zhang, Y., Clarke, J.D., Li, Y., and Dong, X. (1999). Identification and cloning of a negative regulator of systemic acquired resistance, SNlI1, through a screen for suppressors of *npr1–1*. Cell **98:** 329–339.

Li X., Clarke J.D., Zhang Y., and Dong X. (2001). Activation of an EDS1-mediated *R*-gene pathway in the *snc1* mutant leads to constitutive, NPR1-independent pathogen resistance. Mol Plant Microbe In **14,** 1131-1139.

Li Y., Li S., Bi D., Cheng Y.T., Li X., and Zhang Y. (2010a). SRFR1 negatively regulates plant NB-LRR resistance protein accumulation to prevent autoimmunity. PLoS Pathog. **6,** e1001111.

Li Y., Tessaro M.J., Li X., and Zhang Y. (2010b). Regulation of the expression of plant resistance gene SNC1 by a protein with a conserved BAT2 domain. Plant Physiol. **153,** 1425-1434.

Li Y., Dong O.X., Johnson K., and Zhang Y. (2011). MOS1 epigenetically regulates the expression of plant Resistance gene SNC1. Plant. Signal. Behav. **6,** 434-436.

Lin S.S., Martin R., Mongrand S., Vandenabeele S., Chen K.C., Jang I.C., and Chua N.H. (2008). RING1 E3 ligase localizes to plasma membrane lipid rafts to trigger FB1-induced programmed cell death in Arabidopsis. Plant J. **56,** 550-561.

Lipka V., Dittgen J., Bednarek P., Bhat R., Wiermer M., Stein M., Landtag J., Brandt W., Rosahl S., Scheel D., Llorente F., Molina A., Parker J., Somerville S., and Schulze-Lefert P. (2005). Pre- and postinvasion defenses both contribute to nonhost resistance in Arabidopsis. Science **310,** 1180-1183.

Liu C., Lu F., Cui X., and Cao X. (2010). Histone methylation in higher plants. Annu. Rev. Plant. Biol. **61,** 395-420.

Liu J., Li H., Miao M., Tang X., Giovannoni J., Xiao F., and Liu Y. (2012). The tomato UV-damaged DNA-binding protein-1 (DDB1) is implicated in pathogenesis-related (PR) gene expression and resistance to Agrobacterium tumefaciens. Mol. Plant. Pathol. **13,** 123-134.

Liu Y., Schiff M., Serino G., Deng X.W., and Dinesh-Kumar S.P. (2002). Role of SCF ubiquitin-ligase and the COP9 signalosome in the *N* gene-mediated resistance response to *Tobacco mosaic virus*. Plant Cell **14,** 1483-1496.

Long J.A., Ohno C., Smith Z.R., and Meyerowitz E.M. (2006). TOPLESS regulates apical embryonic fate in Arabidopsis. Science **312,** 1520-1523.

Loyer P., Trembley J.H., Grenet J.A., Busson A., Corlu A., Zhao W., Kocak M., Kidd V.J., and Lahti J.M. (2008). Characterization of cyclin L1 and L2 interactions with CDK11 and splicing factors: influence of cyclin L isoforms on splice site selection. J. Biol. Chem. **283,** 7721-7732.

Lu D., Lin W., Gao X., Wu S., Cheng C., Avila J., Heese A., Devarenne T.P., He P., and Shan L. (2011). Direct ubiquitination of pattern recognition receptor FLS2 attenuates plant innate immunity. Science **332,** 1439-1442.

Ma W. and Berkowitz G.A. (2007). The grateful dead: calcium and cell death in plant innate immunity. Cell. Microbiol. **9,** 2571-2585.

Mackey, D., Belkhadir, Y., Alonso, J.M., Ecker, J.R., and Dangl, J.L. (2003). *Arabidopsis* RIN4 is a target of the type III virulence effector AvrRpt2 and modulates RPS2-mediated resistance. Cell **112:** 379–389.

Mackey, D., Holt, B.F., Wiig, A., and Dangl, J.L. (2002). RIN4 interacts with *Pseudomonas syringae* type III effector molecules and is required for RPM1-mediated resistance in *Arabidopsis.* Cell **108:** 743–754.

Maekawa T., Cheng W., Spiridon L.N., Toller A., Lukasik E., Saijo Y., Liu P., Shen Q.H., Micluta M.A., Somssich I.E., Takken F.L., Petrescu A.J., Chai J., and Schulze-Lefert P. (2011). Coiled-coil domain-dependent homodimerization of intracellular barley immune receptors defines a minimal functional module for triggering cell death. Cell. Host Microbe **9,** 187-199.

Magalhaes J.G., Sorbara M.T., Girardin S.E., and Philpott D.J. (2011). What is new with Nods? Curr. Opin. Immunol. **23,** 29-34.

Martin G., Brommonschenkel S., Chunwongse J., Frary A., Ganal M., Spivey R., Wu T., Earle E., and Tanksley S. (1993). Map-based cloning of a protein kinase gene conferring disease resistance in tomato. Science **262**, 1432-1436

Martin, G.B., Bogdanove, A.J., and Sessa, G. (2003). Understanding the functions of plant disease resistance proteins. Annu. Rev. Plant Biol. **54:** 23–61.

Mayor A., Martinon F., De Smedt T., Petrilli V., and Tschopp J. (2007). A crucial function of SGT1 and HSP90 in inflammasome activity links mammalian and plant innate immune responses. Nat. Immunol. **8,** 497-503.

McHale L., Tan X., Koehl P., and Michelmore R.W. (2006). Plant NBS-LRR proteins: adaptable guards. Genome Biol. **7,** 212.

Meyers B.C., Kozik A., Griego A., Kuang H.H., and Michelmore R.W. (2003). Genome-wide analysis of NBS-LRR-encoding genes in Arabidopsis. Plant Cell **15,** 809-834.

Monaghan J., Xu F., Gao M., Zhao Q., Palma K., Long C., Chen S., Zhang Y., and Li X. (2009). Two Prp19-like U-box proteins in the MOS4-associated complex play redundant roles in plant innate immunity. PLoS Pathog. **5,** e1000526.

Monaghan J. and Zipfel C. (2012). Plant pattern recognition receptor complexes at the plasma membrane. Curr. Opin. Plant Biol. **15,** 349-357.

Mou, Z., Fan, W.H., and Dong, X. (2003). Inducers of plant systemic acquired resistance regulate NPR1 function through redox changes. Cell **113:** 935–944.

Munkvold K.R. and Martin G.B. (2009). Advances in experimental methods for the elucidation of Pseudomonas syringae effector function with a focus on AvrPtoB. Mol. Plant. Pathol. **10,** 777-793.

Muskett P.R., Kahn K., Austin M.J., Moisan L.J., Sadanandom A., Shirasu K., Jones J.D., and Parker J.E. (2002). Arabidopsis *RAR1* exerts rate-limiting control of *R* gene-mediated defenses against multiple pathogens. Plant Cell **14,** 979-92.

Navarro L., Zipfel C., Rowland O., Keller I., Robatzek S., Boller T., and Jones J.D. (2004). The transcriptional innate immune response to flg22. Interplay and overlap with Avr gene-dependent defense responses and bacterial pathogenesis. Plant Physiol. **135,** 1113-1128.

Neubauer G., King A., Rappsilber J., Calvio C., Watson M., Ajuh P., Sleeman J., Lamond A., and Mann M. (1998). Mass spectrometry and EST-database searching allows characterization of the multi-protein spliceosome complex. Nat. Genet. **20,** 46-50.

Nicaise V., Roux M., and Zipfel C. (2009). Recent advances in PAMP-triggered immunity against bacteria: pattern recognition receptors watch over and raise the alarm. Plant Physiol. **150,** 1638-1647.

Nielsen R. and Yang Z. (1998). Likelihood models for detecting positively selected amino acid sites and applications to the HIV-1 envelope gene. Genetics **148,** 929-936.

Noel L., Moores T.L., van Der Biezen E.A., Parniske M., Daniels M.J., Parker J.E., and Jones J.D. (1999). Pronounced intraspecific haplotype divergence at the RPP5 complex disease resistance locus of Arabidopsis. Plant Cell **11,** 2099-2112.

Noël, L.D., Cagna, G., Stuttmann, J., Wirthmuller, L., Betsuyaku, S., Witte, C.P., Bhat, R., Pochon, N., Colby, T., and Parker, J.E. (2007). Interaction between SGT1 and cytosolic/nuclear HSC70 chaperones regulates *Arabidopsis* immune responses. Plant Cell **19:** 4061–4076.

Nurnberger T. and Scheel D. (2001). Signal transmission in the plant immune response. Trends Plant Sci. **6,** 372-379.

Nurnberger T. and Lipka V. (2005). Non-host resistance in plants: new insights into an old phenomenon. Molecular Plant Pathology **6,** 335-345.

Palma K., Zhang Y., and Li X. (2005). An importin α homolog, MOS6, plays an important role in plant innate immunity. Curr Biol **15,** 1129-35.

Palma K., Zhao Q., Cheng Y.T., Bi D., Monaghan J., Cheng W., Zhang Y., and Li X. (2007). Regulation of plant innate immunity by three proteins in a complex conserved across the plant and animal kingdoms. Genes Dev. **21,** 1484-1493.

Palma K., Thorgrimsen S., Malinovsky F.G., Fiil B.K., Nielsen H.B., Brodersen P., Hofius D., Petersen M., and Mundy J. (2010). Autoimmunity in Arabidopsis acd11 is mediated by epigenetic regulation of an immune receptor. PLoS Pathog. **6,** e1001137.

Parry G., Ward S., Cernac A., Dharmasiri S., and Estelle M. (2006). The Arabidopsis SUPPRESSOR OF AUXIN RESISTANCE proteins are nucleoporins with an important role in hormone signaling and development. Plant Cell **18,** 1590-1603.

Pei Z.M., Ghassemian M., Kwak C.M., McCourt P., and Schroeder J.I. (1998). Role of farnesyltransferase in ABA regulation of guard cell anion channels and plant water loss. Science **282,** 287-290.

Pickart C.M. and Fushman D. (2004). Polyubiquitin chains: polymeric protein signals. Curr. Opin. Chem. Biol. **8,** 610-616.

Purrington C.B. (2000). Costs of resistance. Curr. Opin. Plant Biol. **3,** 305-308.

Rairdan G.J. and Moffett P. (2006). Distinct domains in the ARC region of the potato resistance protein Rx mediate LRR binding and inhibition of activation. Plant Cell **18,** 2082-2093.

Reed R. (2003). Coupling transcription, splicing and mRNA export. Curr. Opin. Cell Biol. **15,** 326-331.

Reed R. and Cheng H. (2005). TREX, SR proteins and export of mRNA. Curr. Opin. Cell Biol. **17,** 269-273.

Roth, P., Xylourgidis, N., Sabri, N., Uv, A., Fornerod, M., and Samakovlis, C. (2003). The *Drosophila* nucleoporin DNup88 localizes DNup214 and CRM1 on the nuclear envelope and attenuates NES-mediated nuclear export. J. Cell Biol. **163:** 701–706.

Sacco, M.A., Mansoor, S., and Moffett, P. (2007). A RanGAP protein physically interacts with the NB-LRR protein Rx, and is required for Rx-mediated viral resistance. Plant J. **52:** 82–93.
Santner A. and Estelle M. (2009). Recent advances and emerging trends in plant hormone signalling. Nature **459,** 1071-1078.

Schnell J.D. and Hicke L. (2003). Non-traditional functions of ubiquitin and ubiquitin-binding proteins. J. Biol. Chem. **278,** 35857-35860.

Schult K., Meierhoff K., Paradies S., Toller T., Wolff P., and Westhoff P. (2007). The nuclear-encoded factor HCF173 is involved in the initiation of translation of the psbA mRNA in Arabidopsis thaliana. Plant Cell **19,** 1329-1346.

Segonzac C. and Zipfel C. (2011). Activation of plant pattern-recognition receptors by bacteria. Curr. Opin. Microbiol. **14,** 54-61.

Sela H., Spiridon L.N., Petrescu A.J., Akerman M., Mandel-Gutfreund Y., Nevo E., Loutre C., Keller B., Schulman A.H., and Fahima T. (2012). Ancient diversity of splicing motifs and protein surfaces in the wild emmer wheat (Triticum dicoccoides) LR10 coiled coil (CC) and leucine-rich repeat (LRR) domains. Mol. Plant. Pathol. **13,** 276-287.

Shah, J. (2003). The salicylic acid loop in plant defense. Curr. Opin. Plant Biol. **6:** 365–371.

Shen, Q.H., Saijo, Y., Mauch, S., Biskup, C., Bieri, S., Keller, B., Seki, H., Ülker, B., Somssich, I.E., and Schulze-Lefert, P. (2007). Nuclear activity of MLA immune receptors links isolate-specific and basal disease-resistance responses. Science **315:** 1098–1103.

Shen W.H., Parmentier Y., Hellmann H., Lechner E., Dong A., Masson J., Granier F., Lepiniec L., Estelle M., and Genschik P. (2002). Null mutation of AtCUL1 causes arrest in early embryogenesis in Arabidopsis. Mol. Biol. Cell **13,** 1916-1928.

Sheen, J. (2001). Signal transduction in maize and Arabidopsis mesophyll protoplasts. Plant Physiol. **127:** 1466–1475.

Shirano Y., Kachroo P., Shah J., and Klessig D.F. (2002). A gain-of-function mutation in an Arabidopsis Toll Interleukin-1 Receptor-Nucleotide Binding Site-Leucine-Rich Repeat type R gene triggers defense responses and results in enhanced disease resistance. Plant Cell **14,** 3149-3162.

Shirasu K., Lahaye T., Tan M.W., Zhou F., Azevedo C., and Schulze-Lefert P. (1999). A novel class of eukaryotic zinc-binding proteins is required for disease resistance signaling in barley and development in C. elegans. Cell **99,** 355-366.

Shirasu K. (2009). The HSP90-SGT1 chaperone complex for NLR immune sensors. Annu. Rev. Plant. Biol. **60,** 139-164.

Shilatifard A. (2012). The COMPASS family of histone H3K4 methylases: mechanisms of regulation in development and disease pathogenesis. Annu. Rev. Biochem. **81,** 65-95.

Sinapidou E., Williams K., Nott L., Bahkt S., Tor M., Crute I., Bittner-Eddy P., and Beynon J. (2004). Two TIR:NB:LRR genes are required to specify resistance to Peronospora parasitica isolate Cala2 in Arabidopsis. Plant J. **38,** 898-909.

Simonich M.T. and Innes R.W. (1995). A disease resistance gene in Arabidopsis with specificity for the avrPph3 gene of Pseudomonas syringae pv. phaseolicola. Mol. Plant Microbe Interact. **8,** 637-640.

Smalle J. and Vierstra R.D. (2004). The ubiquitin 26S proteasome proteolytic pathway. Annu. Rev. Plant. Biol. **55,** 555-590.

Somers D.E. and Fujiwara S. (2009). Thinking outside the F-box: novel ligands for novel receptors. Trends Plant Sci. **14,** 206-213.

Song W.Y., Wang G.L., Chen L.L., Kim H.S., Pi L.Y., Holsten T., Gardner J., Wang B., Zhai W.X., Zhu L.H., Fauquet C., and Ronald P. (1995). A receptor kinase-like protein encoded by the rice disease resistance gene, Xa21. Science **270,** 1804-1806.

Sorek N., Bloch D., and Yalovsky S. (2009). Protein lipid modifications in signaling and subcellular targeting. Curr. Opin. Plant Biol. **12,** 714-720.

Stein M., Dittgen J., Sanchez-Rodriguez C., Hou B.H., Molina A., Schulze-Lefert P., Lipka V., and Somerville S. (2006). Arabidopsis PEN3/PDR8, an ATP binding cassette transporter, contributes to nonhost resistance to inappropriate pathogens that enter by direct penetration. Plant Cell **18,** 731-746.

Steiner T., Kaiser J.T., Marinkovic S., Huber R., and Wahl M.C. (2002). Crystal structures of transcription factor NusG in light of its nucleic acid- and protein-binding activities. EMBO J. **21,** 4641-4653.

Stone S.L., Hauksdottir H., Troy A., Herschleb J., Kraft E., and Callis J. (2005). Functional analysis of the RING-type ubiquitin ligase family of Arabidopsis. Plant Physiol. **137,** 13-30.

Stone S.L., Williams L.A., Farmer L.M., Vierstra R.D., and Callis J. (2006). KEEP ON GOING, a RING E3 ligase essential for Arabidopsis growth and development, is involved in abscisic acid signaling. Plant Cell **18,** 3415-3428.

Sun L. and Chen Z.J. (2004). The novel functions of ubiquitination in signaling. Curr. Opin. Cell Biol. **16,** 119-126.

Szemenyei H., Hannon M., and Long J.A. (2008). TOPLESS mediates auxin-dependent transcriptional repression during Arabidopsis embryogenesis. Science **319,** 1384-1386.

Tada, Y., Spoel, S.H., Pajerowska-Mukhtar, K., Mou, Z., Song, J., and Dong, X. (2008). Plant immunity requires conformational changes of NPR1 via S-nitrosylation and thioredoxins. Science **321:** 952–956.

Takahashi A., Casais C., Ichimura K., and Shirasu K. (2003). HSP90 interacts with RAR1 and SGT1 and is essential for RPS2-mediated disease resistance in *Arabidopsis*. Proc Natl Acad Sci **100,** 11777-11782.

Takahashi, N., van Kilsdonk, J.W., Ostendorf, B., Smeets, R., Bruggeman, S.W., Alonso, A., van de Loo, F., Schneider, M., van den Berg, W.B., and Swart, G.W. (2008). Tumor marker nucleoporin 88 kDa regulates nucleocytoplasmic transport of NF-κB. Biochem. Biophys. Res. Commun. **374:** 424–430.

Takken F.L., Albrecht M., and Tameling W.I. (2006). Resistance proteins: molecular switches of plant defence. Curr. Opin. Plant Biol. **9,** 383-390.

Takken F.L. and Tameling W.I. (2009). To nibble at plant resistance proteins. Science **324,** 744-746.

Tamada Y., Yun J.Y., Woo S.C., and Amasino R.M. (2009). ARABIDOPSIS TRITHORAX-RELATED7 is required for methylation of lysine 4 of histone H3 and for transcriptional activation of FLOWERING LOCUS C. Plant Cell **21,** 3257-3269.

Tameling, W.I., and Baulcombe, D.C. (2007). Physical association of the NB-LRR resistance protein Rx with a Ran GTPase-activating protein is required for extreme resistance to *Potato virus X*. Plant Cell **19:** 1682–1694.

Tan X., Meyers B.C., Kozik A., West M.A., Morgante M., St Clair D.A., Bent A.F., and Michelmore R.W. (2007). Global expression analysis of nucleotide binding site-leucine rich repeat-encoding and related genes in Arabidopsis. BMC Plant. Biol. **7,** 56.

Tao Y., Xie Z.Y., Chen W.Q., Glazebrook J., Chang H.S., Han B., Zhu T., Zou G.Z., and Katagiri F. (2003). Quantitative nature of Arabidopsis responses during compatible and incompatible interactions with the bacterial pathogen *Pseudomonas syringae*. Plant Cell **15,** 317-330.

Tasset C., Bernoux M., Jauneau A., Pouzet C., Briere C., Kieffer-Jacquinod S., Rivas S., Marco Y., and Deslandes L. (2010). Autoacetylation of the Ralstonia solanacearum effector PopP2 targets a lysine residue essential for RRS1-R-mediated immunity in Arabidopsis. PLoS Pathog. **6,** e1001202.

Terry, L.J., Shows, E.B., and Wente, S.R. (2007). Crossing the nuclear envelope: hierarchical regulation of nucleocytoplasmic transport. Science **318:** 1412–1416.

Thilmony R., Underwood W., and He S.Y. (2006). Genome-wide transcriptional analysis of the Arabidopsis thaliana interaction with the plant pathogen Pseudomonas syringae pv. tomato DC3000 and the human pathogen Escherichia coli O157:H7. Plant J. **46,** 34-53.

Thrower J.S., Hoffman L., Rechsteiner M., and Pickart C.M. (2000). Recognition of the polyubiquitin proteolytic signal. EMBO J. **19,** 94-102.

Ting J.P. and Davis B.K. (2005). CATERPILLER: a novel gene family important in immunity, cell death, and diseases. Annu. Rev. Immunol. **23,** 387-414.

Ting J.P., Kastner D.L., and Hoffman H.M. (2006). CATERPILLERs, pyrin and hereditary immunological disorders. Nat. Rev. Immunol. **6,** 183-195.

Tör M., Gordon P., Cuzick A., Eulgem T., Sinapidou E., Mert-Türk F., Can C., Dangl J.L., and Holub E.B. (2002). Arabidopsis SGT1b is required for defense signaling conferred by several downy mildew resistance genes. Plant Cell **14,** 993-1003.

Trujillo M., Ichimura K., Casais C., and Shirasu K. (2008). Negative regulation of PAMP-triggered immunity by an E3 ubiquitin ligase triplet in Arabidopsis. Curr. Biol. **18,** 1396-1401.

Truman W., de Zabala M.T., and Grant M. (2006). Type III effectors orchestrate a complex interplay between transcriptional networks to modify basal defence responses during pathogenesis and resistance. Plant J. **46,** 14-33.

Tsuchiya T. and Eulgem T. (2010). The Arabidopsis defense component EDM2 affects the floral transition in an FLC-dependent manner. Plant J. **62,** 518-528.

Tsuda K., Sato M., Glazebrook J., Cohen J.D., and Katagiri F. (2008). Interplay between MAMP-triggered and SA-mediated defense responses. Plant J. **53,** 763-775.

Tzfira T., Vaidya M., and Citovsky V. (2004). Involvement of targeted proteolysis in plant genetic transformation by Agrobacterium. Nature **431,** 87-92.

Umebayashi K. (2003). The roles of ubiquitin and lipids in protein sorting along the endocytic pathway. Cell Struct. Funct. **28,** 443-453.

Underwood W., Melotto M., and He S.Y. (2007). Role of plant stomata in bacterial invasion. Cell. Microbiol. **9,** 1621-1629.

Uv, A.E., Roth, P., Xylourgidis, N., Wickberg, A., Cantera, R., and Samakovlis, C. (2000). *members only* encodes a *Drosophila* nucleoporin required for Rel protein import and immune response activation. Genes Dev. **14:** 1945–1957.

van den Burg H.A., Tsitsigiannis D.I., Rowland O., Lo J., Rallapalli G., Maclean D., Takken F.L., and Jones J.D. (2008). The F-box protein ACRE189/ACIF1 regulates cell death and defense responses activated during pathogen recognition in tobacco and tomato. Plant Cell **20,** 697-719.

van der Biezen, E.A., Freddie, C.T., Kahn, K., Parker, J.E., and Jones, J.D. (2002). *Arabidopsis RPP4* is a member of the *RPP5* multigene family of TIR-NB-LRR genes and confers downy mildew resistance through multiple signalling components. Plant J. **29:** 439–451.

Vasu S., Shah S., Orjalo A., Park M., Fischer W.H., and Forbes D.J. (2001). Novel vertebrate nucleoporins Nup133 and Nup160 play a role in mRNA export. J Cell Bio **155,** 339-54.

Vernooij, B., Friedrich, L., Morse, A., Reist, R., Kolditz-Jawhar, R., Ward, E., Uknes, S., Kessmann, H., and Ryals, J. (1994). Salicylic acid is not the translocated signal responsible for inducing systemic acquired resistance but is required in signal transduction. Plant Cell **6:** 959–965.

Vierstra R.D. (2009). The ubiquitin-26S proteasome system at the nexus of plant biology. Nat. Rev. Mol. Cell Biol. **10,** 385-397.

Wang Y.S., Pi L.Y., Chen X., Chakrabarty P.K., Jiang J., De Leon A.L., Liu G.Z., Li L., Benny U., Oard J., Ronald P.C., and Song W.Y. (2006). Rice XA21 binding protein 3 is a ubiquitin ligase required for full Xa21-mediated disease resistance. Plant Cell **18,** 3635-3646.

Warren R.F., Merritt P.M., Holub E., and Innes R.W. (1999). Identification of three putative signal transduction genes involved in *R* gene-specified disease resistance in *Arabidopsis*. Genetics **152,** 401-412.

Weissman A.M. (2001). Themes and variations on ubiquitylation. Nat. Rev. Mol. Cell Biol. **2,** 169-178.

Weissman A.M., Shabek N., and Ciechanover A. (2011). The predator becomes the prey: regulating the ubiquitin system by ubiquitylation and degradation. Nat. Rev. Mol. Cell Biol. **12,** 605-620.

Wiermer M., Feys B.J., and Parker J.E. (2005). Plant immunity: the EDS1 regulatory node. Curr Opin Plant Biol **8,** 383-389.

Wirthmueller, L., Zhang, Y., Jones, J.D., and Parker, J.E. (2007). Nuclear accumulation of the *Arabidopsis* immune receptor RPS4 is necessary for triggering EDS1-dependent defense. Curr. Biol. **17:** 2023–2029.

Xu F., Xu S., Wiermer M., Zhang Y., and Li X. (2012). The cyclin L homolog MOS12 and the MOS4-associated complex are required for the proper splicing of plant resistance genes. Plant J. **70,** 916-928.

Xu S., Zhang Z., Jing B., Gannon P., Ding J., Xu F., Li X., and Zhang Y. (2011). Transportin-SR is required for proper splicing of resistance genes and plant immunity. PLoS Genet. **7,** e1002159.

Xylourgidis N., Roth P., Sabri N., Tsarouhas V., and Samakovlis C. (2006). The nucleoporin Nup214 sequesters CRM1 at the nuclear rim and modulates NFkappaB activation in Drosophila. J. Cell. Sci. **119,** 4409-4419.

Yaeno T. and Iba K. (2008). BAH1/NLA, a RING-type ubiquitin E3 ligase, regulates the accumulation of salicylic acid and immune responses to Pseudomonas syringae DC3000. Plant Physiol. **148,** 1032-1041.

Yaeno T., Li H., Chaparro-Garcia A., Schornack S., Koshiba S., Watanabe S., Kigawa T., Kamoun S., and Shirasu K. (2011). Phosphatidylinositol monophosphate-binding interface in the oomycete RXLR effector AVR3a is required for its stability in host cells to modulate plant immunity. Proc Natl Acad Sci **108,** 14682-14687.

Yan N., Doelling J.H., Falbel T.G., Durski A.M., and Vierstra R.D. (2000). The ubiquitin-specific protease family from Arabidopsis. AtUBP1 and 2 are required for the resistance to the amino acid analog canavanine. Plant Physiol. **124,** 1828-1843.

Yang C.W., Gonzalez-Lamothe R., Ewan R.A., Rowland O., Yoshioka H., Shenton M., Ye H., O'Donnell E., Jones J.D., and Sadanandom A. (2006). The E3 ubiquitin ligase activity of Arabidopsis PLANT U-BOX17 and its functional tobacco homolog ACRE276 are required for cell death and defense. Plant Cell **18,** 1084-1098.

Yang Z. and Bielawski J.P. (2000). Statistical methods for detecting molecular adaptation. Trends Ecol. Evol. **15,** 496-503.

Yang Z., Nielsen R., Goldman N., and Pedersen A.M. (2000). Codon-substitution models for heterogeneous selection pressure at amino acid sites. Genetics **155,** 431-449.

Yang Z. (2007). PAML 4: phylogenetic analysis by maximum likelihood. Mol. Biol. Evol. **24,** 1586-1591.

Yee D. and Goring D.R. (2009). The diversity of plant U-box E3 ubiquitin ligases: from upstream activators to downstream target substrates. J. Exp. Bot. **60,** 1109-1121.

Yen H.C. and Elledge S.J. (2008). Identification of SCF ubiquitin ligase substrates by global protein stability profiling. Science **322,** 923-929.

Yi H. and Richards E.J. (2009). Gene duplication and hypermutation of the pathogen Resistance gene SNC1 in the Arabidopsis bal variant. Genetics **183,** 1227-1234.

Yoo, S.D., Cho, Y.H., and Sheen, J. (2007). Arabidopsis mesophyll protoplasts: A versatile cell system for transient gene expression analysis. Nat. Protoc. **2:** 1565–1572.

Yu G.L., Katagiri F., and Ausubel F.M. (1993). Arabidopsis mutations at the RPS2 locus result in loss of resistance to Pseudomonas syringae strains expressing the avirulence gene avrRpt2. Mol. Plant Microbe Interact. **6,** 434-443.

Yuan Y., Zhong S., Li Q., Zhu Z., Lou Y., Wang L., Wang J., Wang M., Li Q., Yang D., and He Z. (2007). Functional analysis of rice NPR1-like genes reveals that OsNPR1/NH1 is the rice orthologue conferring disease resistance with enhanced herbivore susceptibility. Plant. Biotechnol. J. **5,** 313-324.

Zeng L.R., Qu S., Bordeos A., Yang C., Baraoidan M., Yan H., Xie Q., Nahm B.H., Leung H., and Wang G.L. (2004). Spotted leaf11, a negative regulator of plant cell death and defense, encodes a U-box/armadillo repeat protein endowed with E3 ubiquitin ligase activity. Plant Cell **16,** 2795-2808.

Zhang M., Kadota Y., Prodromou C., Shirasu K., and Pearl L.H. (2010). Structural basis for assembly of Hsp90-Sgt1-CHORD protein complexes: implications for chaperoning of NLR innate immunity receptors. Mol. Cell **39,** 269-281.

Zhang, Y., Fan, W., Kinkema, M., Li, X., and Dong, X. (1999). Interaction of NPR1 with basic leucine zipper protein transcription factors that bind sequences required for salicylic acid induction of the *PR-1* gene. Proc. Natl. Acad. Sci. USA **96:** 6523–6528.

Zhang, Y., Goritschnig, S., Dong, X., and Li, X. (2003a). A gain-of-function mutation in a plant disease resistance gene leads to constitutive activation of downstream signal transduction pathways in *suppressor of npr1-1, constitutive 1.* Plant Cell **15:** 2636–2646.

Zhang, Y., Tessaro, M.J., Lassner, M., and Li, X. (2003b). Knockout analysis of *Arabidopsis* transcription factors *TGA2*, *TGA5*, and *TGA6* reveals their redundant and essential roles in systemic acquired resistance. Plant Cell **15:** 2647–2653.

Zhang Y., Cheng Y.T., Bi D., Palma K., and Li X. (2005). MOS2, a protein containing G-patch and KOW motifs, is essential for innate immunity in Arabidopsis thaliana. Curr. Biol. **15,** 1936-1942.

Zhang Y. and Li X. (2005). A Putative Nucleoporin 96 Is Required for Both Basal Defense and Constitutive Resistance Responses Mediated by *suppressor of npr1-1*, *constitutive 1*. Plant Cell **17,** 1306-1316.

Zhu Z., Xu F., Zhang Y., Cheng Y.T., Wiermer M., Li X., and Zhang Y. (2010). Arabidopsis resistance protein SNC1 activates immune responses through association with a transcriptional corepressor. Proc Natl Acad Sci **107,** 13960-13965.